Hydraulic problems in flooding: from data to theory and from theory to practice

by Donald W Knight

The University of Birmingham, UK

Experimental & computational solutions of hydraulic problems

International School of Hydraulics
May 2012
Lochow, Poland

Personal details

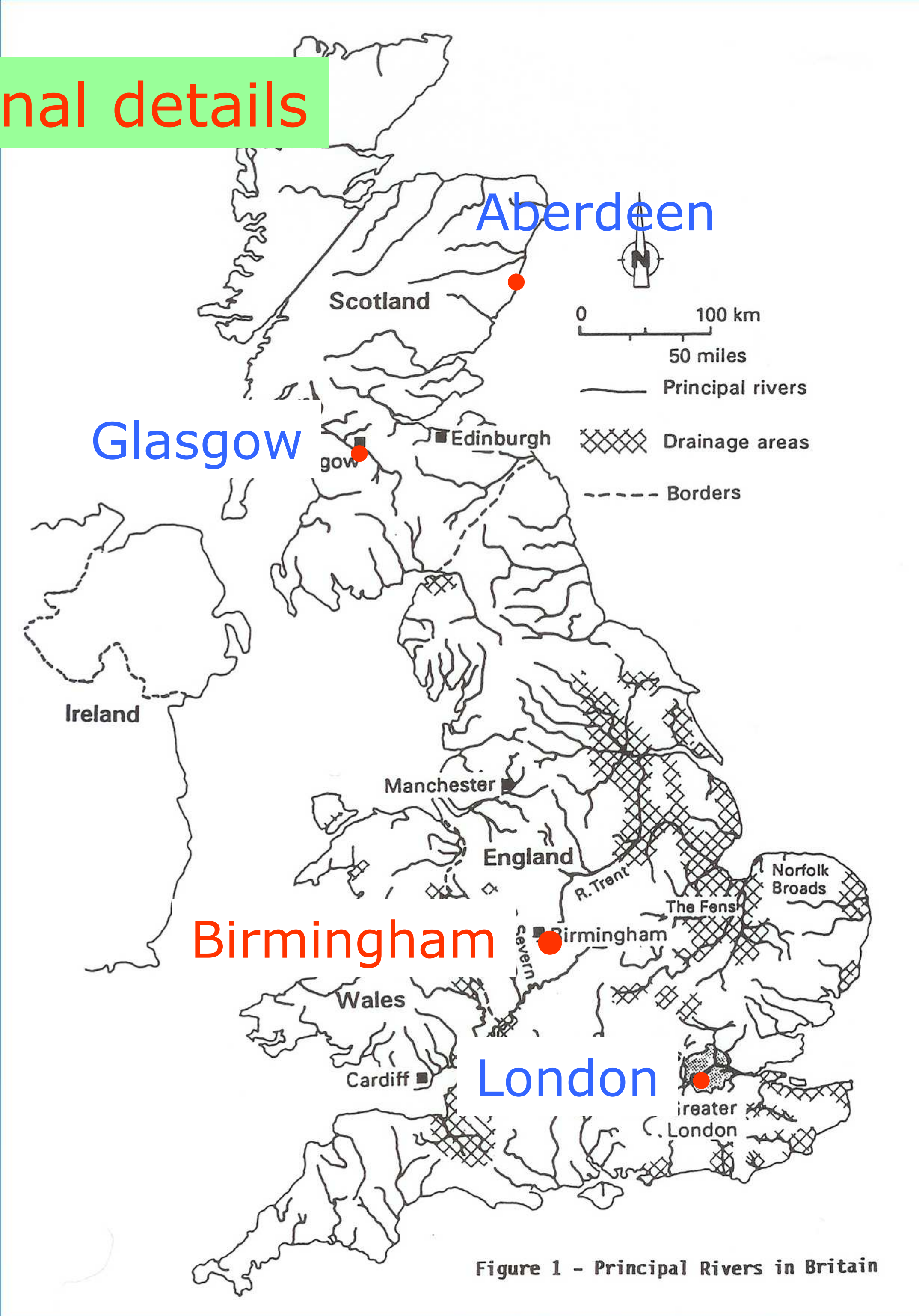

1965-68
PhD at
Aberdeen University

1963-65
Hydraulics research
London & Glasgow

1968
Lecturer at
Birmingham

1960-63
Undergraduate at
Imperial College

Outline of presentation

1. Floods and disaster management
2. What are some of the problems in modelling flows in rivers?
3. General approach to solving problems
4. Constructing a model
5. Testing a theoretical model
6. Using a model in practice
7. Conclusions

Knight, D.W. and Samuels, P.G., 2007, Examples of recent floods in Europe, *Journal of Disaster Research*, Fuji Technology Press, Tokyo, Japan, Vol. 2, No. 3, 190-199.

Examples of rivers in flood – and the damage they cause

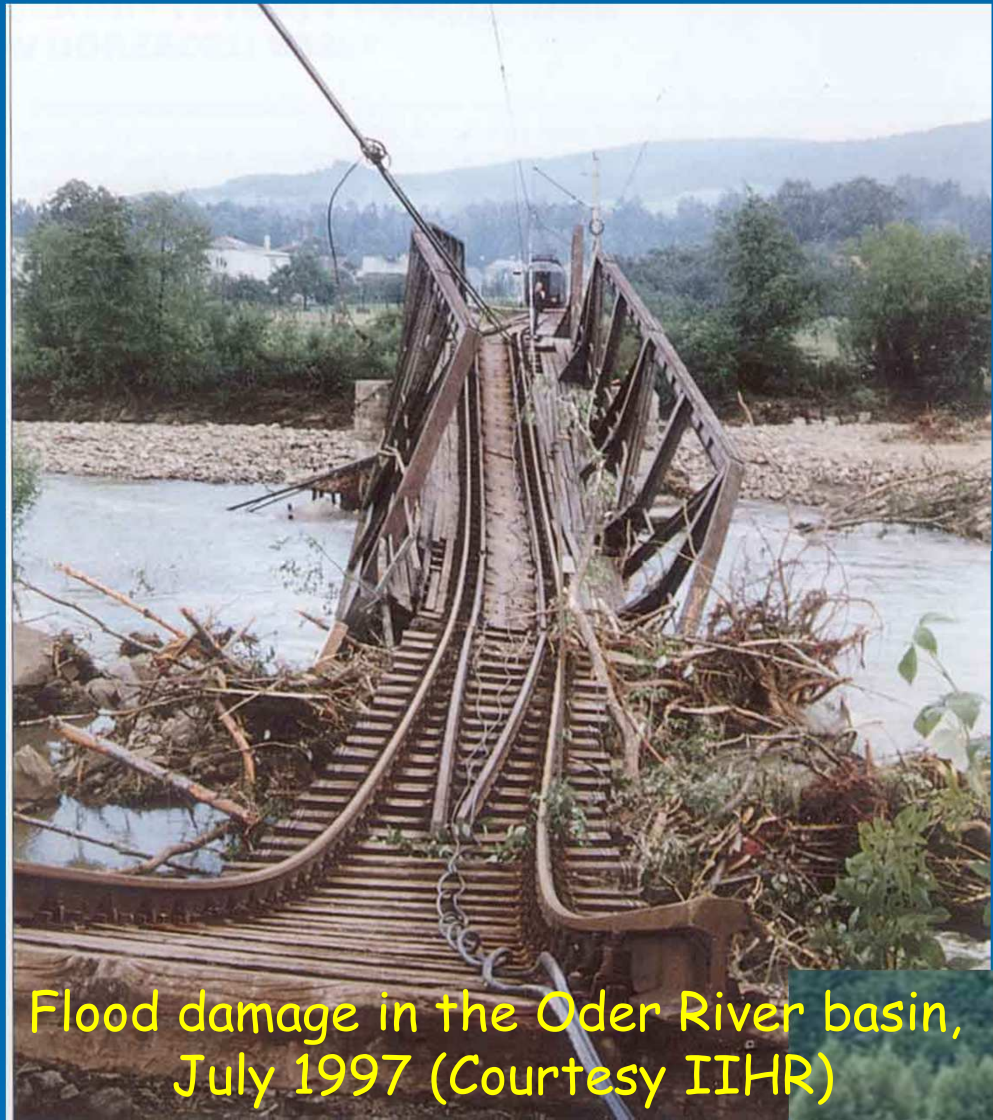

Flood damage in the Oder River basin,
July 1997 (Courtesy IIHR)

110 people died, 200,000 were evacuated and the economic loss was ~ $3bn

Poland, 1997
River Odra,

China, 2006

China, 2006

Disaster “La Josefina”

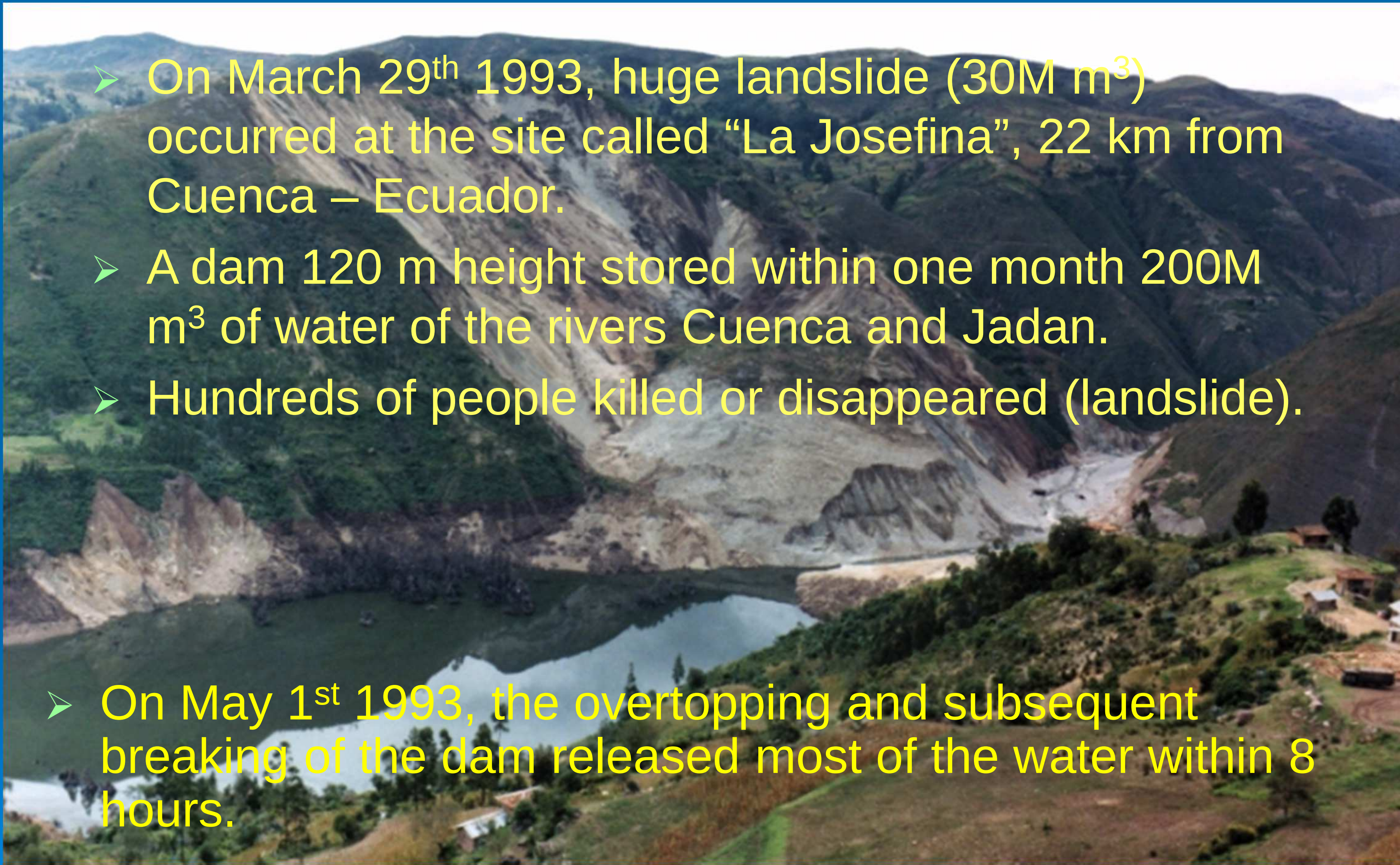

- On March 29th 1993, huge landslide (30M m^3) occurred at the site called “La Josefina”, 22 km from Cuenca – Ecuador.
- A dam 120 m height stored within one month 200M m^3 of water of the rivers Cuenca and Jadan.
- Hundreds of people killed or disappeared (landslide).
- On May 1st 1993, the overtopping and subsequent breaking of the dam released most of the water within 8 hours.

Disaster "La Josefina": Hydrograph

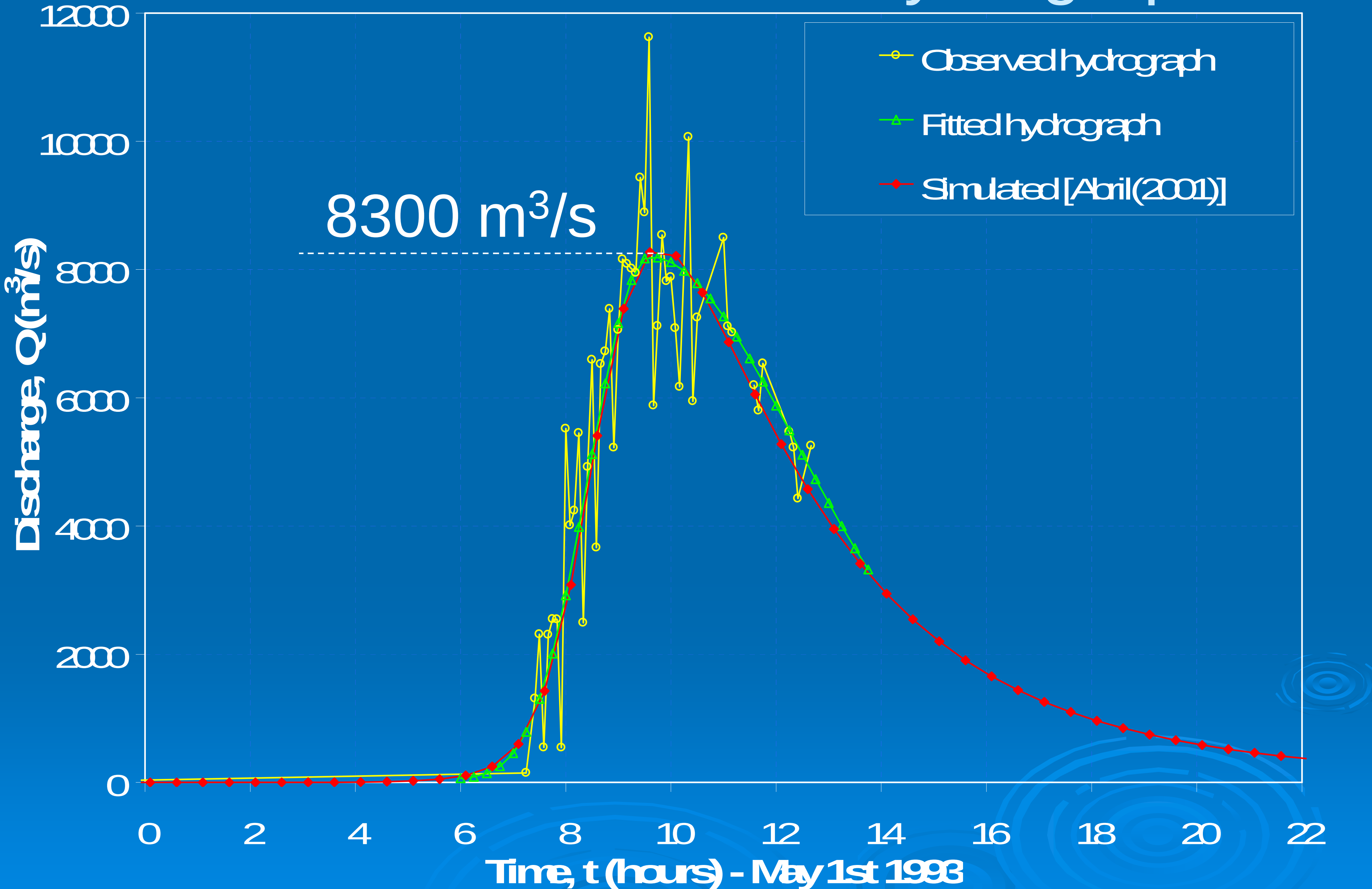

Morphologic changes: factors

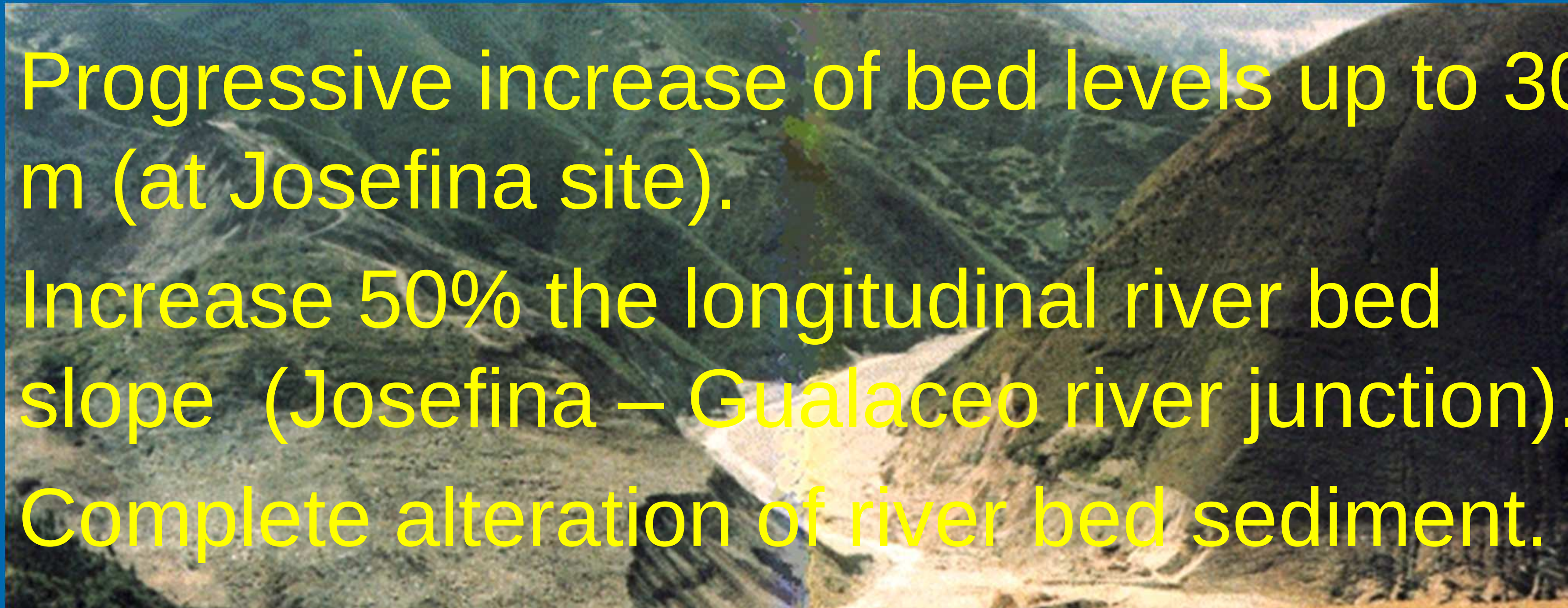

- Progressive increase of bed levels up to 30 m (at Josefina site).
- Increase 50% the longitudinal river bed slope (Josefina – Gualaceo river junction).
- Complete alteration of river bed sediment.

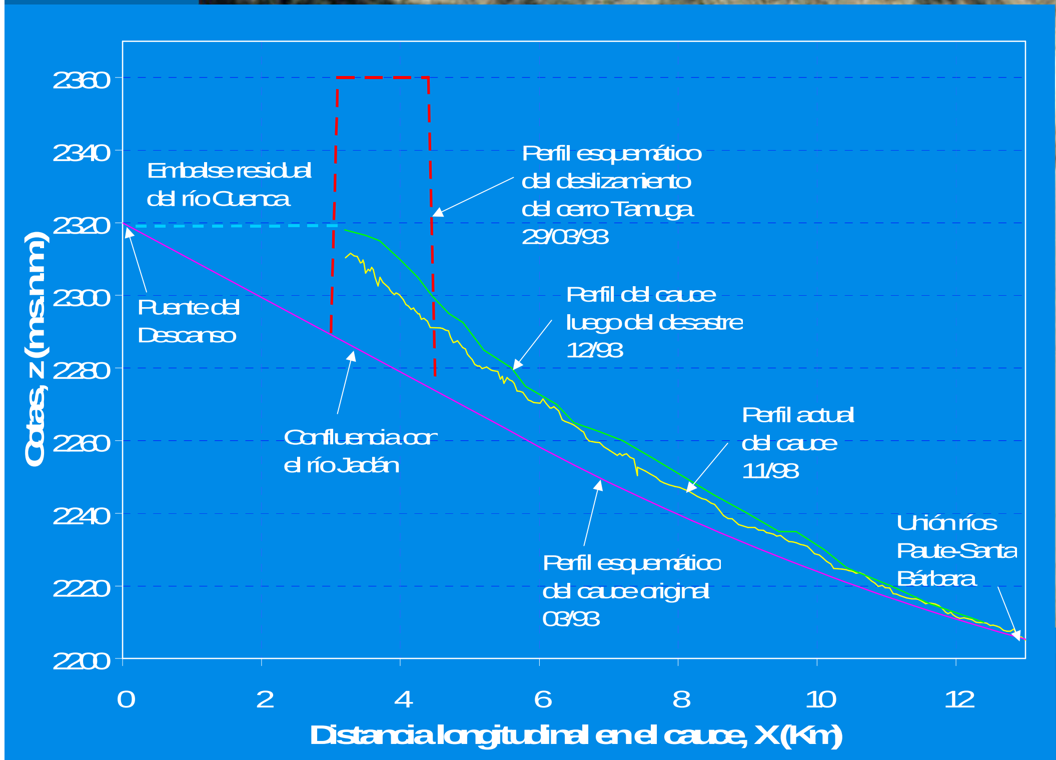

Morphologic changes: Sedimentation

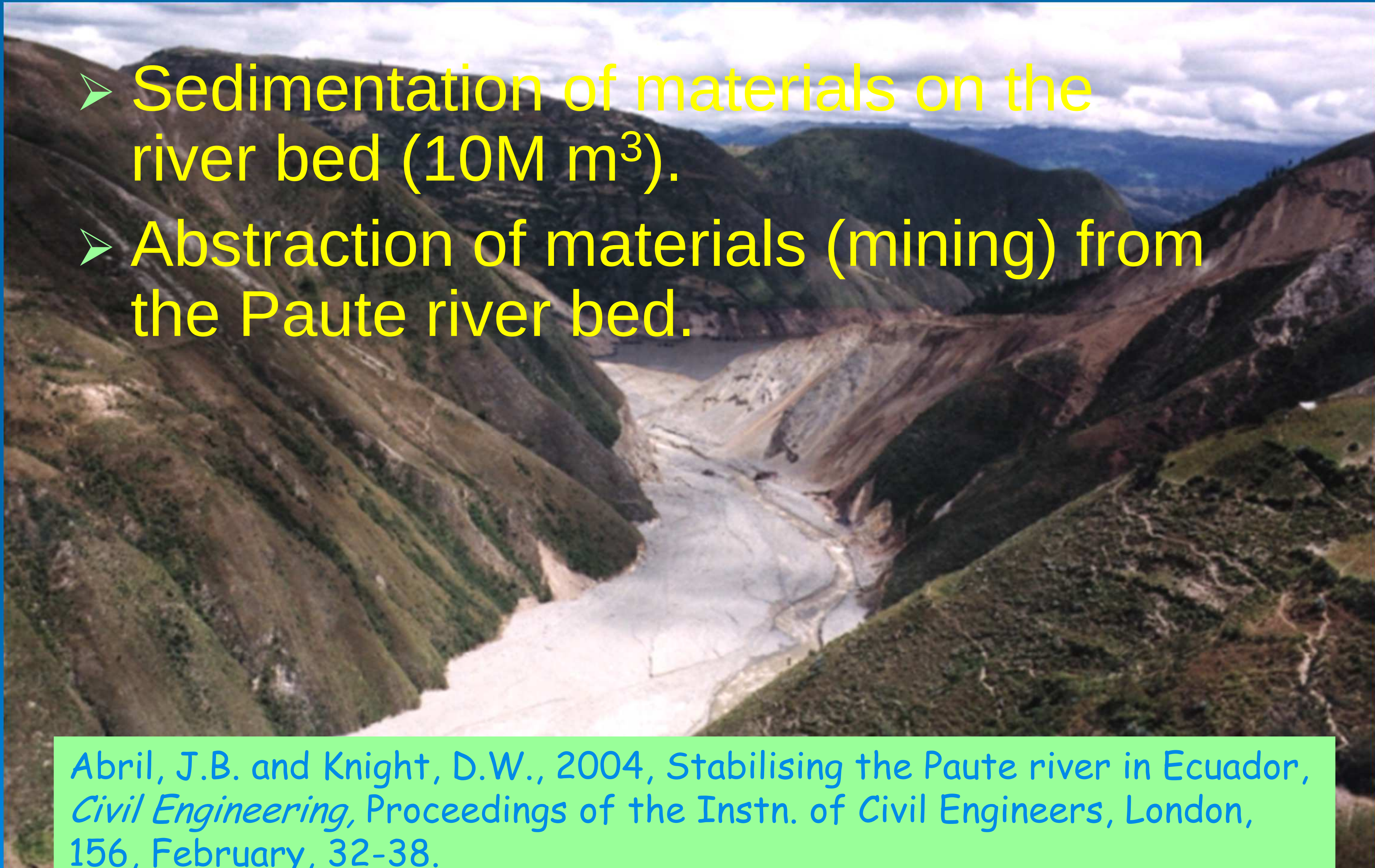

- Sedimentation of materials on the river bed (10M m^3).
- Abstraction of materials (mining) from the Paute river bed.

Abril, J.B. and Knight, D.W., 2004, Stabilising the Paute river in Ecuador, *Civil Engineering,* Proceedings of the Instn. of Civil Engineers, London, 156, February, 32-38.

2. What are some of the problems in modelling flows in rivers?

THE UNIVERSITY OF BIRMINGHAM

2.1 High discharges

2.2 Channel geometry and roughness

2.3 Unsteadiness in flow

2.4 Data for model calibration

International School of Hydraulics
May 2012
Lochow, Poland

Q1. How does one predict the stage-discharge relationship at a gauging station?

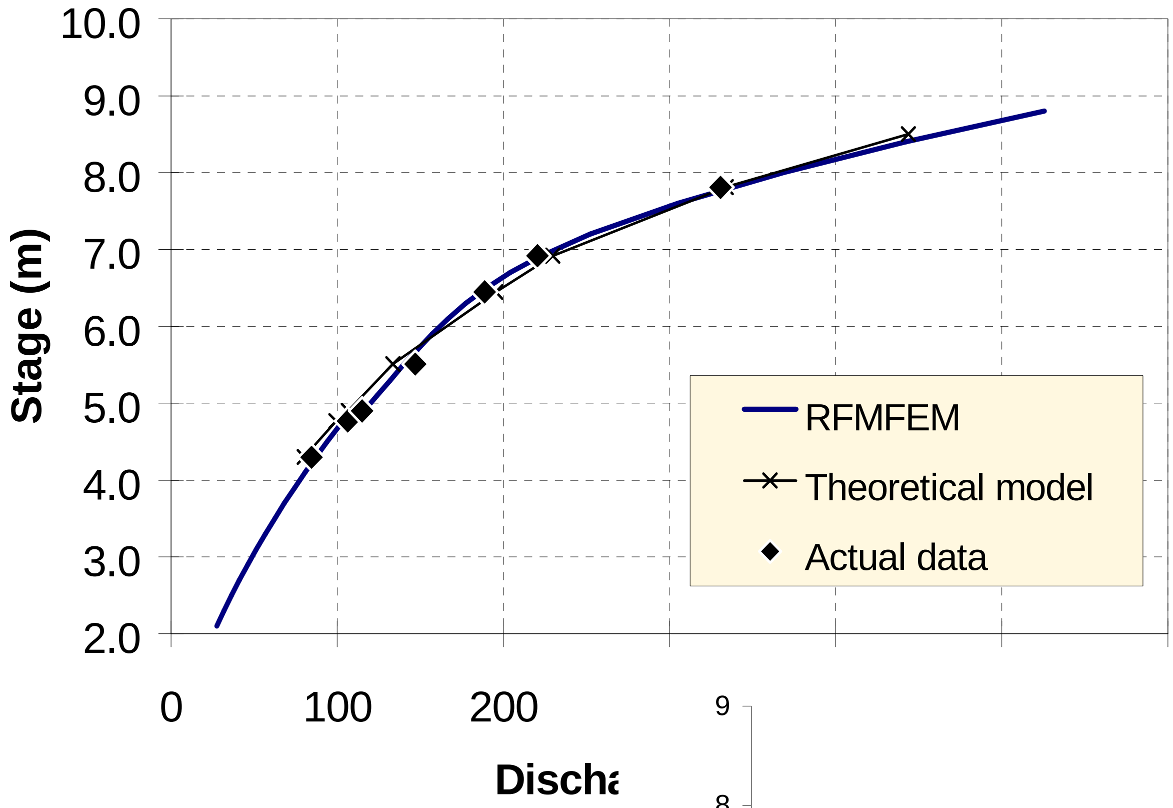

River Sev

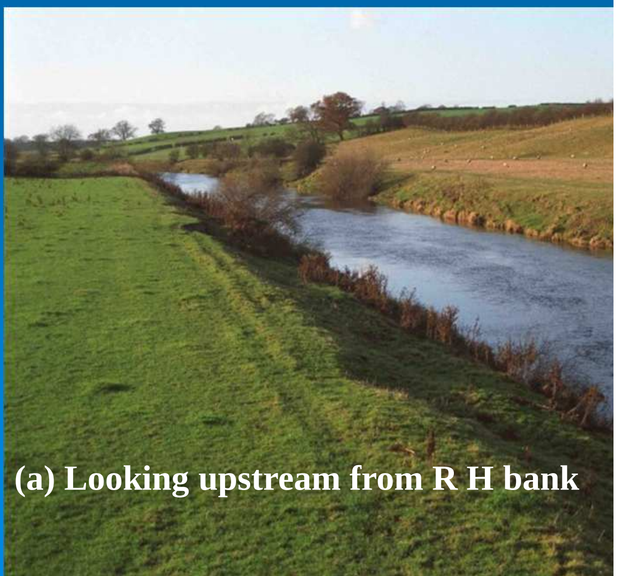

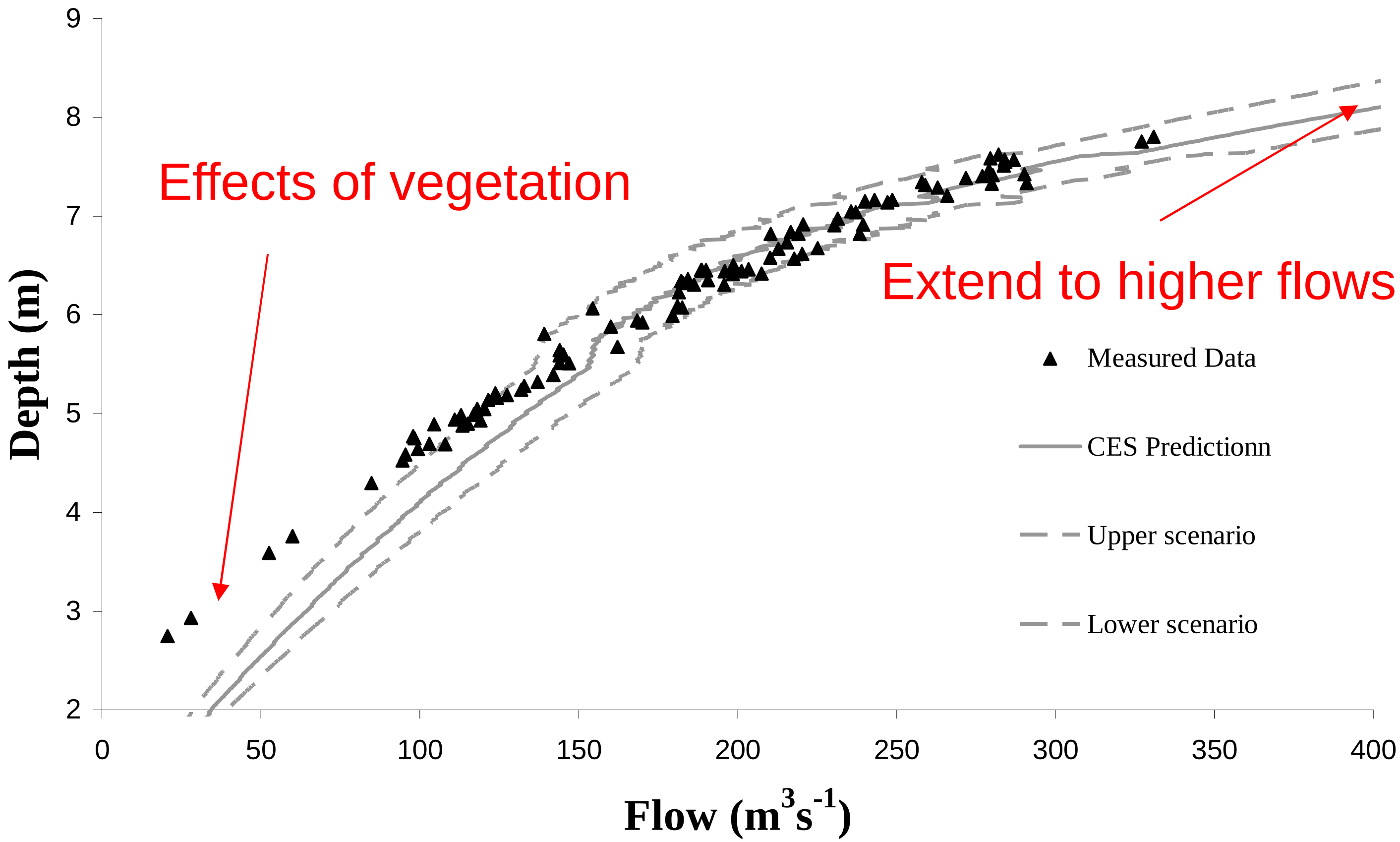

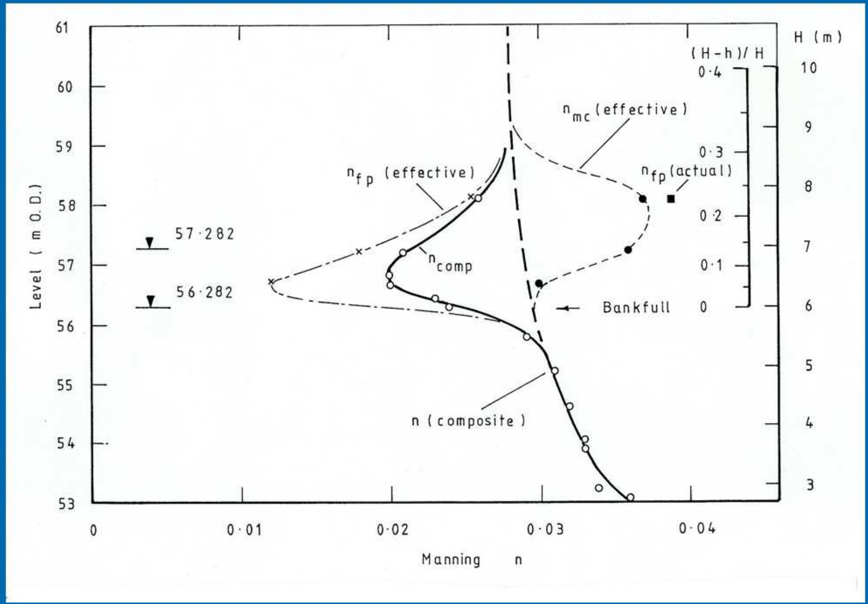

Fig. 1 Variation of overall and zonal Manning's *n* values with depth for overbank flow in the River Severn at Montford bridge

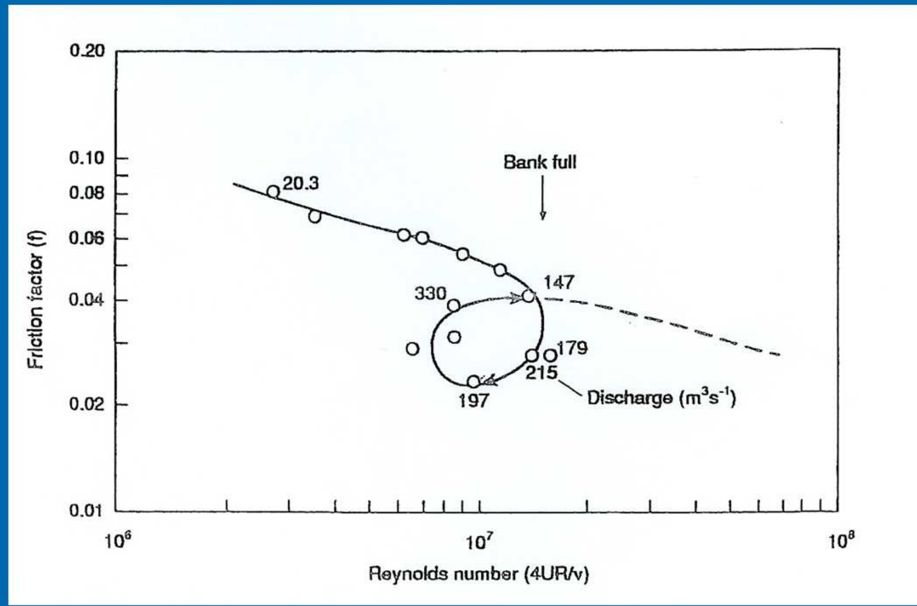

Fig. 2 Variation of overall, *f*, with *Re* for River Severn for Q = 20.3 to 330m^3s^{-1}, showing transition from inbank to overbank flows (bankfull, *Q*b = 170m3s-1)

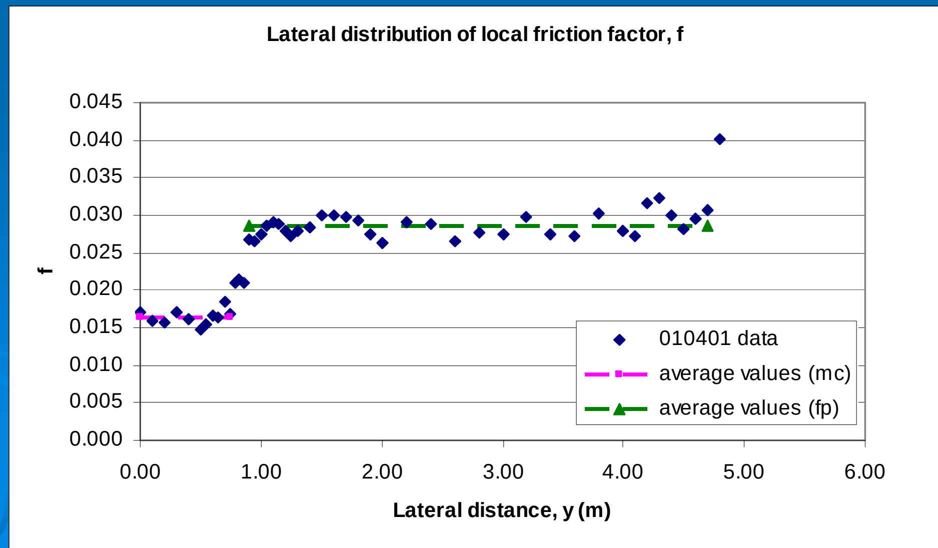

Fig. 3 Lateral variation of local friction factors: main channel (mc) to floodplain (fp)

Definition of friction factors

$$\tau_o = \left(\frac{f}{8}\right)\rho U_A^2$$

global
(1-D models)

$$\tau_z = \left(\frac{f_z}{8}\right)\rho U_z^2$$

zonal/sub-area
(1-D models)

$$\tau_b = \left(\frac{f_b}{8}\right)\rho U_d^2$$

depth-averaged
(2-D models)

τ_b = function of k_s or surface roughness

local
(3-D models)

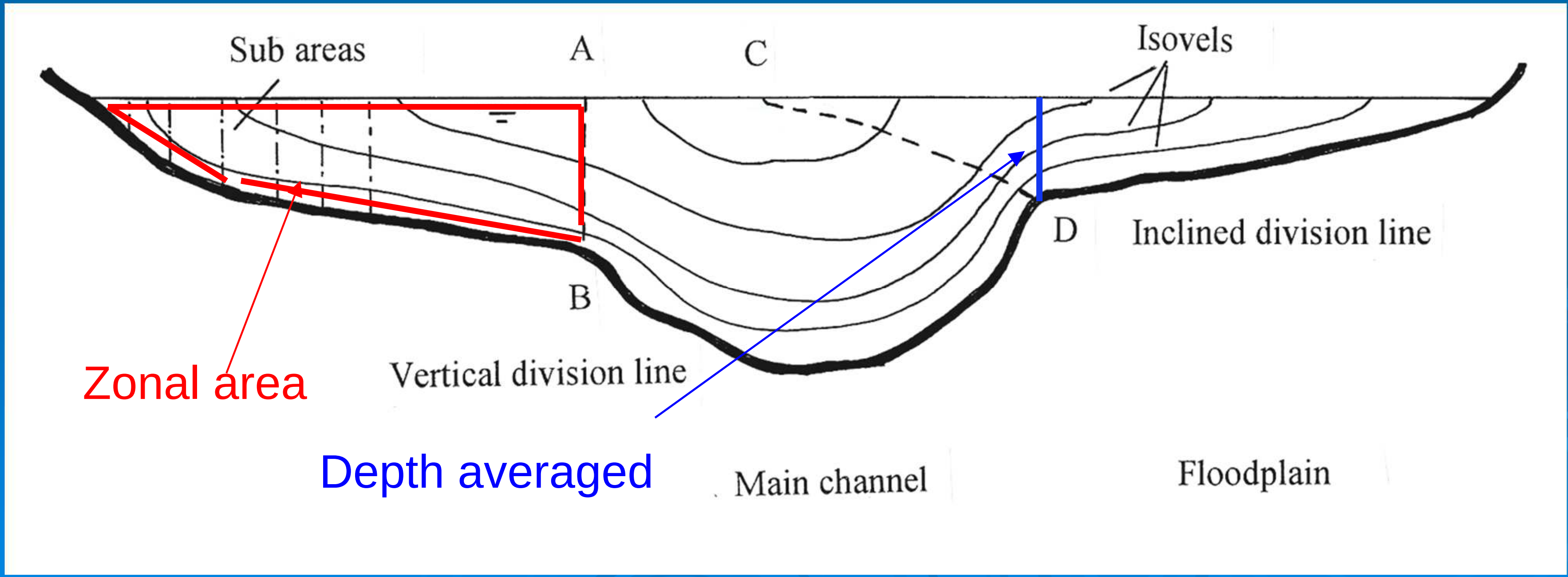

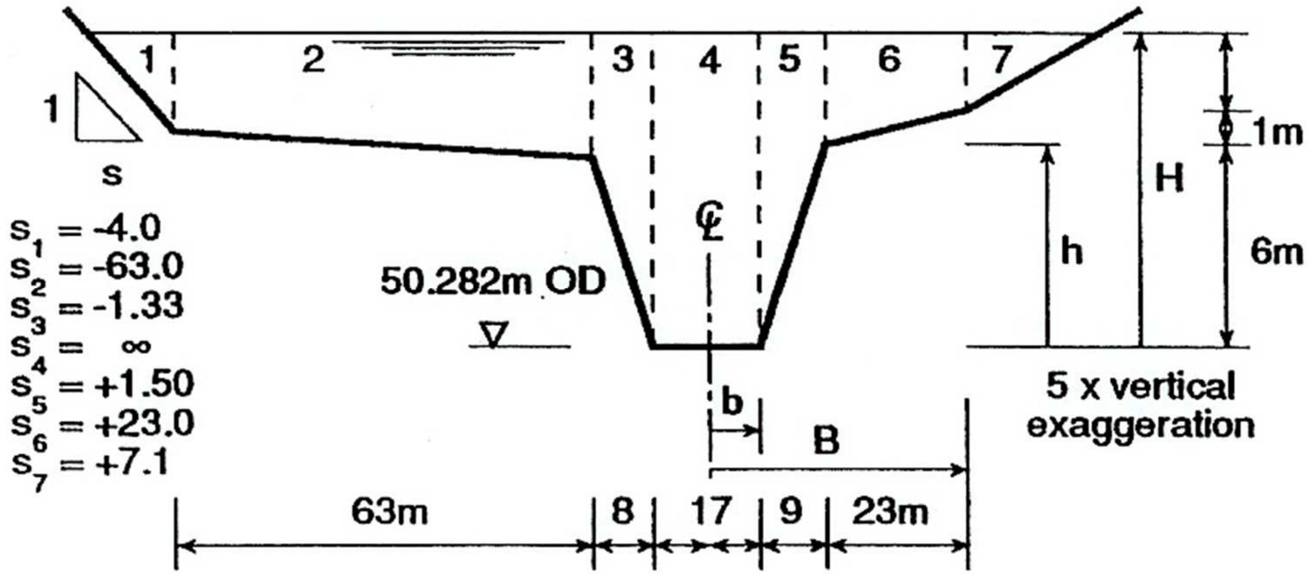

Cross-section of River Severn at Montford bridge
(Knight,Shiono & Pirt, 1989)

Geometric properties
(single section values)

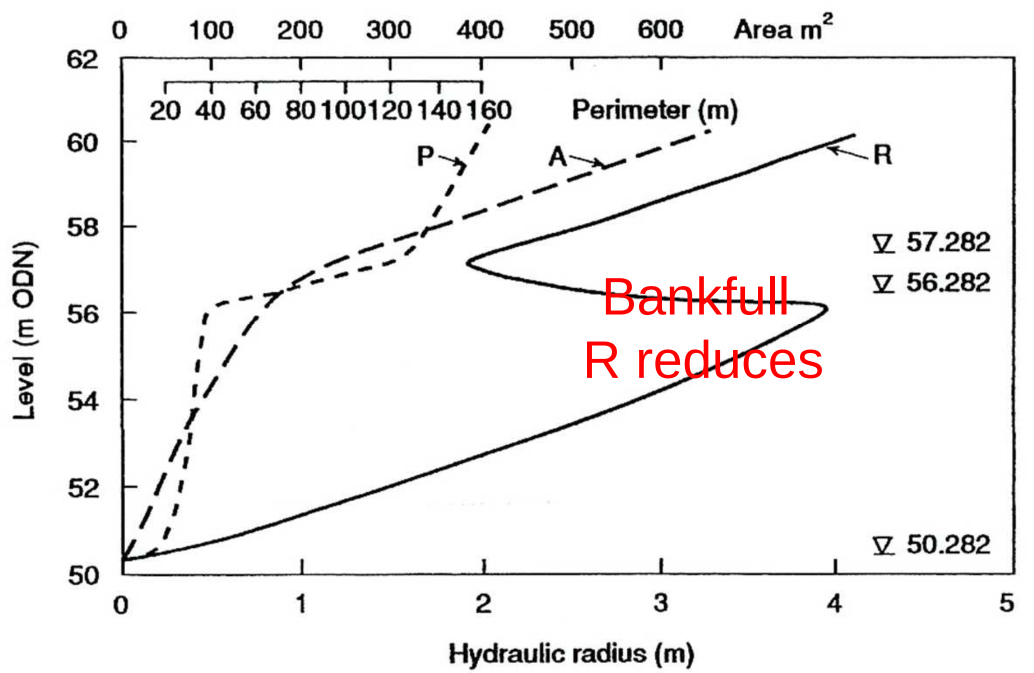

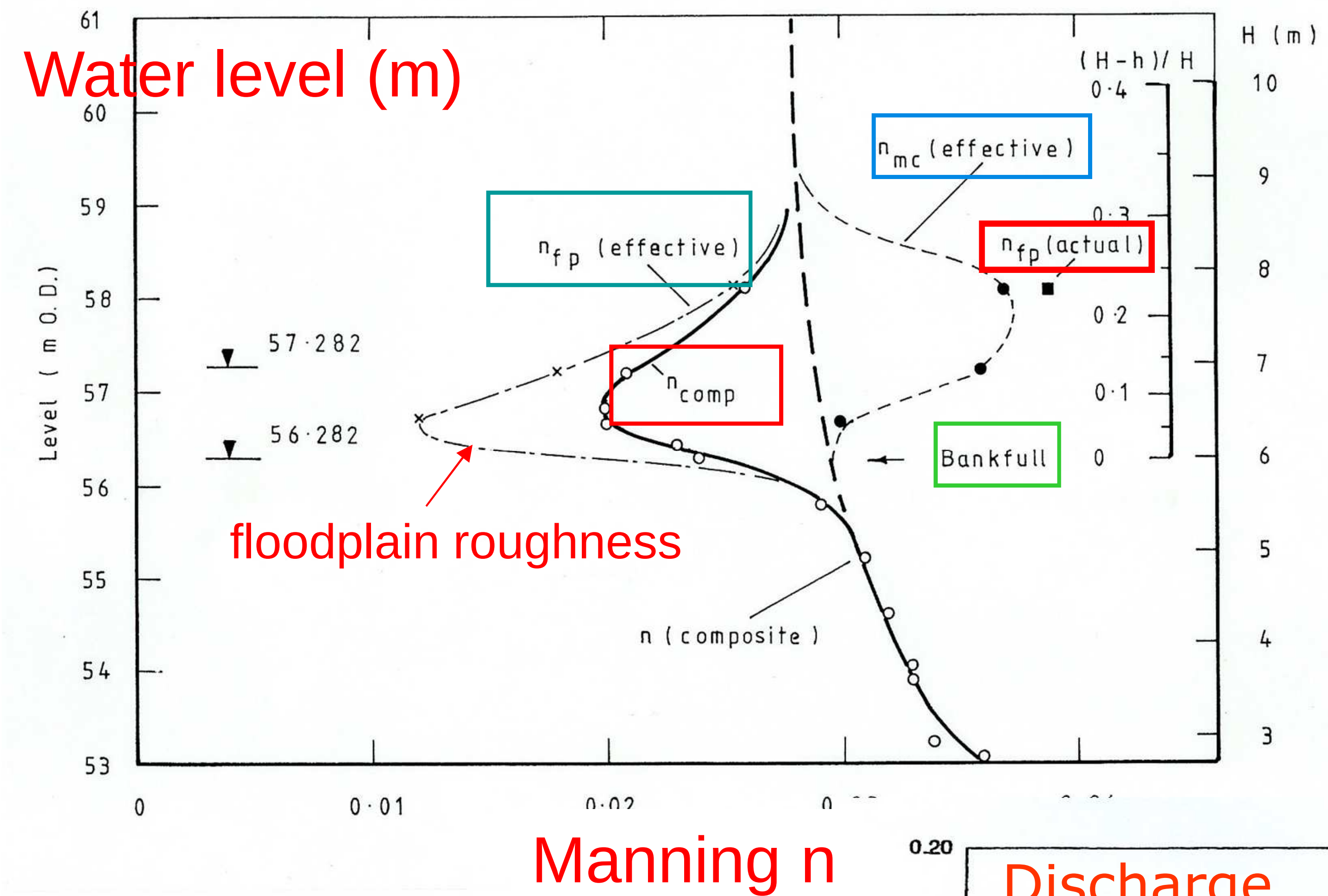

Variation of Manning n with water level

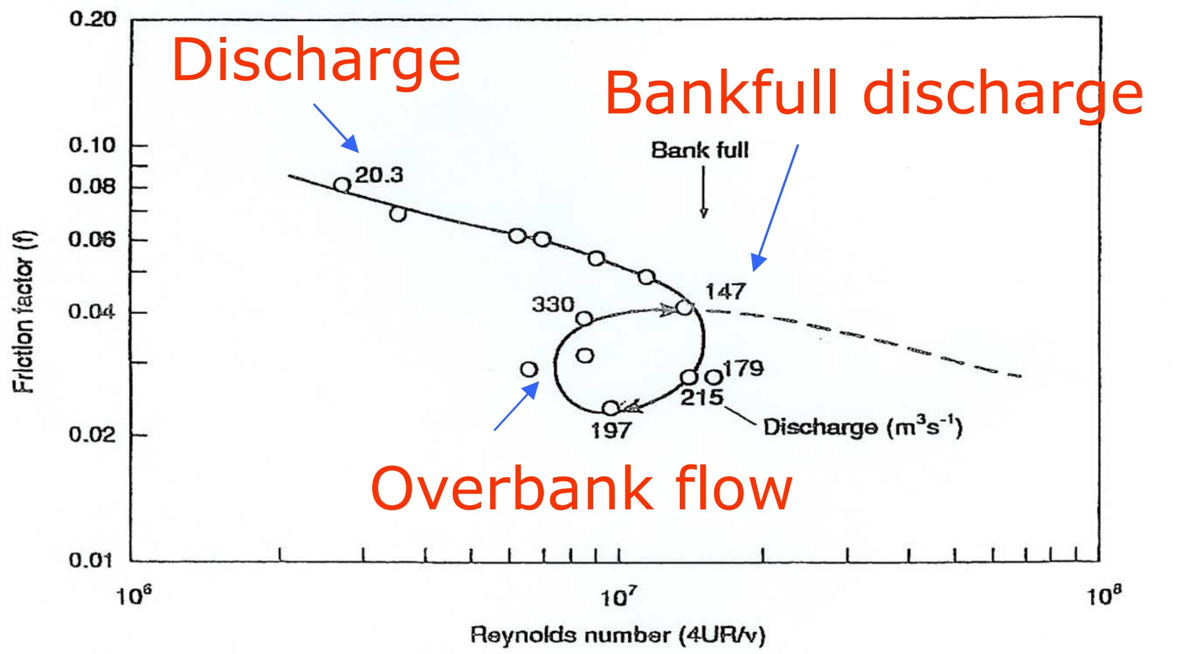

Variation of Darcy f with Reynolds number

Laboratory data

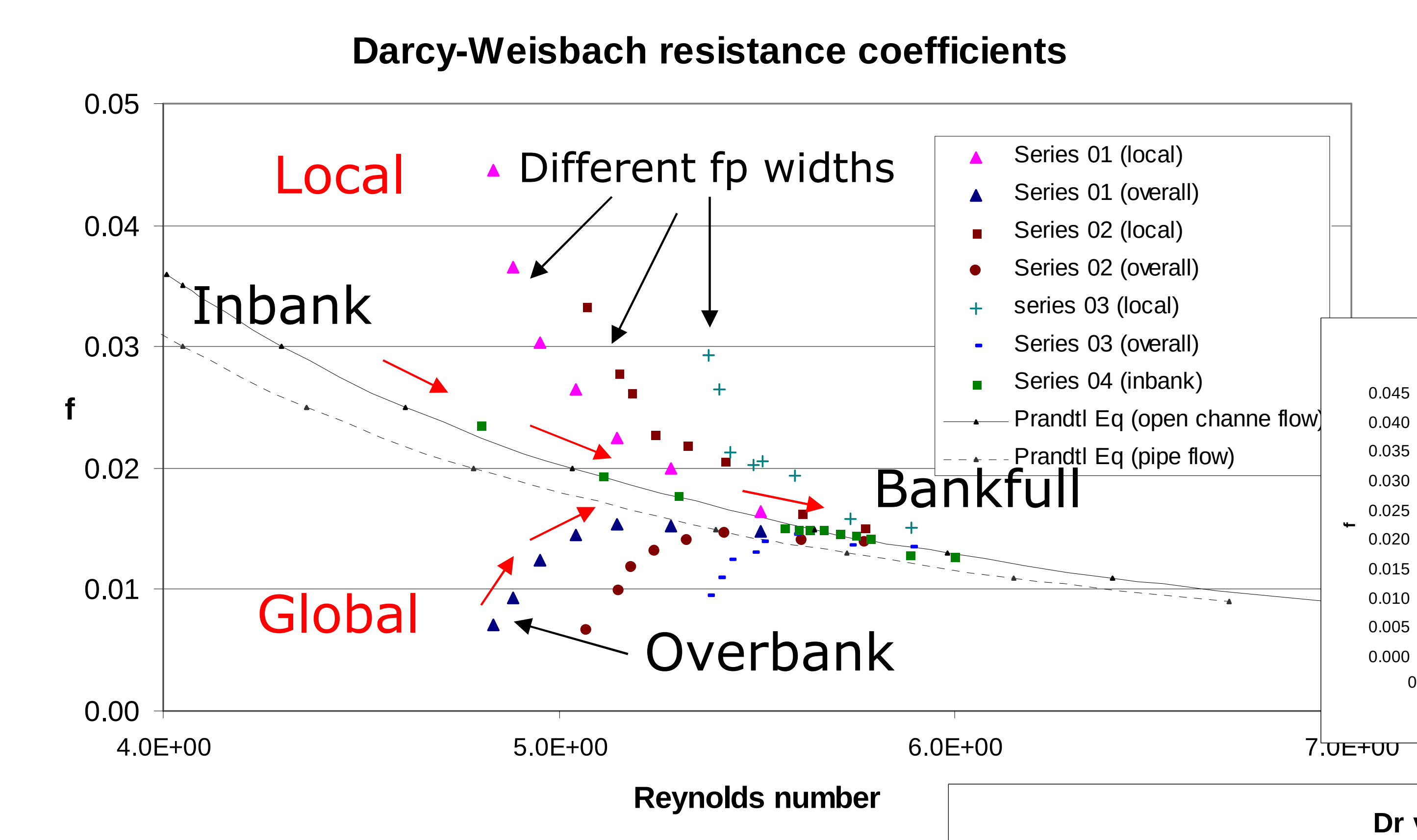

Fig. 4 Overall and local friction factors for FCF data (Series 01-04)

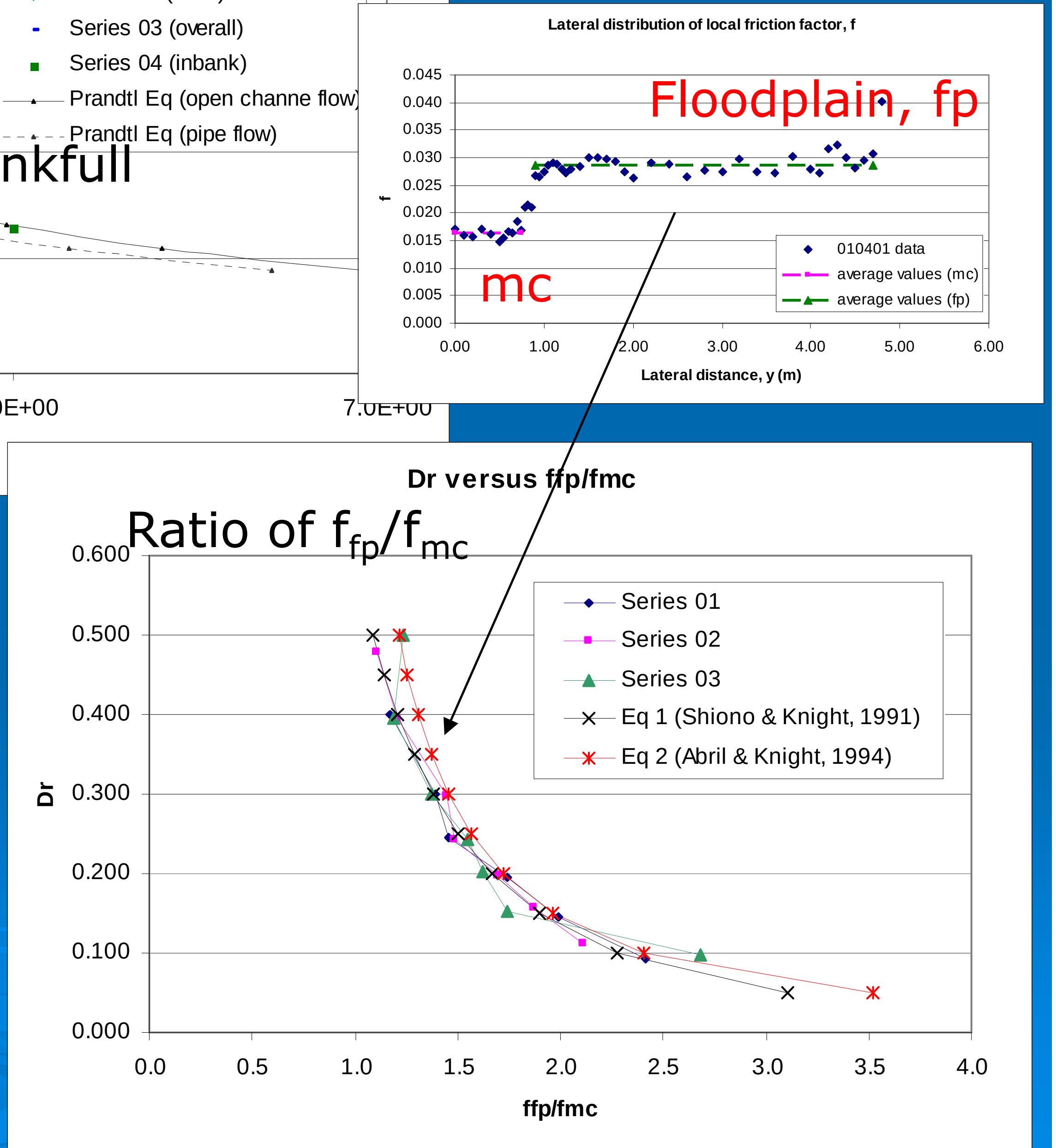

Fig. 5 Variation of local friction factors between the main channel and a floodplain with *Dr*

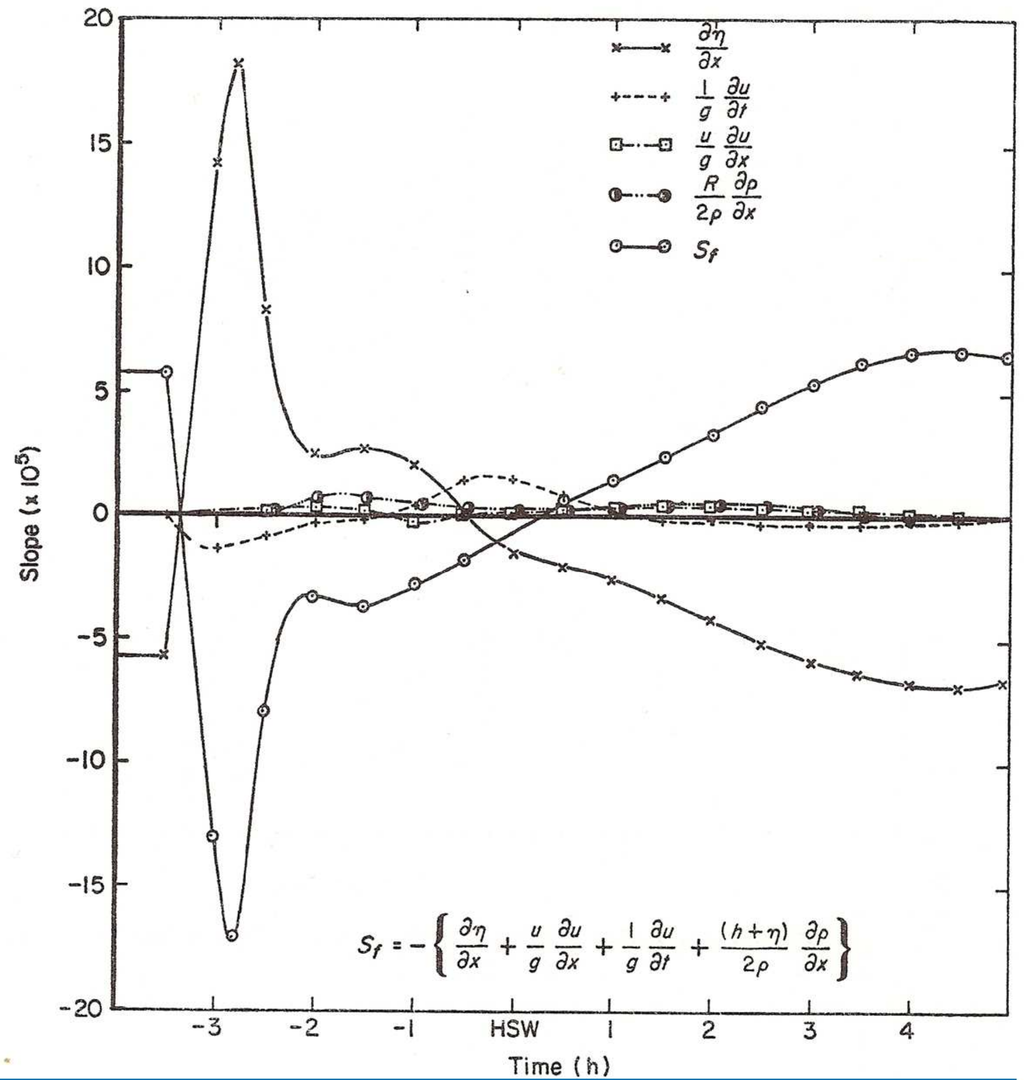

Fig. 6 Resistance data for Conwy estuary showing terms in the 1-D St Venant eq. (after Knight, 1981)

N.B. Slope = 1 x 10^{-5}, so over 1km, water surface difference is ~ 20-200mm. Great accuracy is required

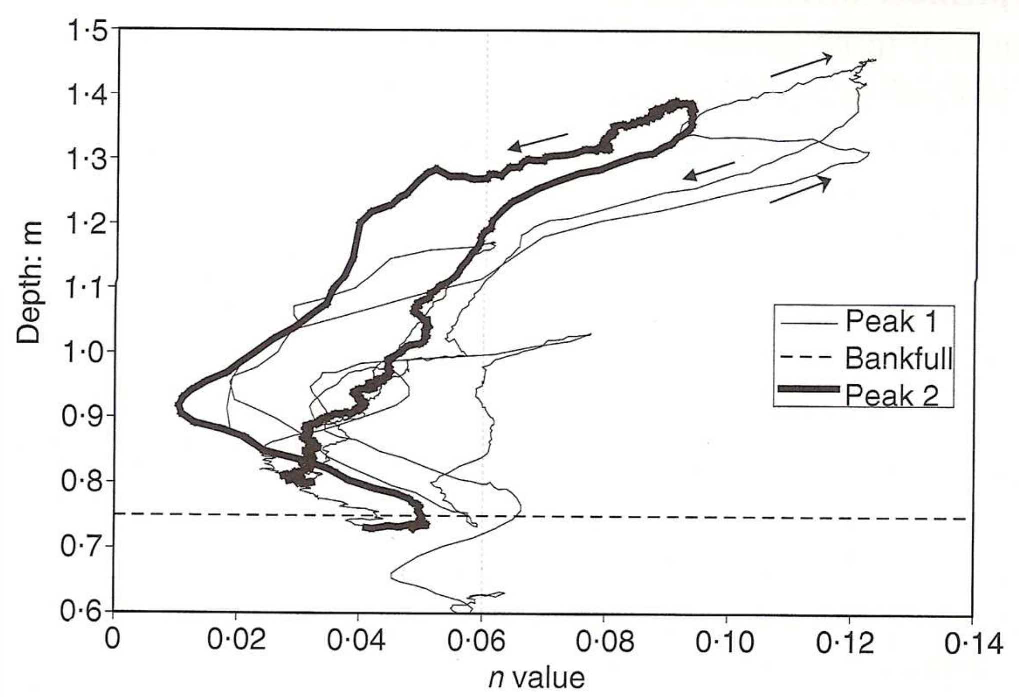

Fig. 7 Looped resistance relationships for a two-stage channel with vegetated floodplains

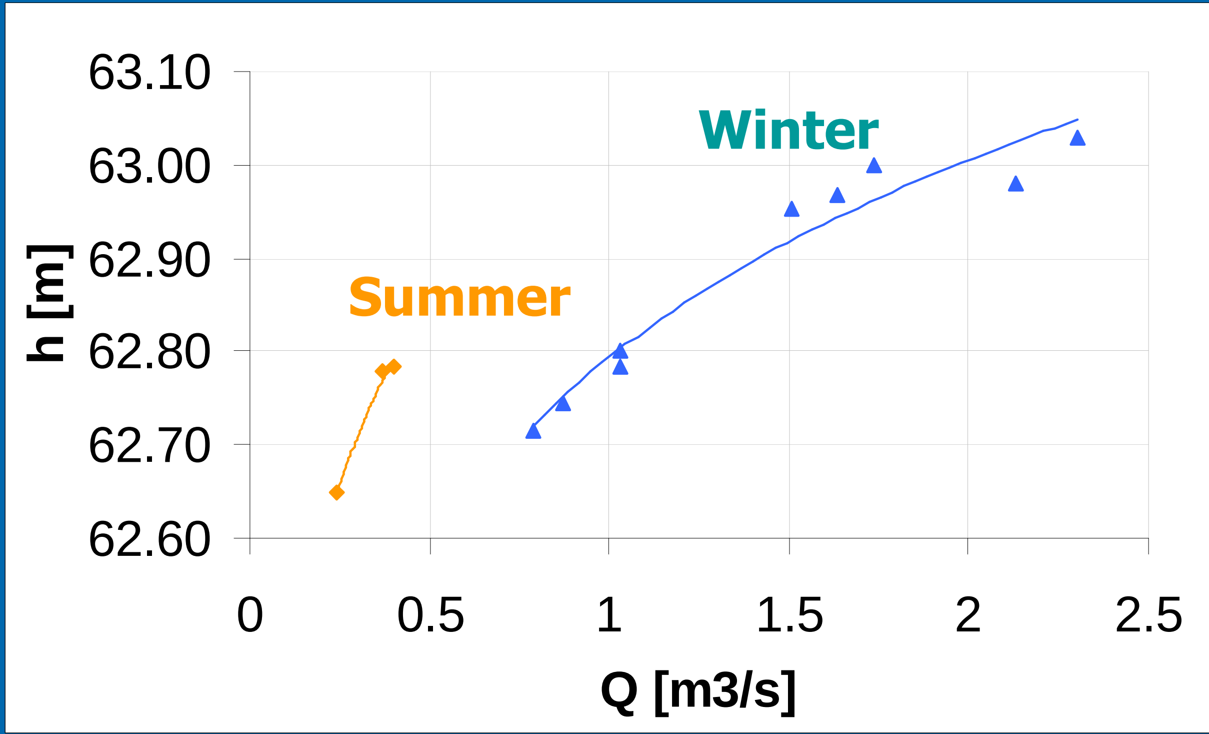

Stage-discharge relationship are often affected by seasonal growth of vegetation

River Blackwater, Hampshire, UK

3. General approach to solving problems

THE UNIVERSITY OF BIRMINGHAM

3.1 Defining the problem:

mathematically, equations, gaps, key fudges, review of literature

3.2 Acquiring data:

assess any primary data oneself, obtain field & laboratory data,

design apparatus with errors in mind, set rigorous procedures

fully developed uniform flow,

collaborative experimental work

3.3 Recognising physical and theoretical concepts

over …

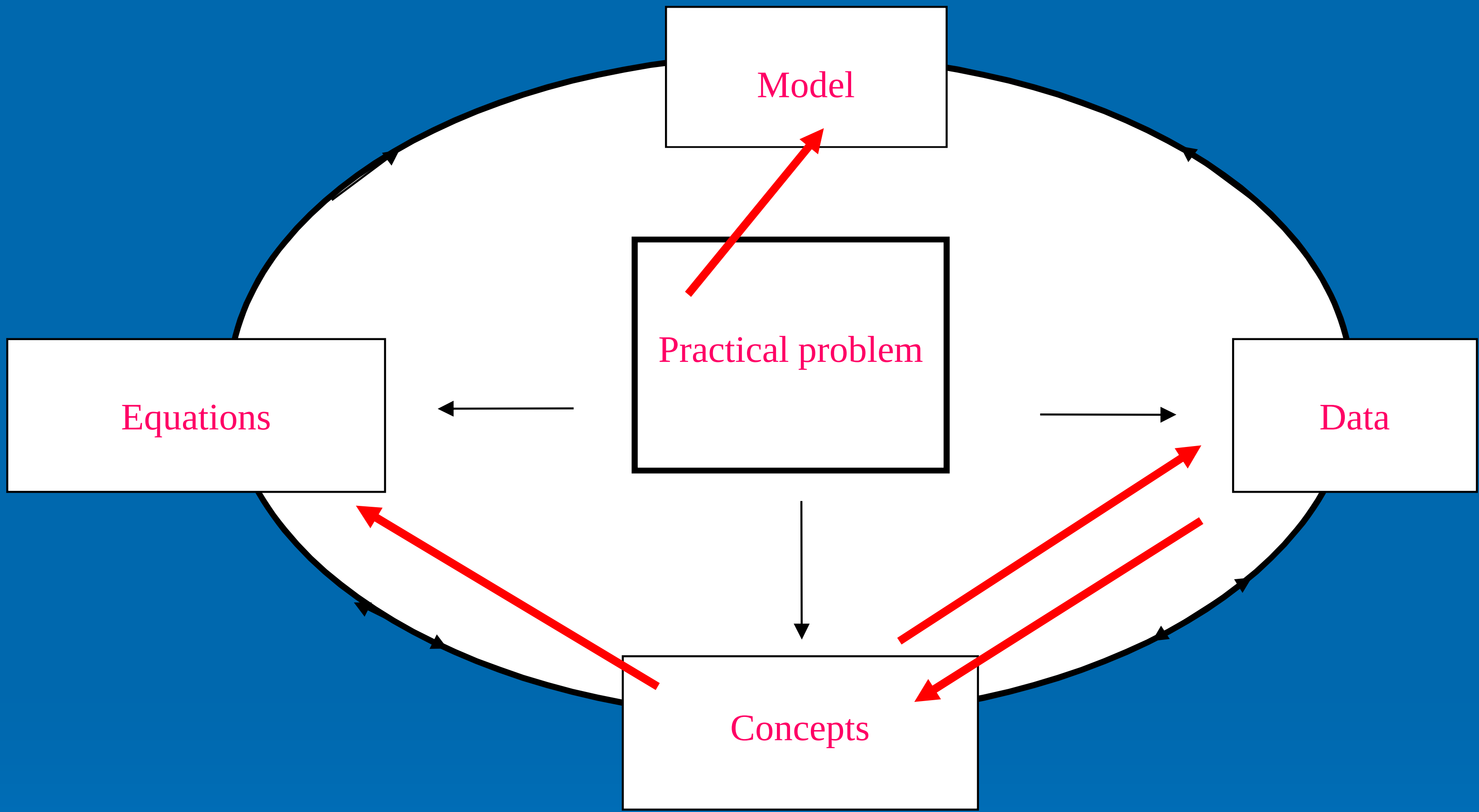

Fig. 8 Solving a practical problem - where to start?

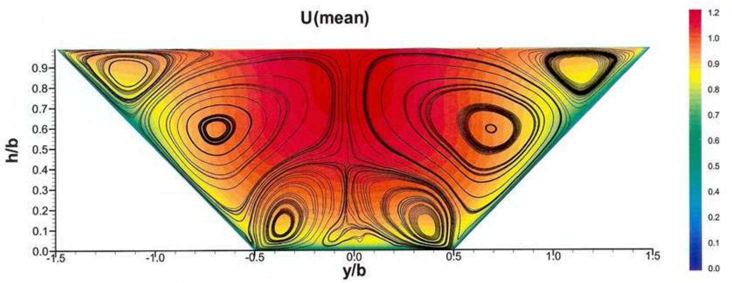

Figure 4. Streamlines from Thorsten's LES results.

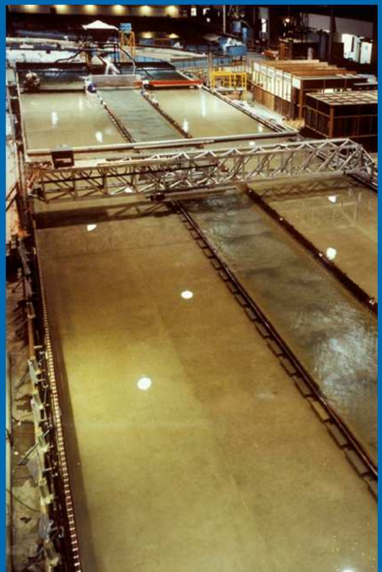

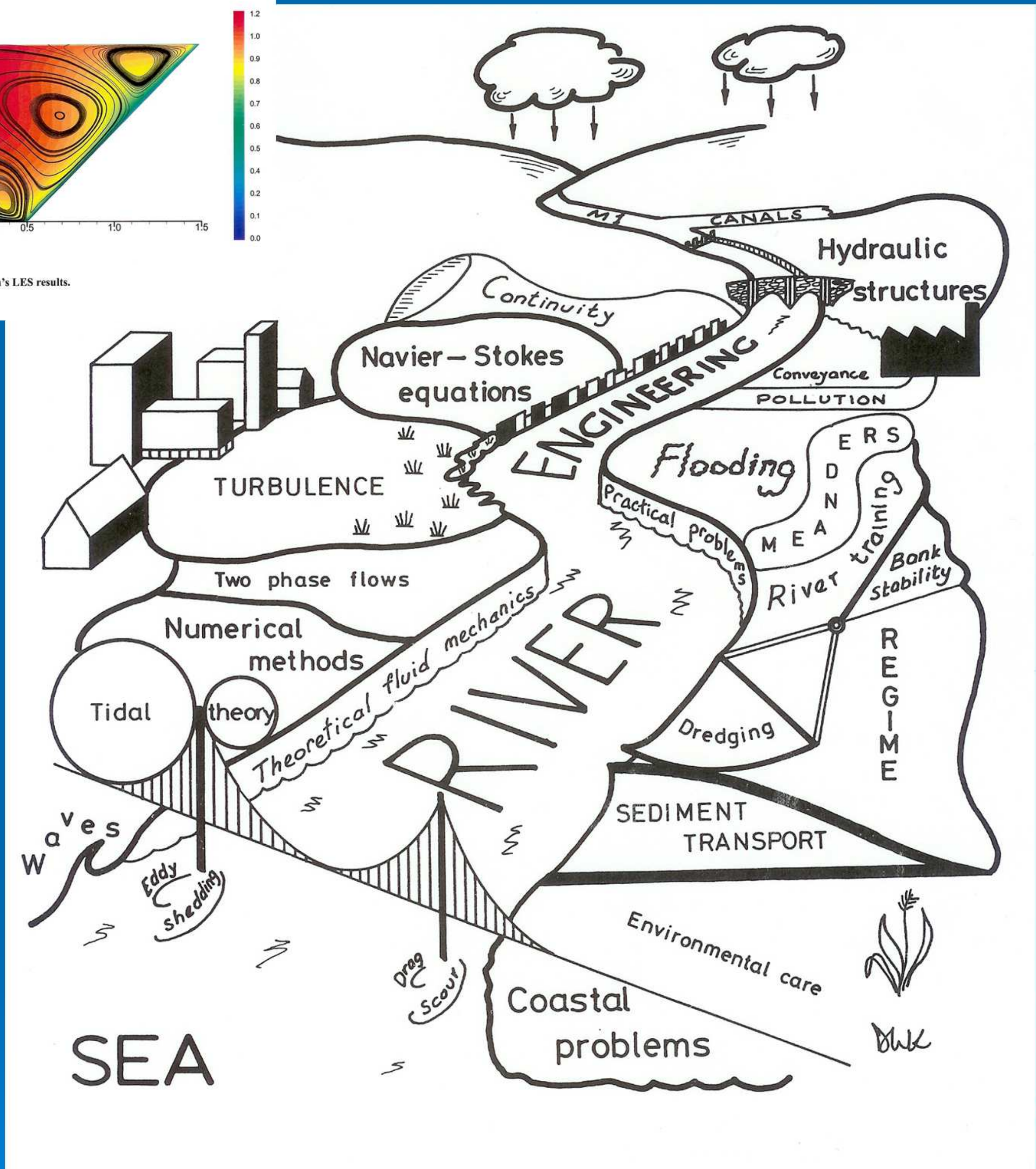

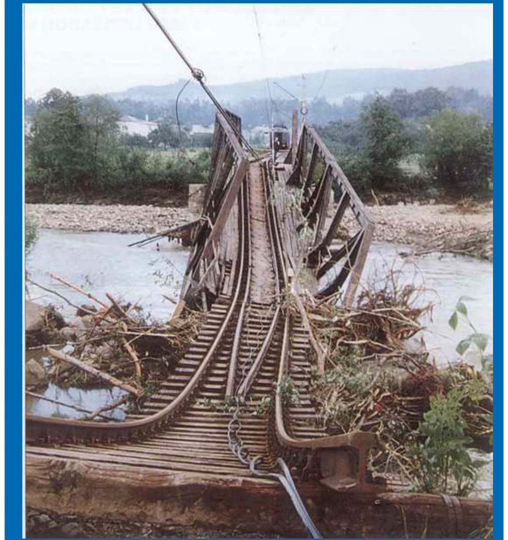

Fig. 9 The art and science of river engineering (after Knight) [reproduced from Nakato & Ettema, (1996), page 448]

4. Constructing a model

THE UNIVERSITY OF BIRMINGHAM

4.1 Getting the concepts

4.2 Defining the scope of the model

4.3 Defining the physical coefficients

4.4 Defining simple equations for the physical coefficients

International School of Hydraulics
May 2012
Lochow, Poland

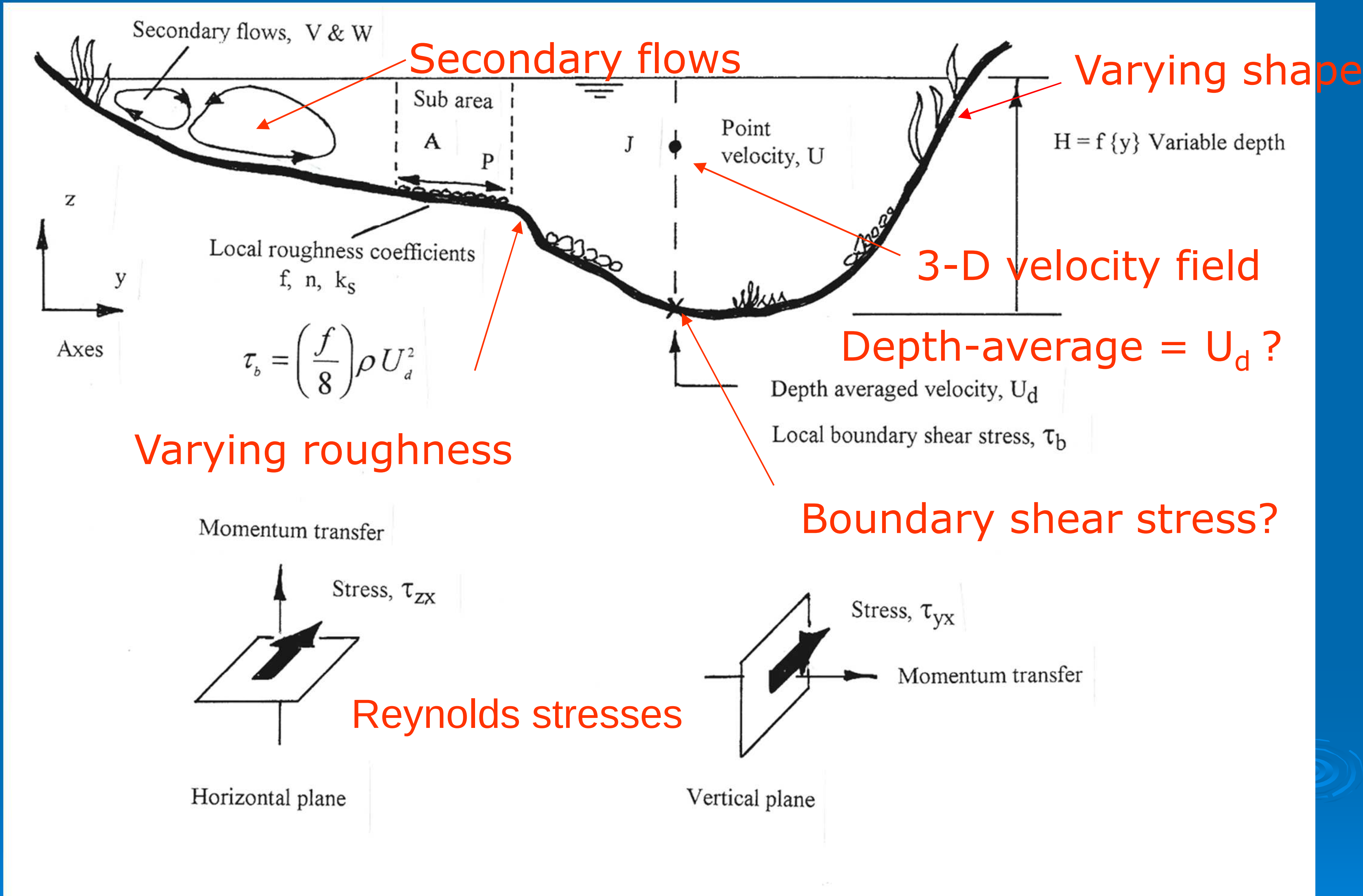

Conceptualized flow in a natural channel (by Knight & Shiono, 1996)

Reynolds-averaged Navier–Stokes equation at a point (streamwise direction)

$$\rho\left[\frac{\partial UV}{\partial y}+\frac{\partial UW}{\partial z}\right]=\rho g S_0+\frac{\partial}{\partial y}\left(-\rho\overline{uv}\right)+\frac{\partial}{\partial z}\left(-\rho\overline{uw}\right)$$

(I) (II) (III) (IV)

The physical meaning of the terms in the equation are:

(I) = secondary flow term (advective term)

(II) = weight component term

(III) = lateral gradient of Reynolds stress, τ_{yx} , on a vertical plane

(IV) = vertical gradient of Reynolds stress, τ_{zx}, on a horizontal plane

Depth-averaged form of the Navier–Stokes equation

$$\rho g H S_o - \tfrac{1}{8}\rho f U_d^2\left(1+\frac{1}{s^2}\right)^{1/2} + \frac{\partial}{\partial y}\left\{\rho\lambda H^2\left(\frac{f}{8}\right)^{1/2} U_d \frac{\partial U_d}{\partial y}\right\} = \frac{\partial}{\partial y}\left[H(\rho UV)_d\right]$$

where $$U_d = \frac{1}{H}\int_0^H U\,dz$$ Depth –averaged velocity

$$\tau_b = \left(\frac{f_b}{8}\right)\rho U_d^2$$ Boundary shear stress

$$\bar{\tau}_{yx} = \rho\bar{\varepsilon}_{yx}\frac{\partial U_d}{\partial y}$$

$$\bar{\varepsilon}_{yx} = \lambda U_* H$$

Depth-averaged Reynolds shear stress

$$\frac{\partial (H\rho UV)_d}{\partial y} = \Gamma$$ Secondary flow term

Equations for coefficients

Resistance

$$\frac{f}{f_{mc}} = 0.669 + 0.331 Dr^{-0.719}$$

Dimensionless eddy viscosity

$$\frac{\lambda}{\lambda_{mc}} = -0.20 + 1.20 Dr^{-1.44}$$

Secondary flow (advection) term

$$\Gamma^*_{mc} = \frac{\Gamma_{mc}}{H} = 0.15 \rho g S_o$$

$$\Gamma^*_{fp} = \frac{\Gamma_{fp}}{(H-h)} = -0.25 \rho g S_o$$

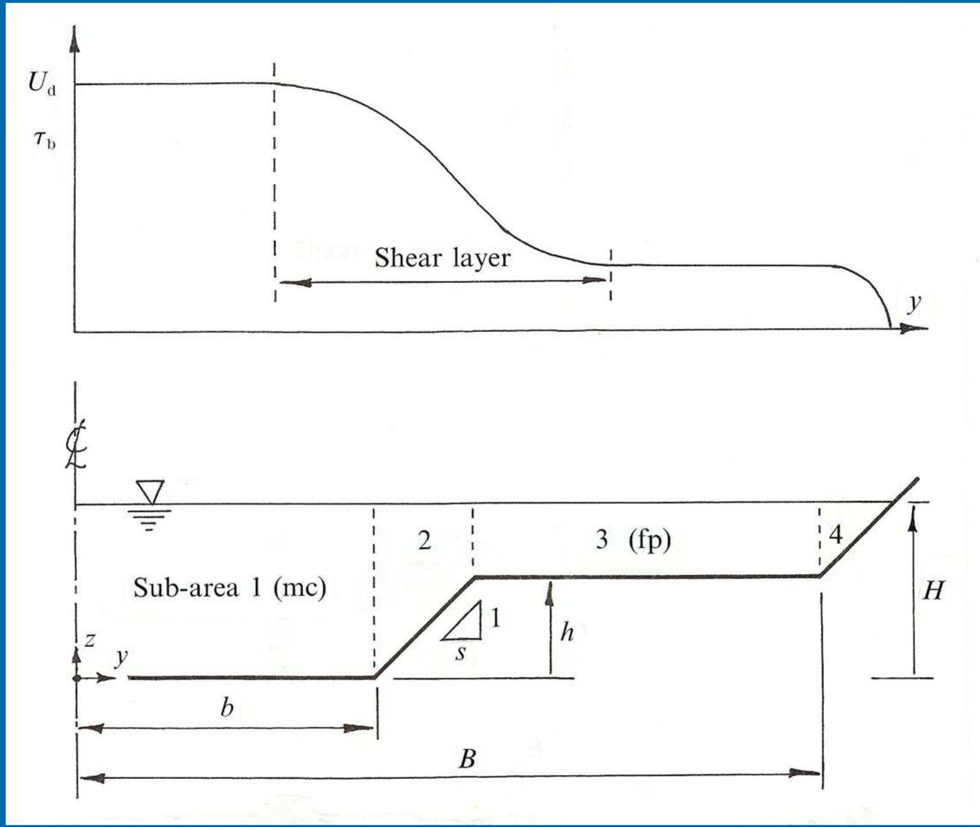

Fig. 10 Flood Channel Facility (FCF) notation

$$Dr = (H-h)/H$$

The data - for *Dr* = 0.5 to 0.05

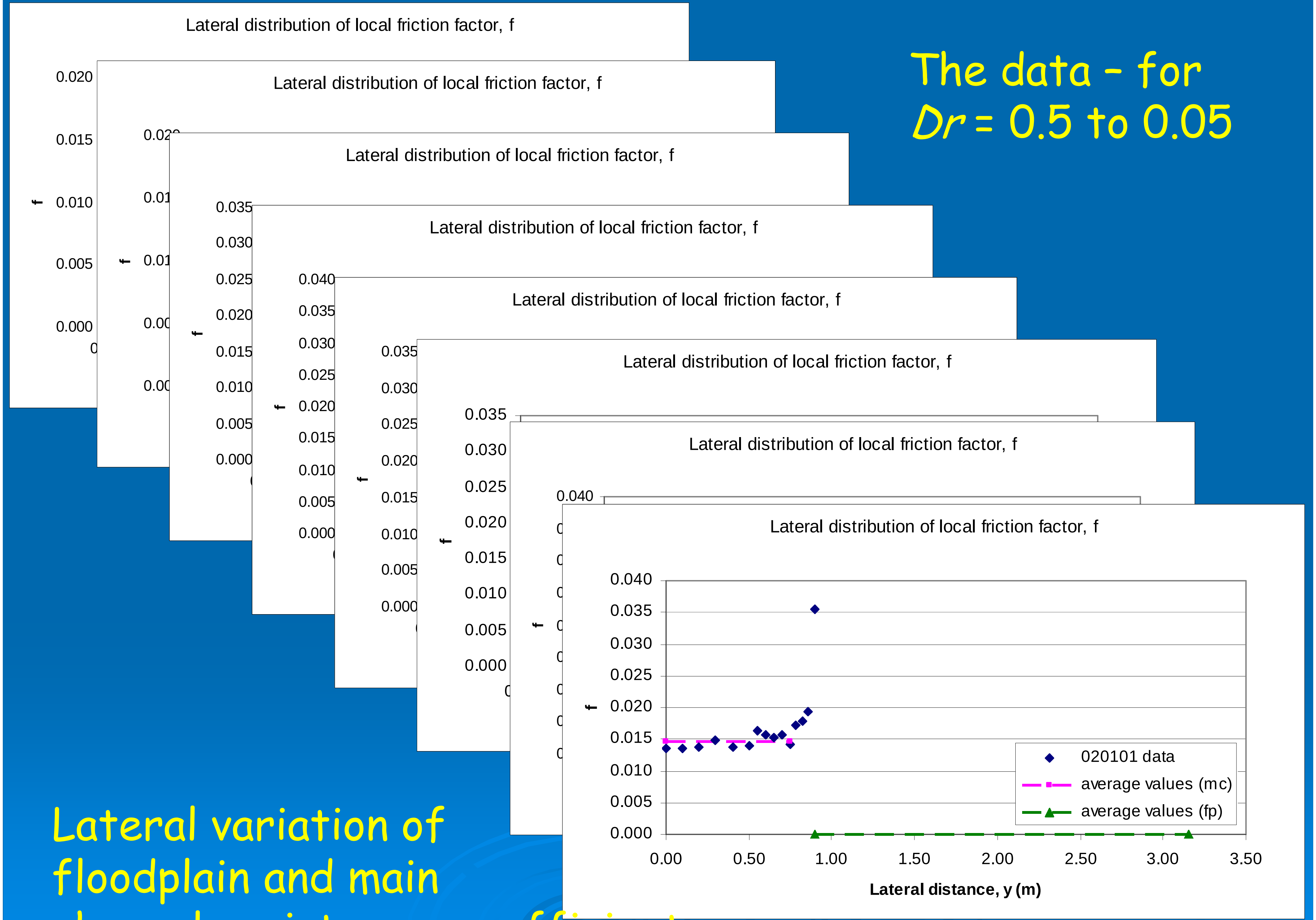

Lateral variation of floodplain and main channel resistance coefficients

Formulating an equation

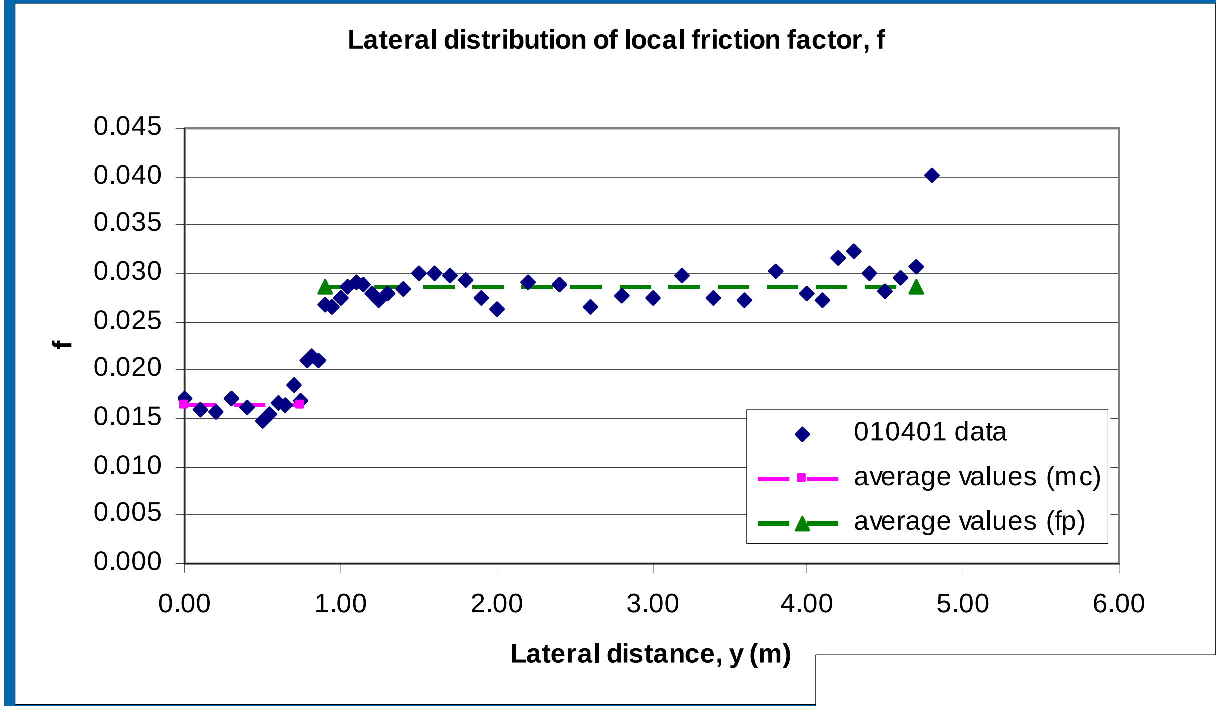

Resistance

$$\frac{f}{f_{mc}} = 0.669 + 0.331 Dr^{-0.719}$$

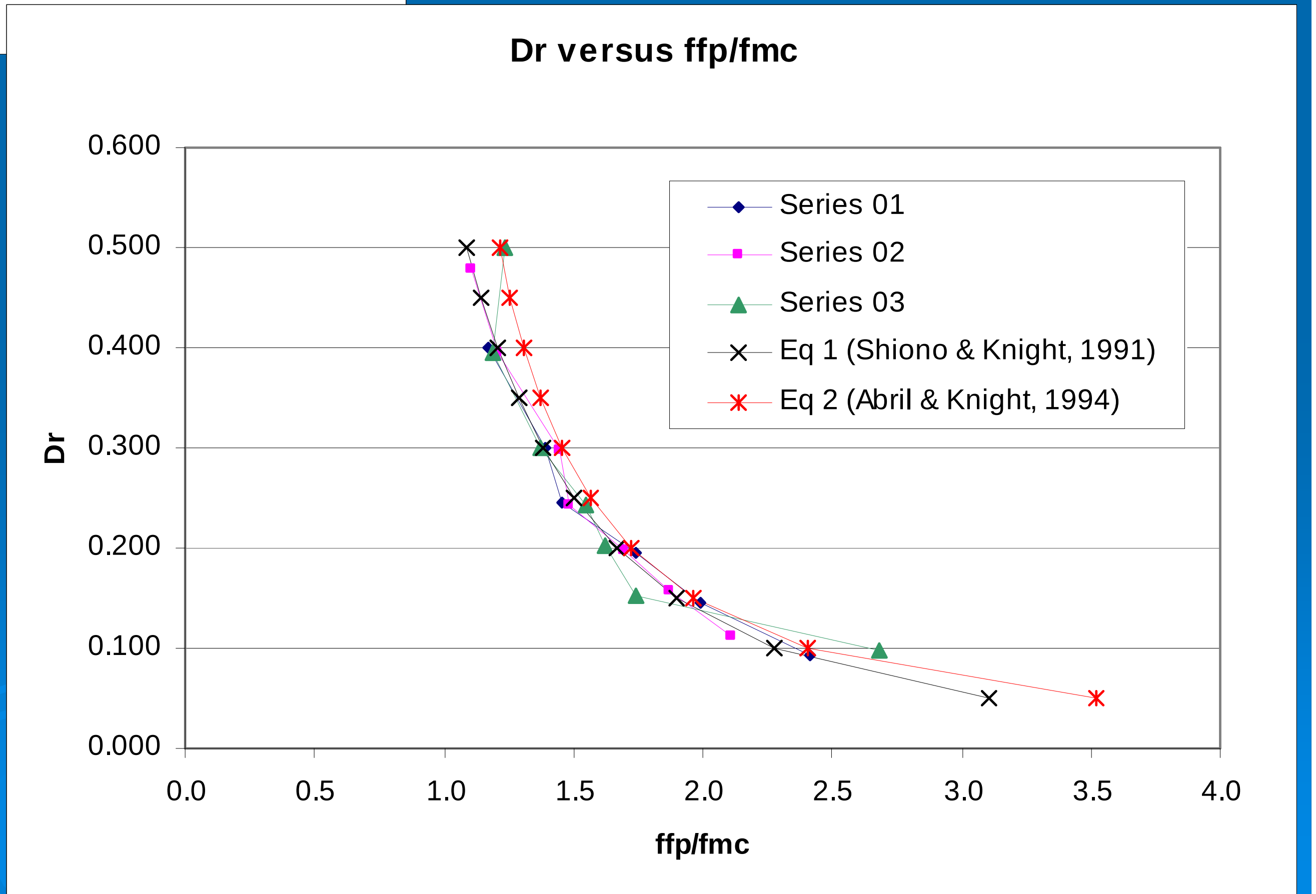

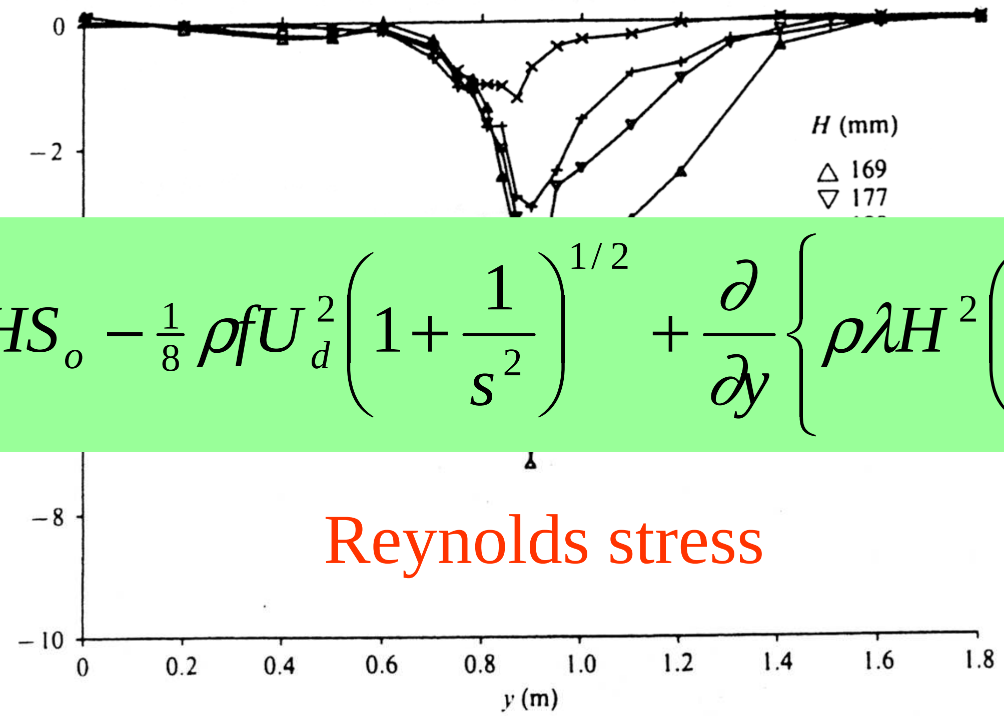

Planform vorticity

$$\rho g H S_o - \tfrac{1}{8}\rho f U_d^2\left(1+\frac{1}{s^2}\right)^{1/2} + \frac{\partial}{\partial y}\left\{\rho\lambda H^2\left(\frac{f}{8}\right)^{1/2} U_d \frac{\partial U_d}{\partial y}\right\} = \frac{\partial}{\partial y}\left[H\left(\rho UV\right)_d\right]$$

Reynolds stress

τ_{yx}, for different depths, H, in FCF Series 02

Secondary flow dispersion

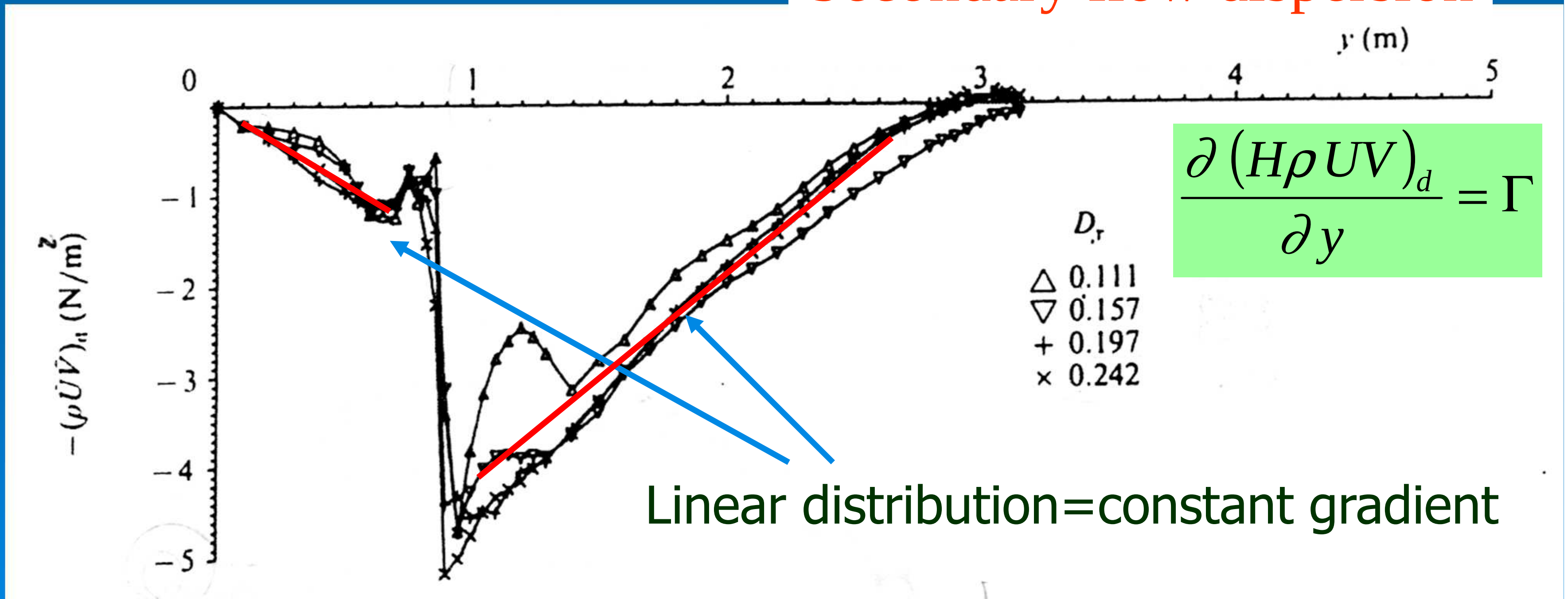

$$\frac{\partial\left(H\rho UV\right)_d}{\partial y} = \Gamma$$

Linear distribution=constant gradient

Fig. 14 Lateral variation of apparent shear stress, for *Dr* = 0.111 to 0.242 (Series 02

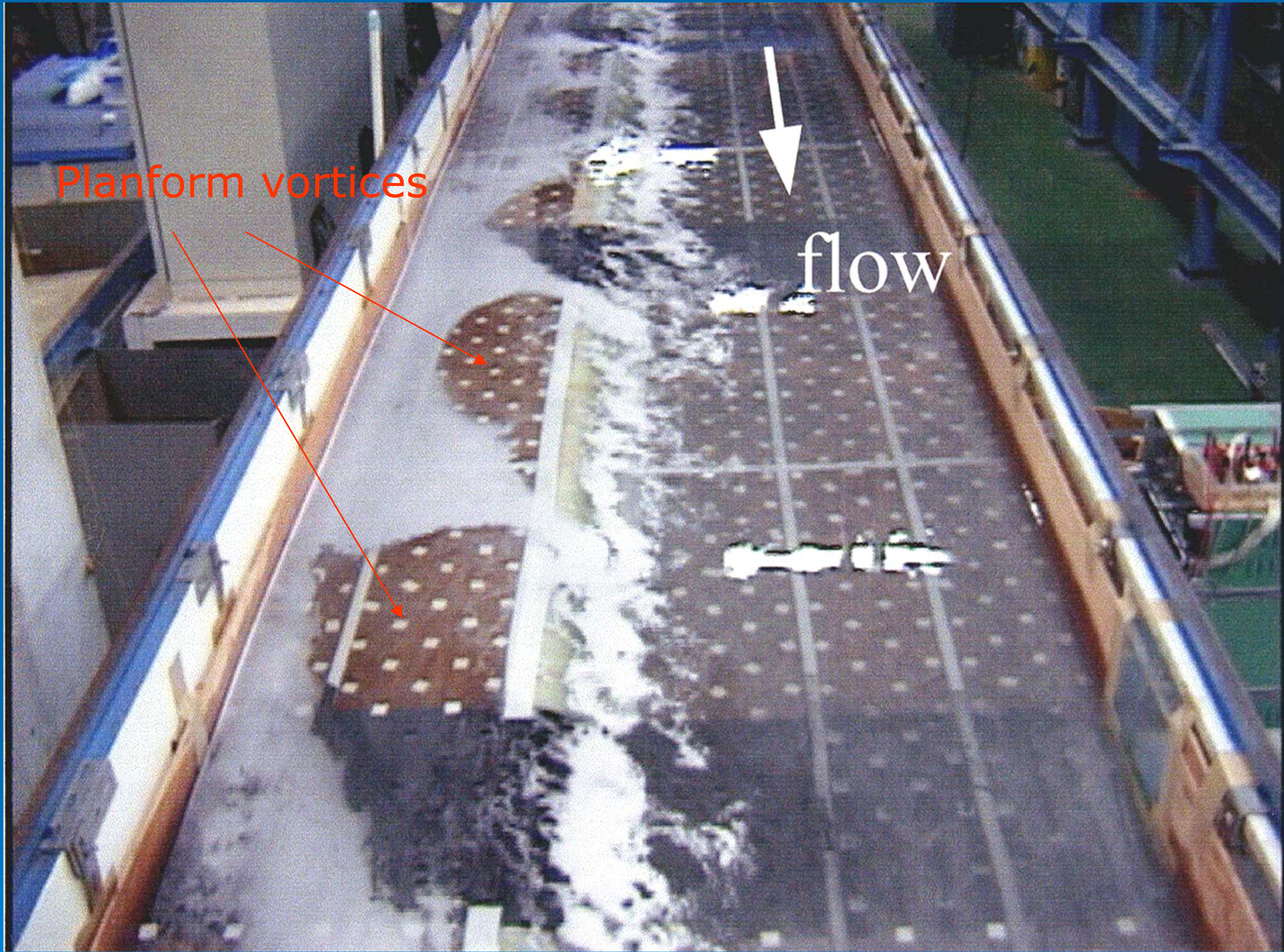

Planform flow structure at low relative depth, Dr = 0.180

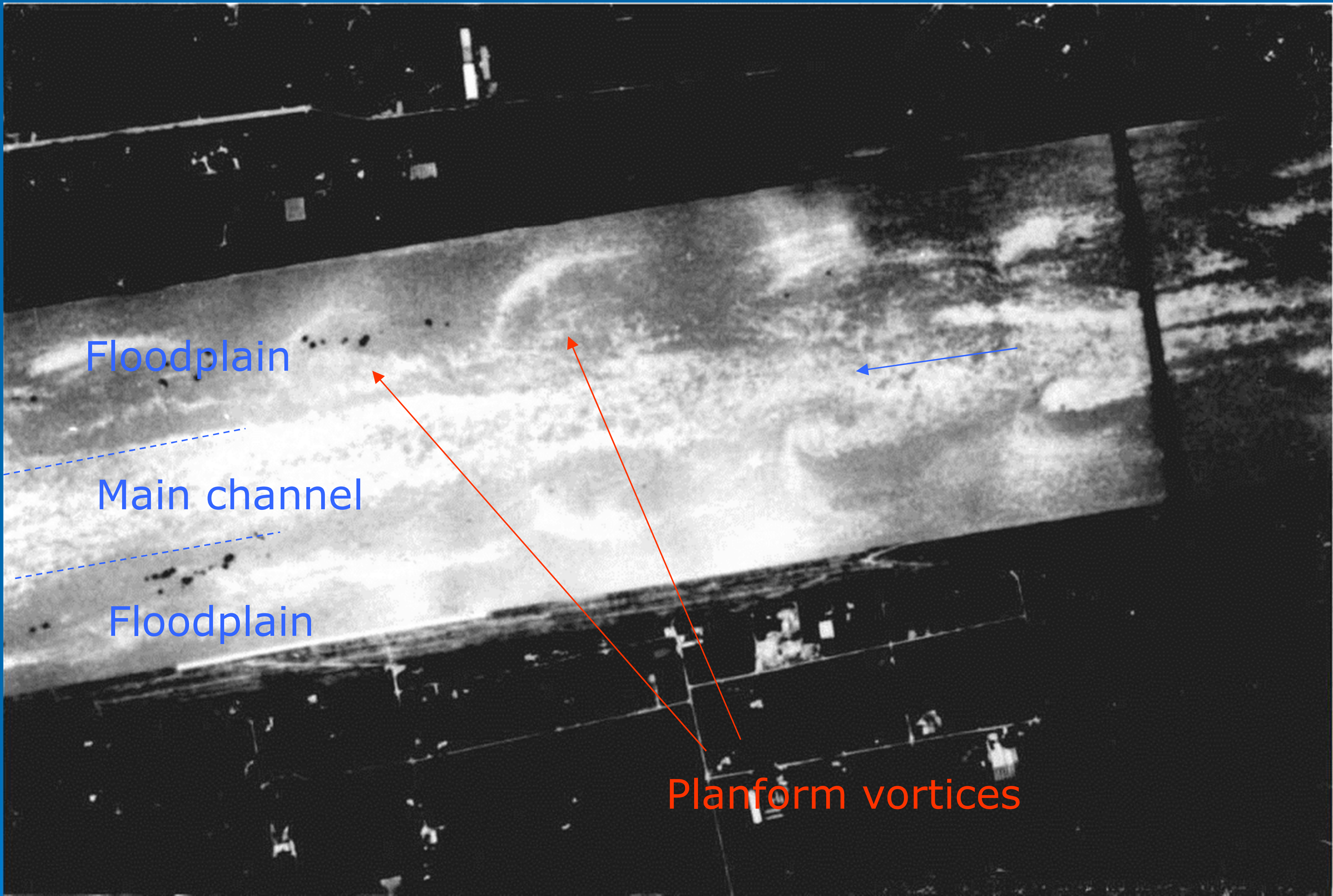

Planform flow structure on Tone River, Japan

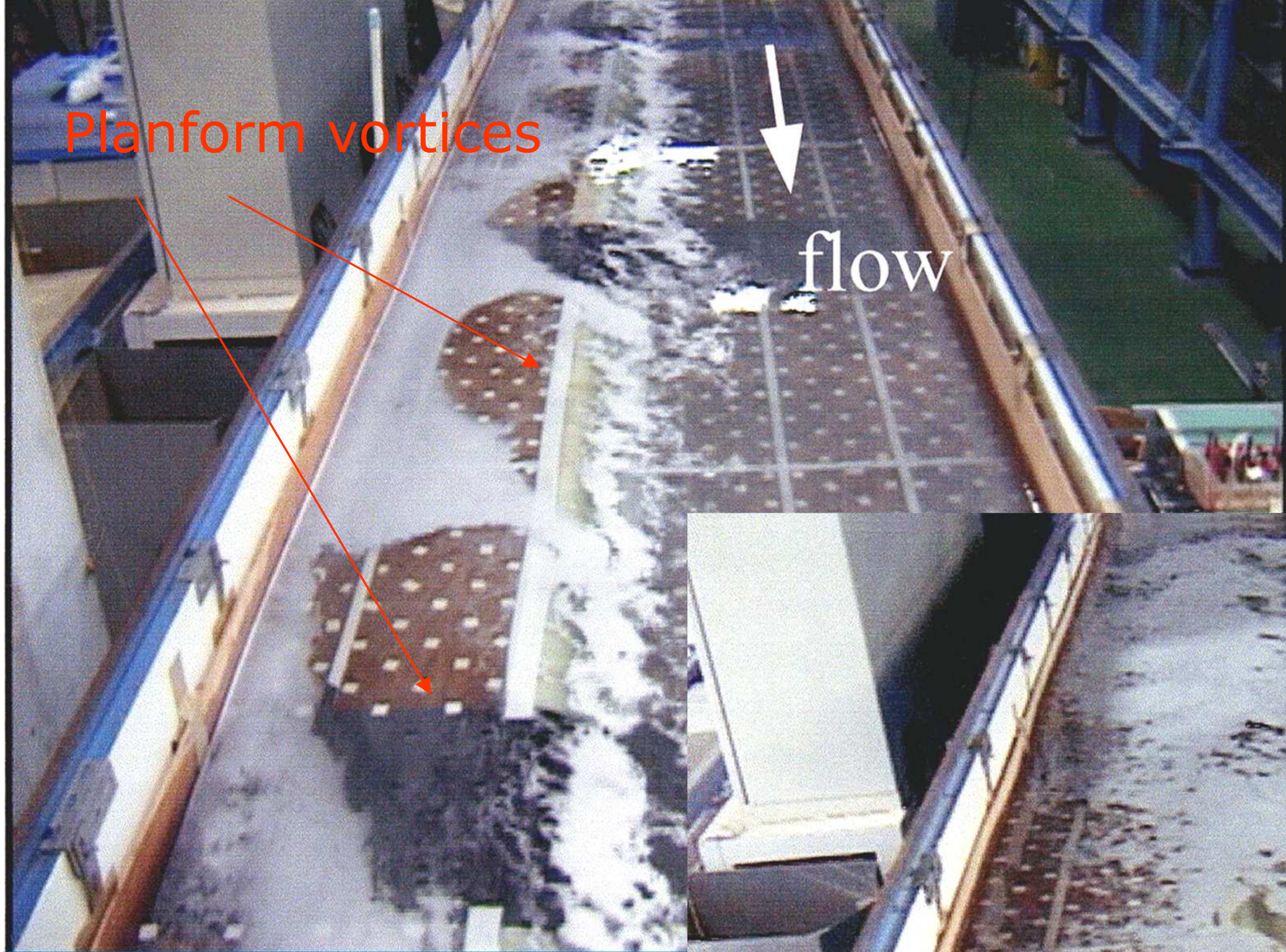

Flow structure at low relative depth, Dr = 0.180

Flow structure at high relative depth, Dr = 0.344

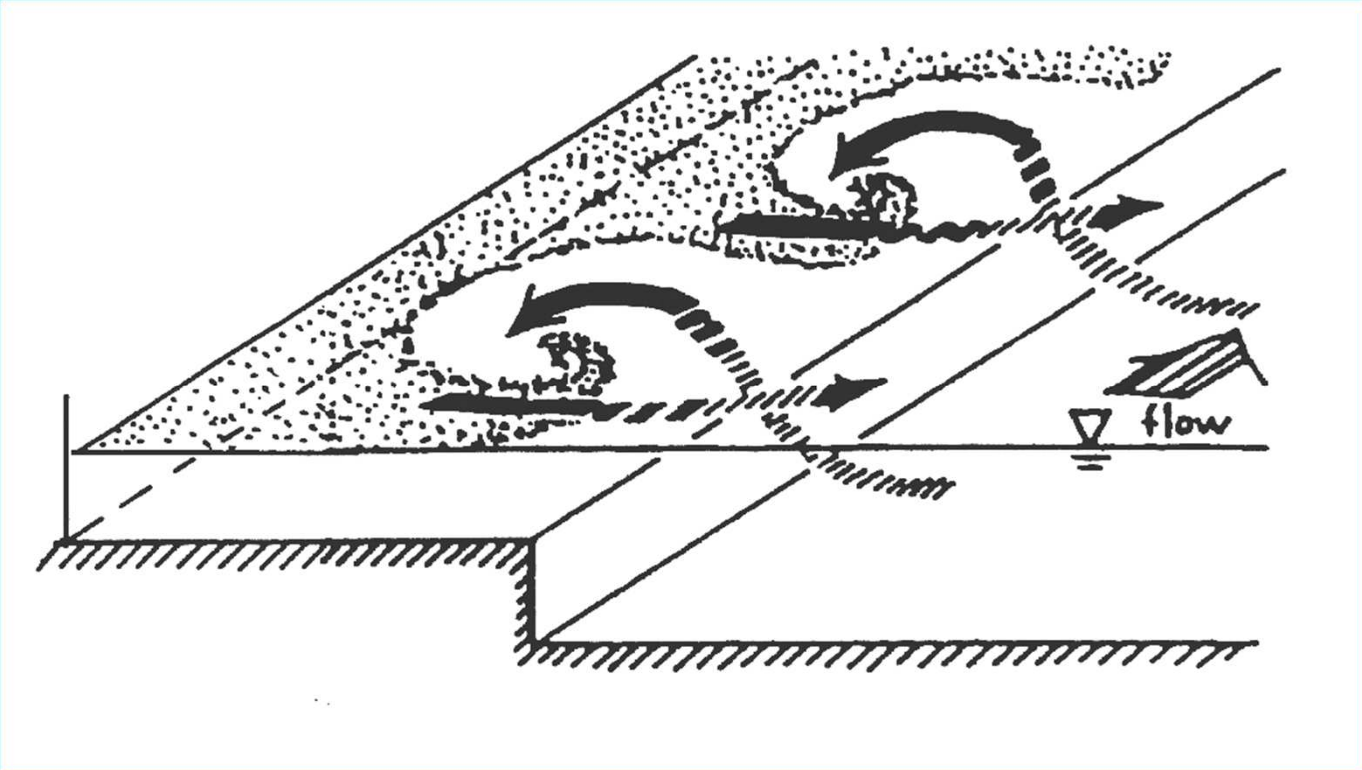

Flow structures in a straight two-stage channel (after Fukuoka & Fujita, 1989)

Sketch of vortex (after van Prooijen, 2004)

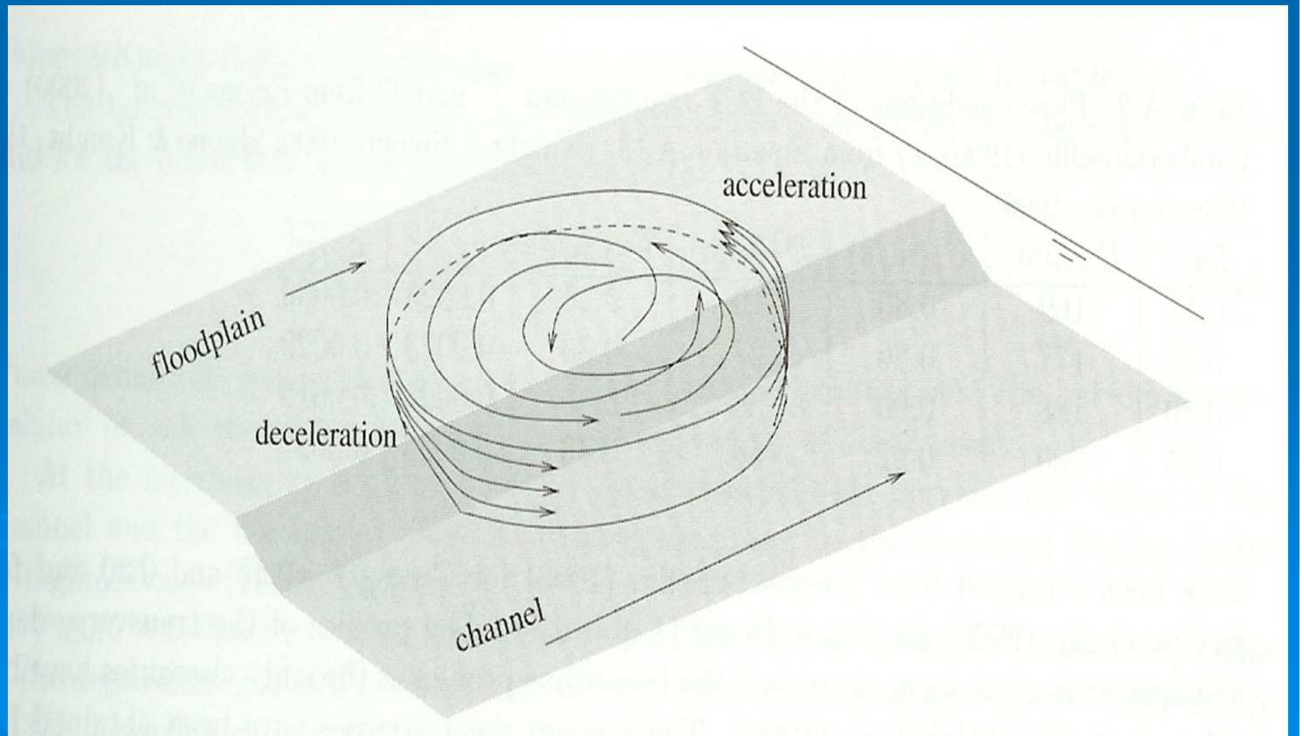

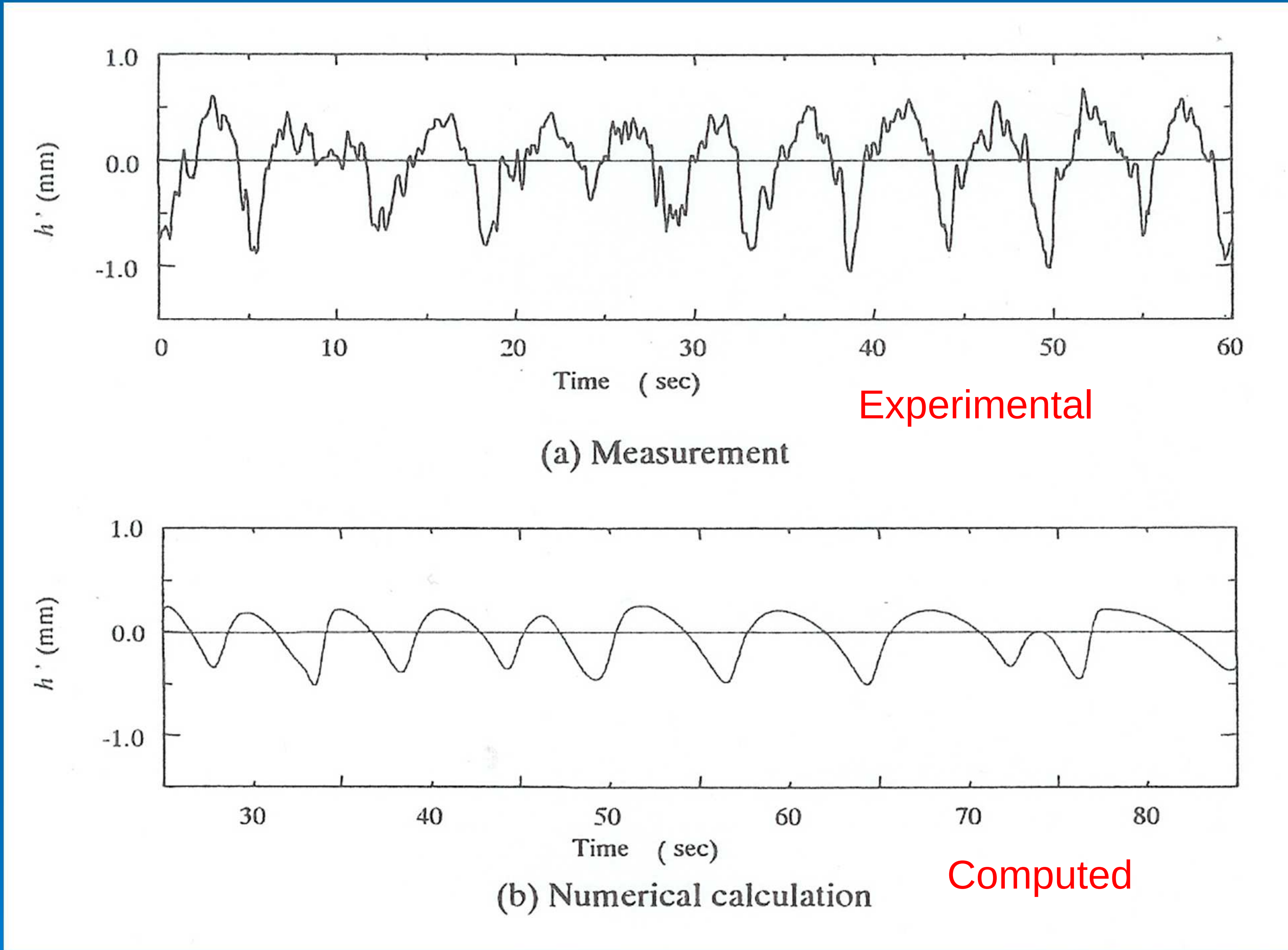

Free surface oscillations

Equations for coefficients

Resistance

$$\frac{f}{f_{mc}} = 0.669 + 0.331 Dr^{-0.719}$$

Dimensionless eddy viscosity

$$\frac{\lambda}{\lambda_{mc}} = -0.20 + 1.20 Dr^{-1.44}$$

Secondary flow (advection) term

$$\Gamma^*_{mc} = \frac{\Gamma_{mc}}{H} = 0.15 \rho g S_o$$

$$\Gamma^*_{fp} = \frac{\Gamma_{fp}}{(H-h)} = -0.25 \rho g S_o$$

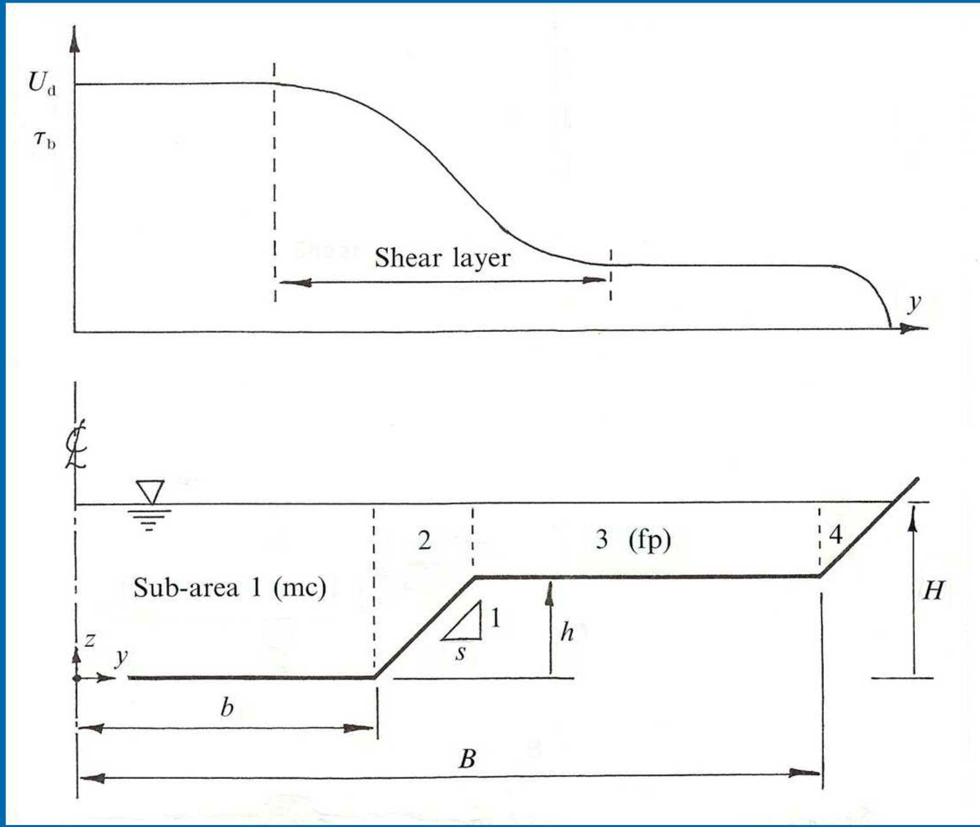

Fig. 10 Flood Channel Facility (FCF) notation

$$Dr = (H-h)/H$$

Low sinuosity compound channel (Toyohira River, Japan)

Large flumes – Flood Channel Facility (FCF)

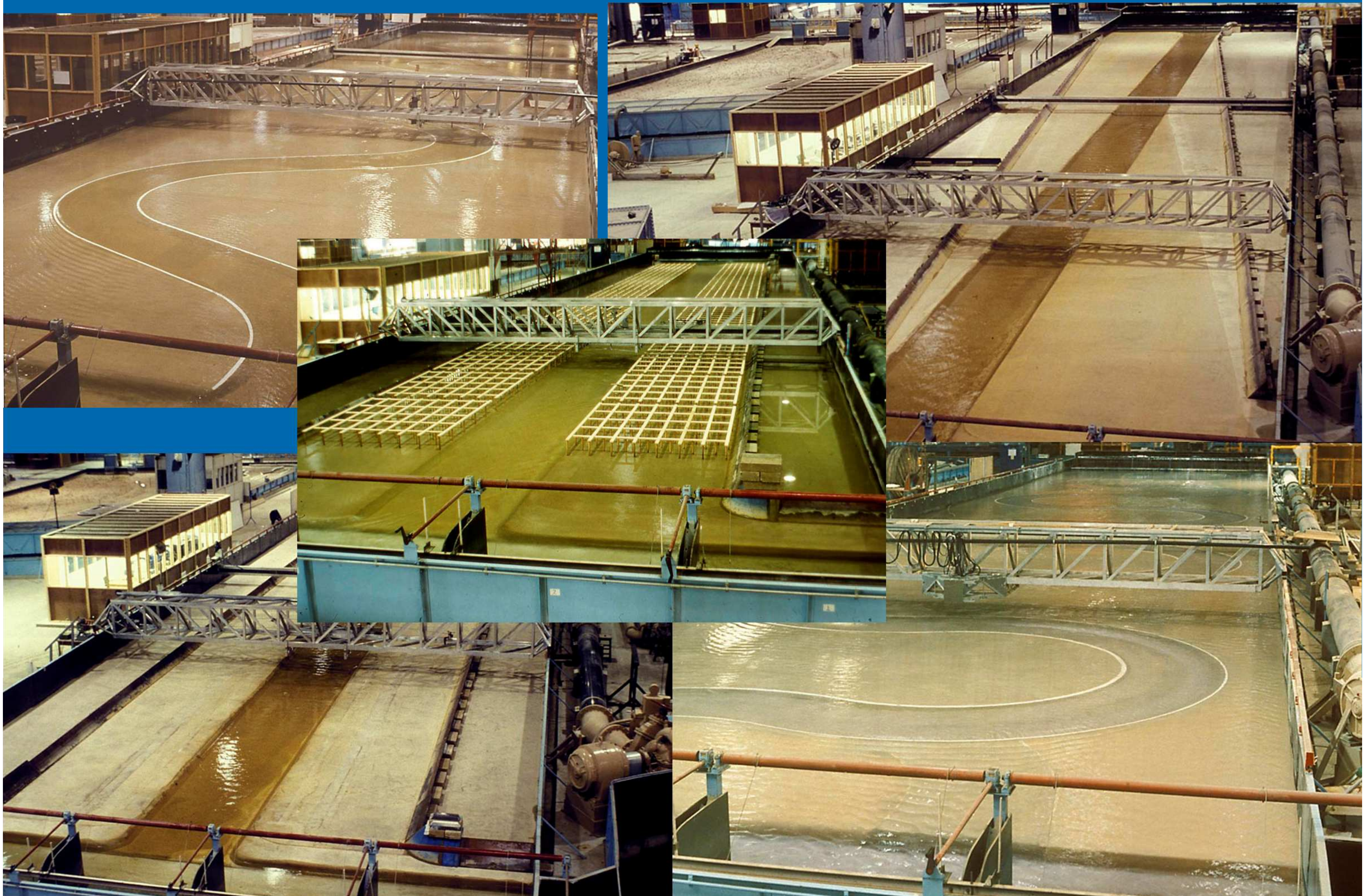

Flood Channel Facility (FCF), with sediment re-circulation system

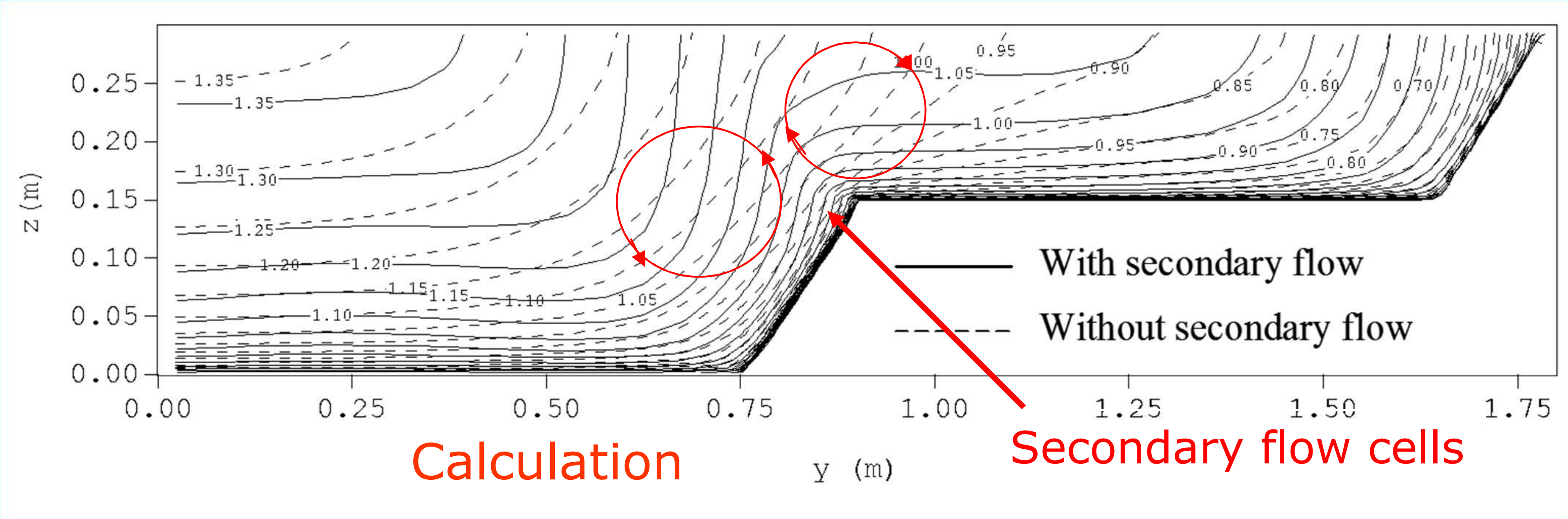

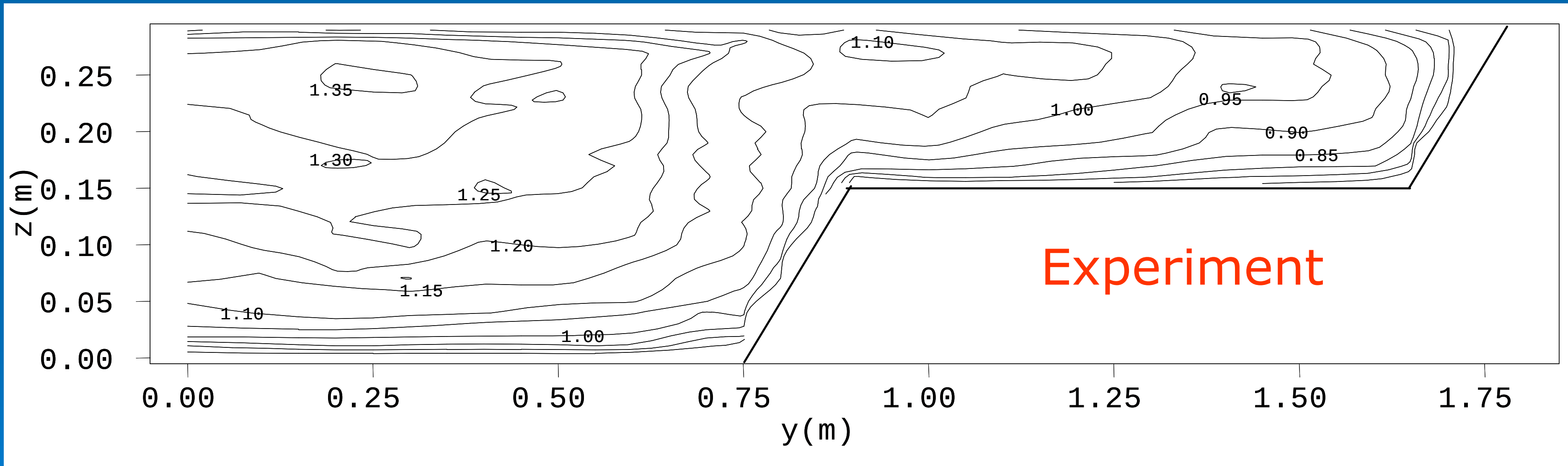

Streamwise secondary flow effects on the primary velocity at re-entrant corners

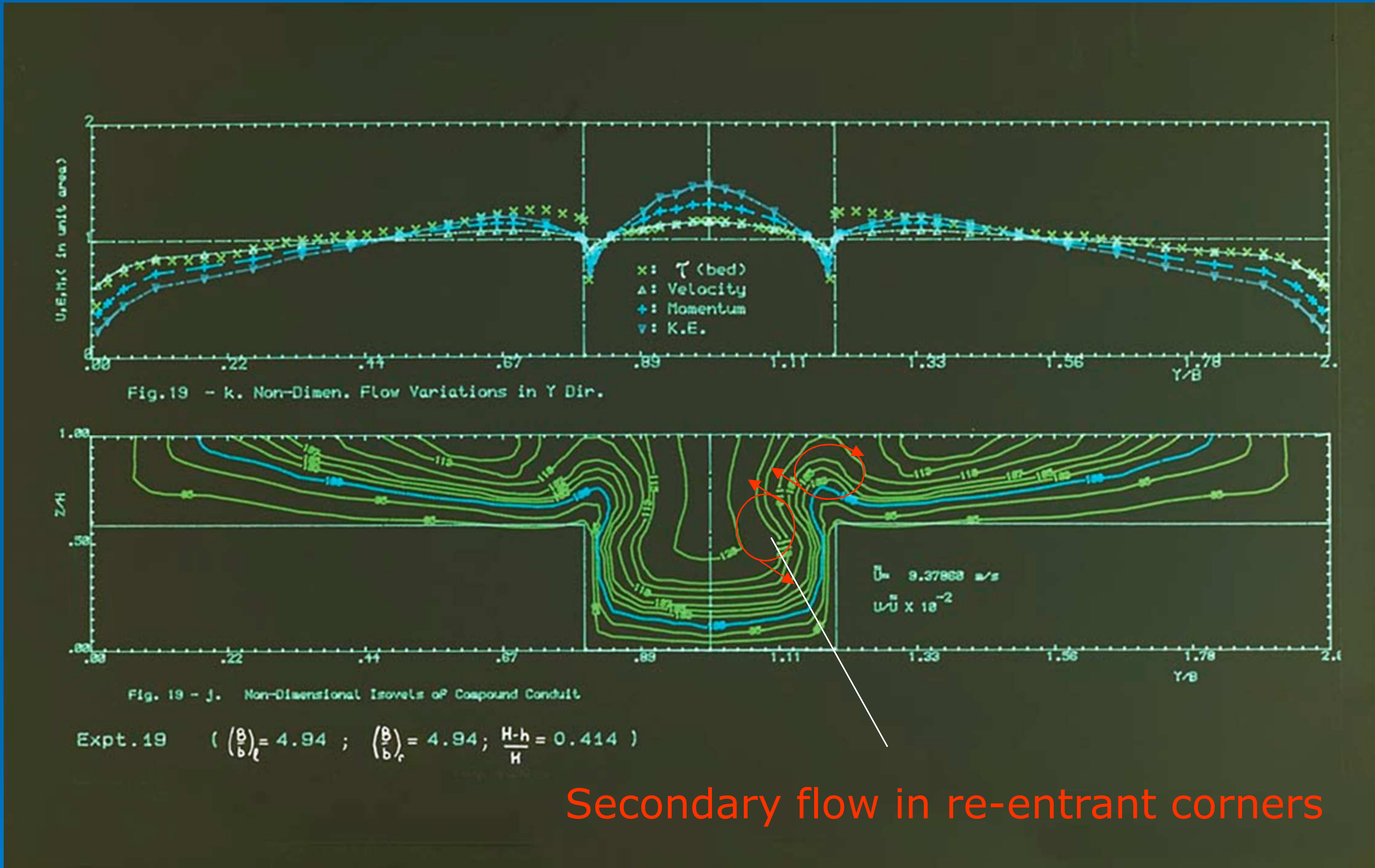

Velocity and boundary shear stress data at high relative depth, (H-h)/H = 0.414 (small wind tunnel)

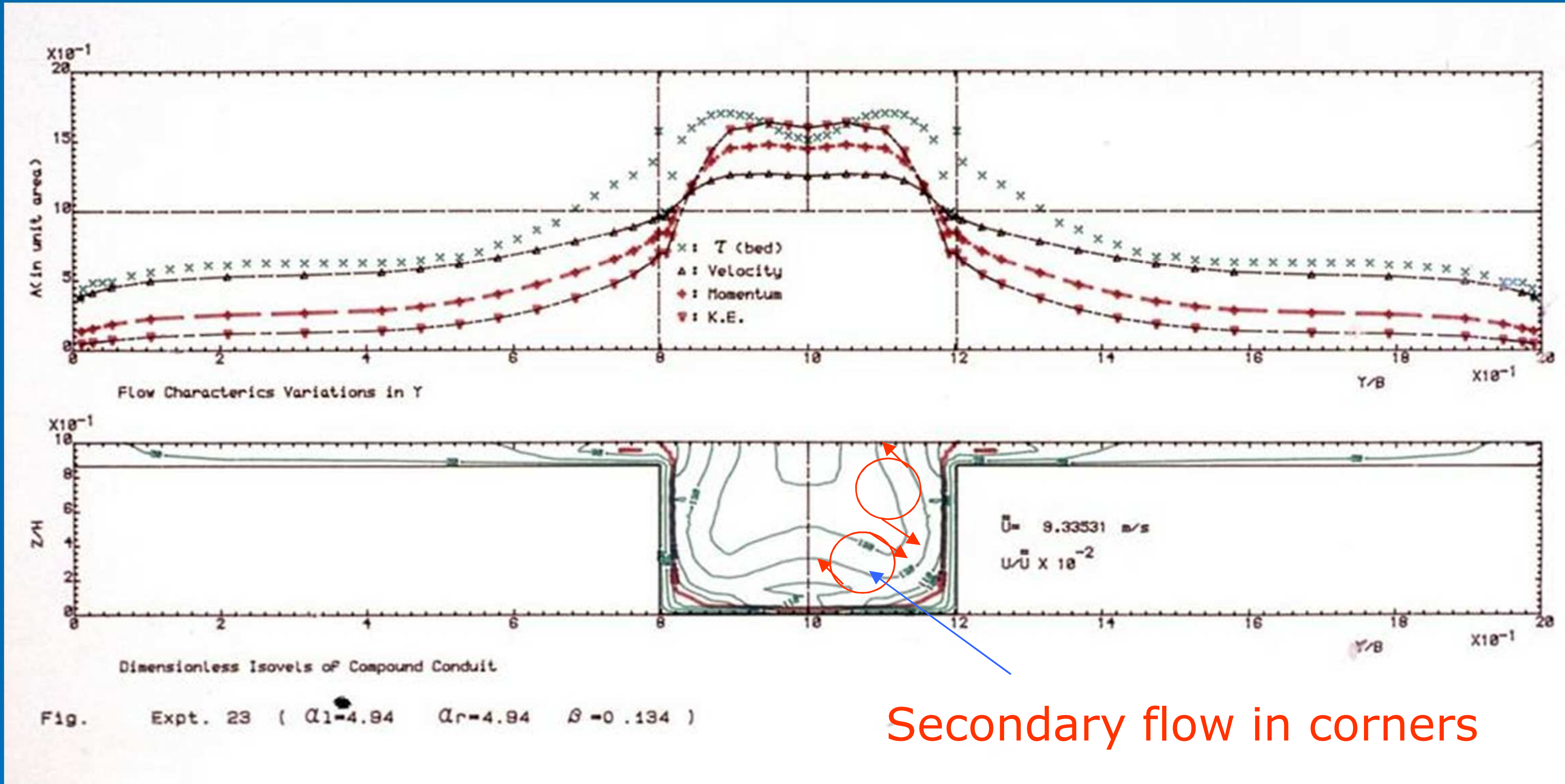

Velocity and boundary shear stress data at low relative depth, (H-h)/H = 0.134 (small wind tunnel)

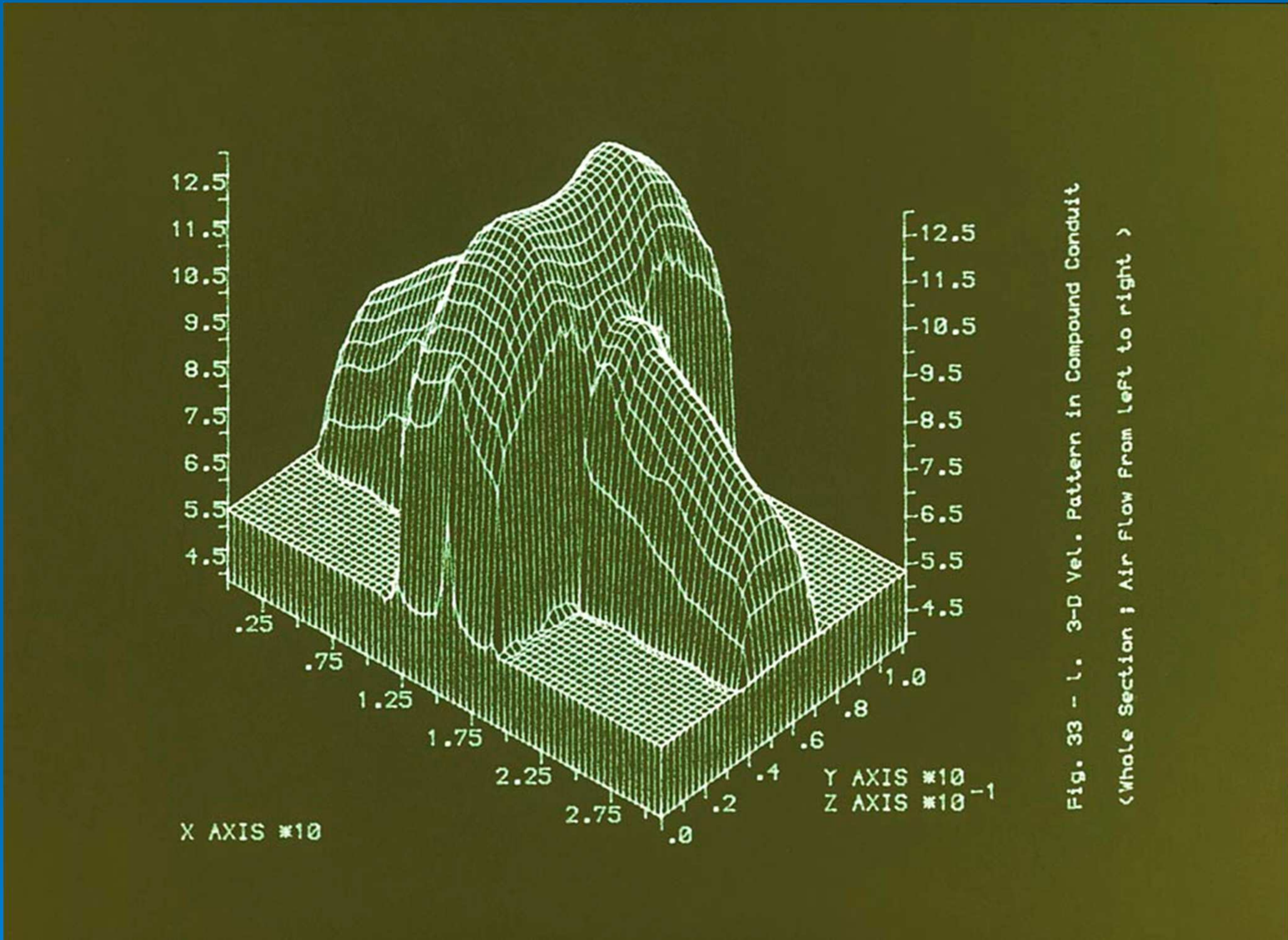

Isometric view of velocity data in small wind tunnel

(a) Inbank flows

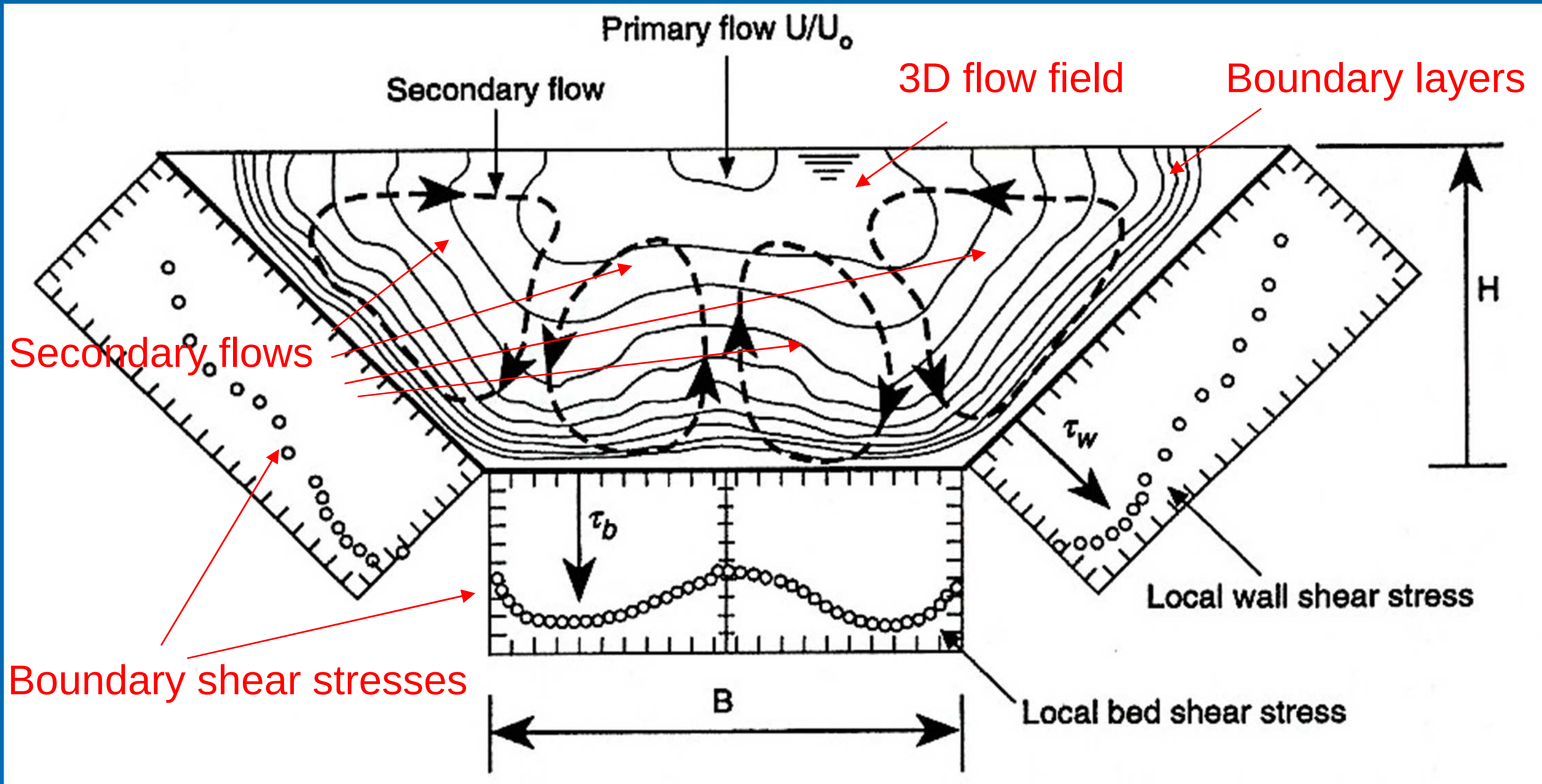

Secondary flows in corner regions - and their influence on isovels and boundary shear stresses in a simple trapezoidal channel (after Knight *et al*., 1994)

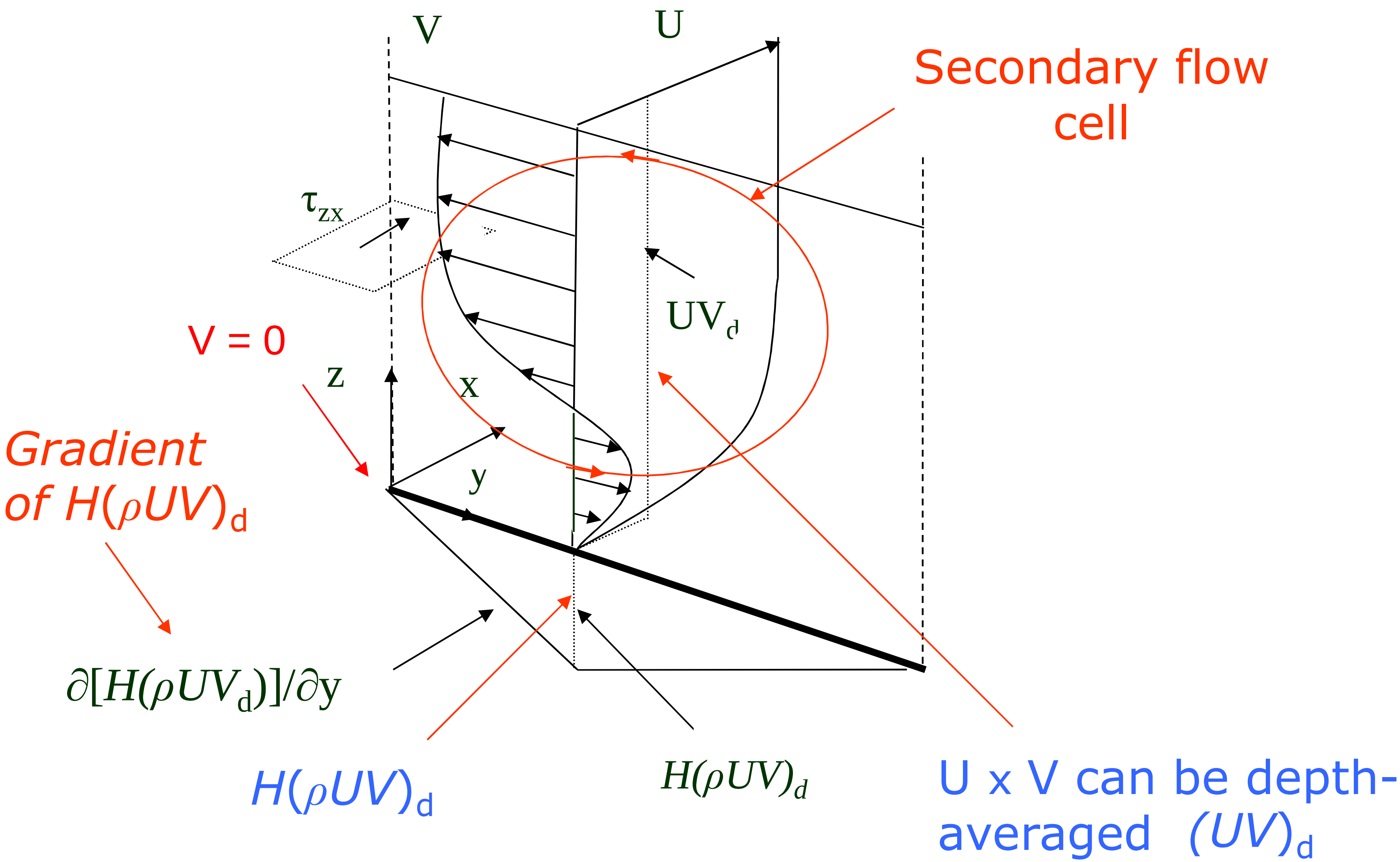

Modelling depth-averaged secondary flow in SKM

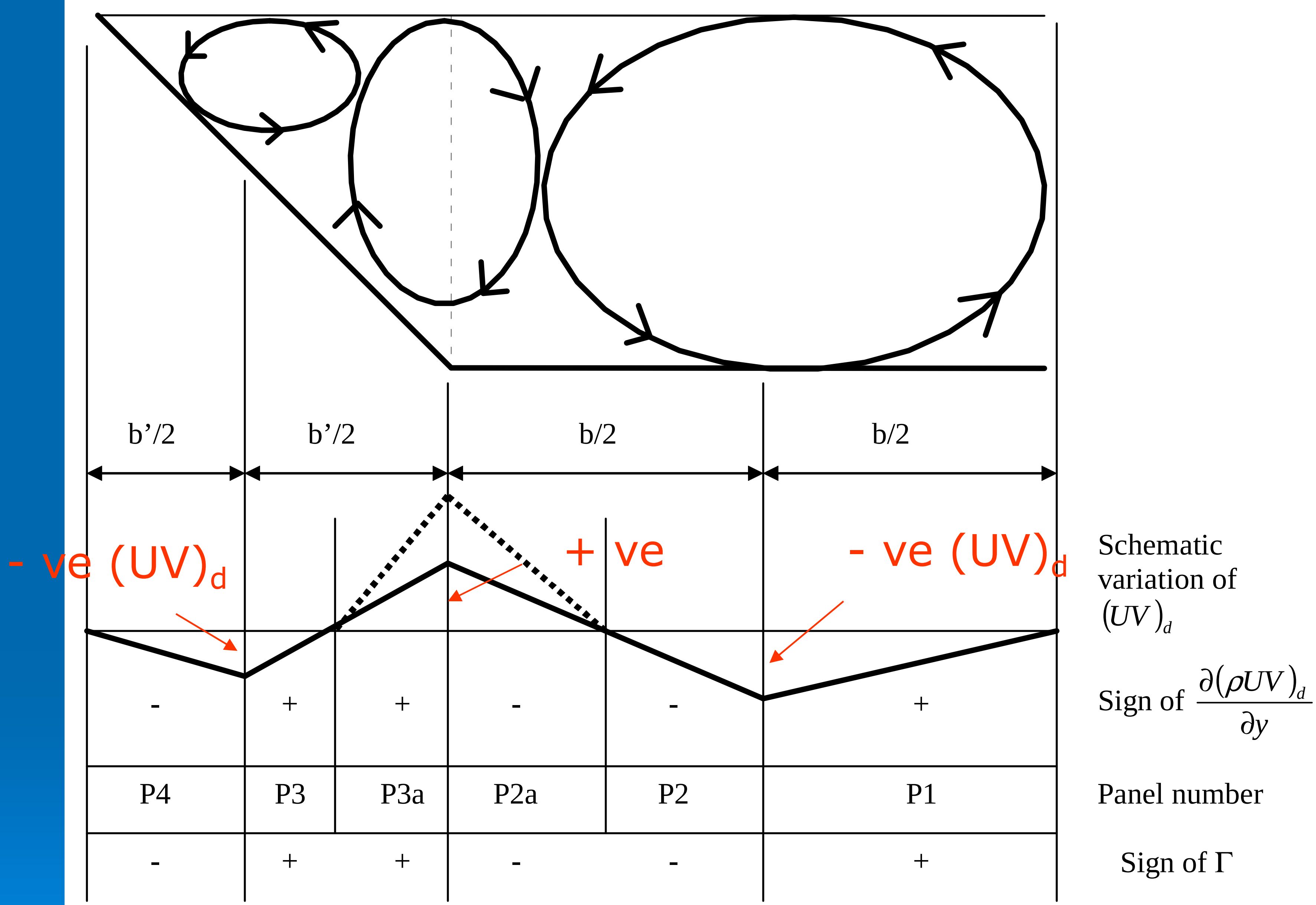

Use of 4 or 6 panels to model flow in a trapezoidal channel, and signs of secondary current term, Γ

SKM approach

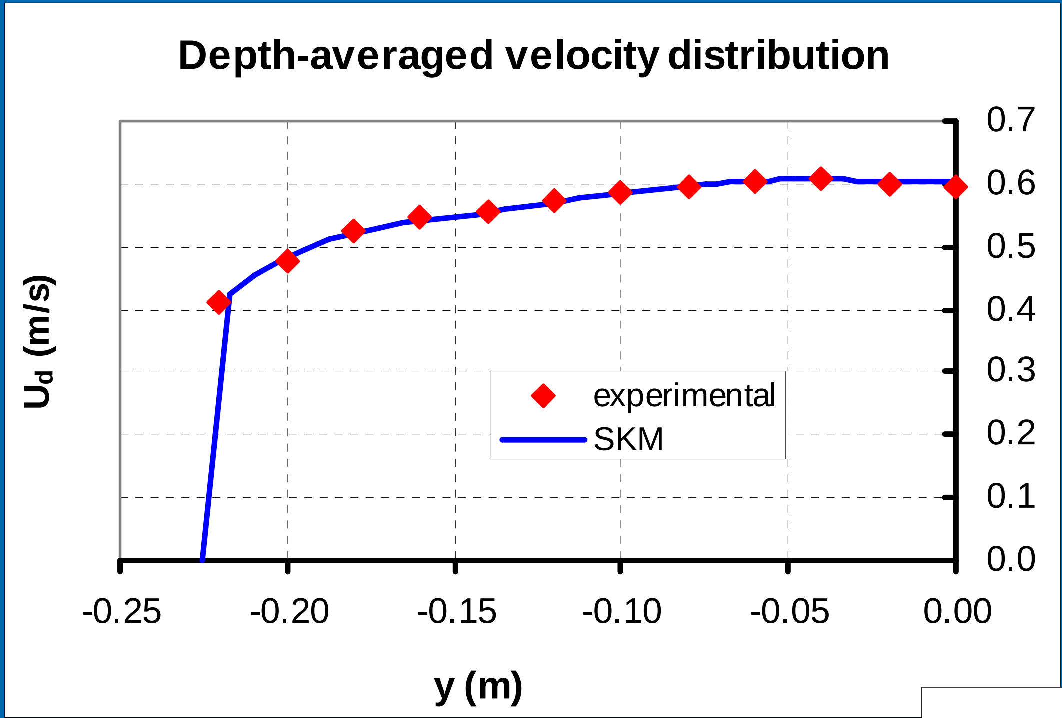

Predicted U_d
using 4 panels
(Exp 16; Yuen)

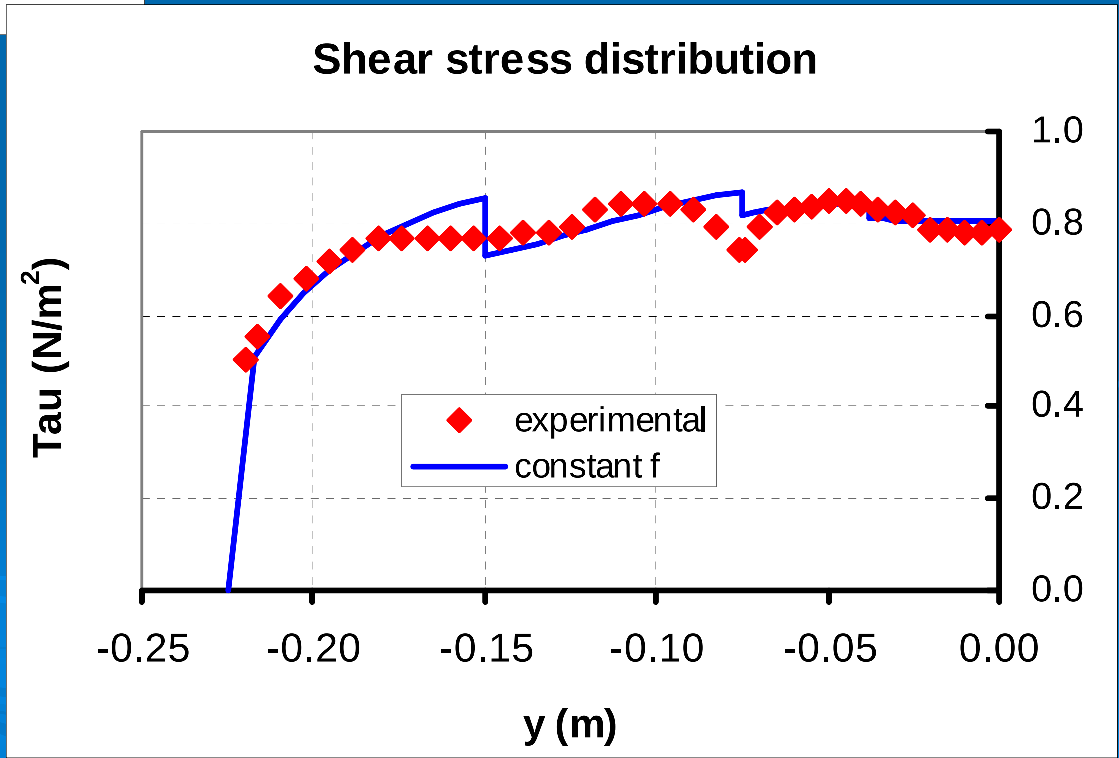

Predicted τ_b
using 4 panels
(Exp 16; Yuen)

SKM approach

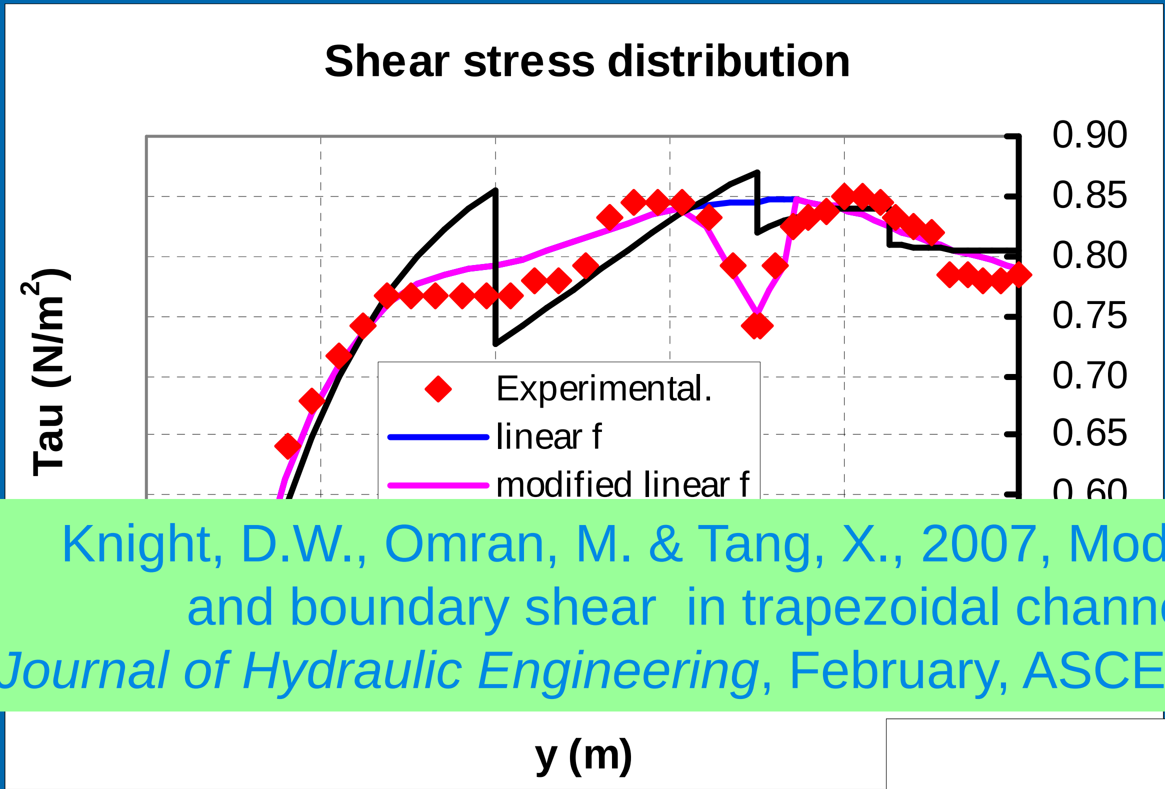

(a) Predicted τ_b using 6 panels (constant λ)

Knight, D.W., Omran, M. & Tang, X., 2007, Modelling depth-averaged velocity and boundary shear in trapezoidal channels with secondary flows, *Journal of Hydraulic Engineering*, February, ASCE, Vol. 133, No. 1, January, 39-47.

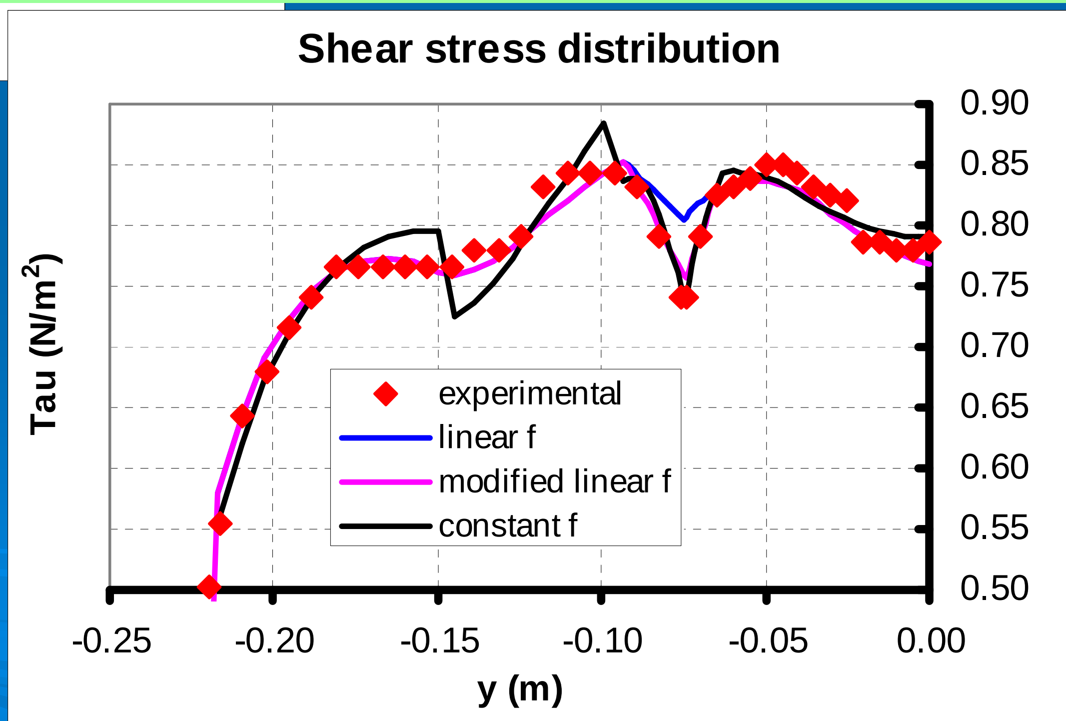

(b) Predicted τ_b using 6 panels (variable λ)

Large Eddy Simulation (rectangular channels)

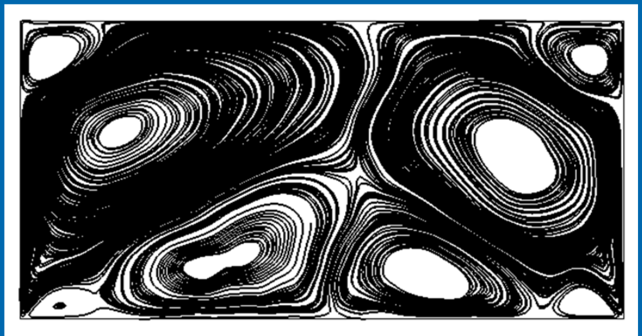

Dr = 2.0

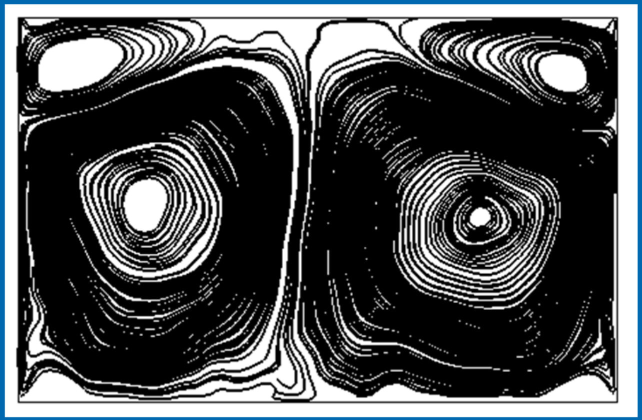

Dr = 1.6

Dr = 1.3

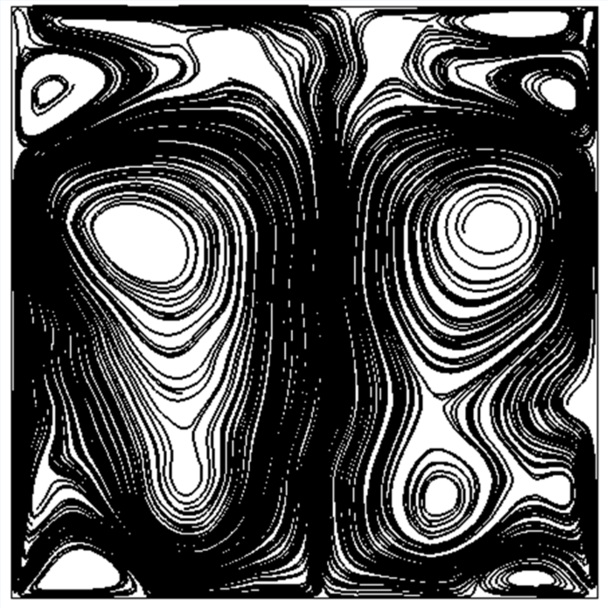

Dr = 1.0

LES Results (rectangular channels)

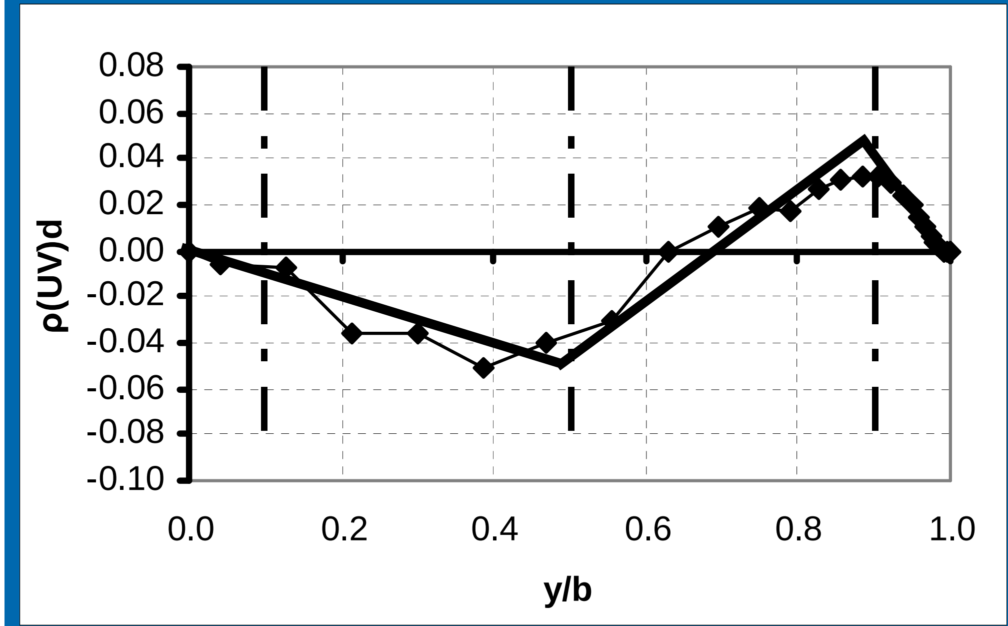

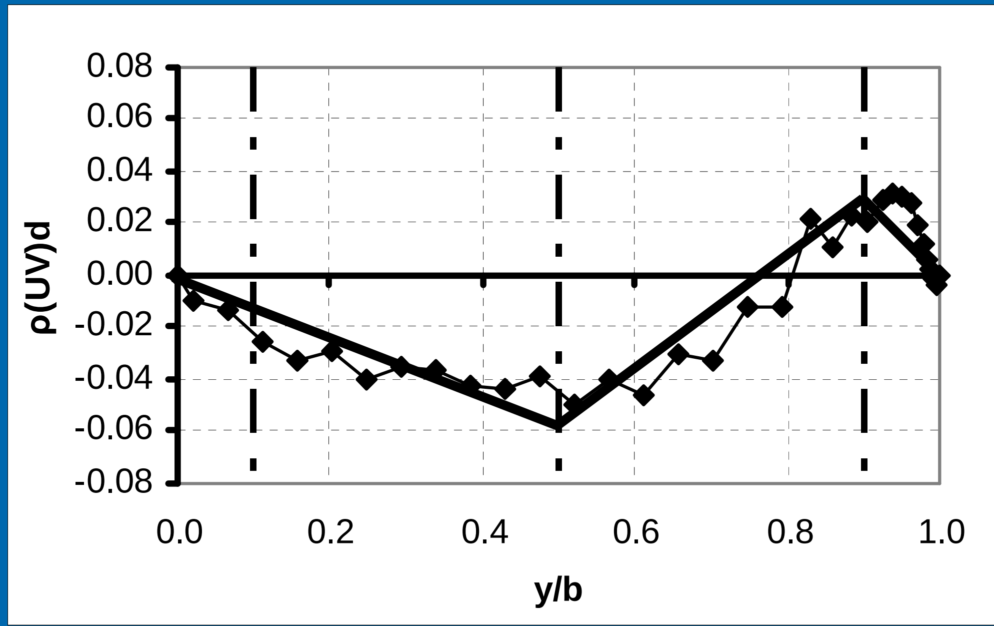

Dr = 1.6

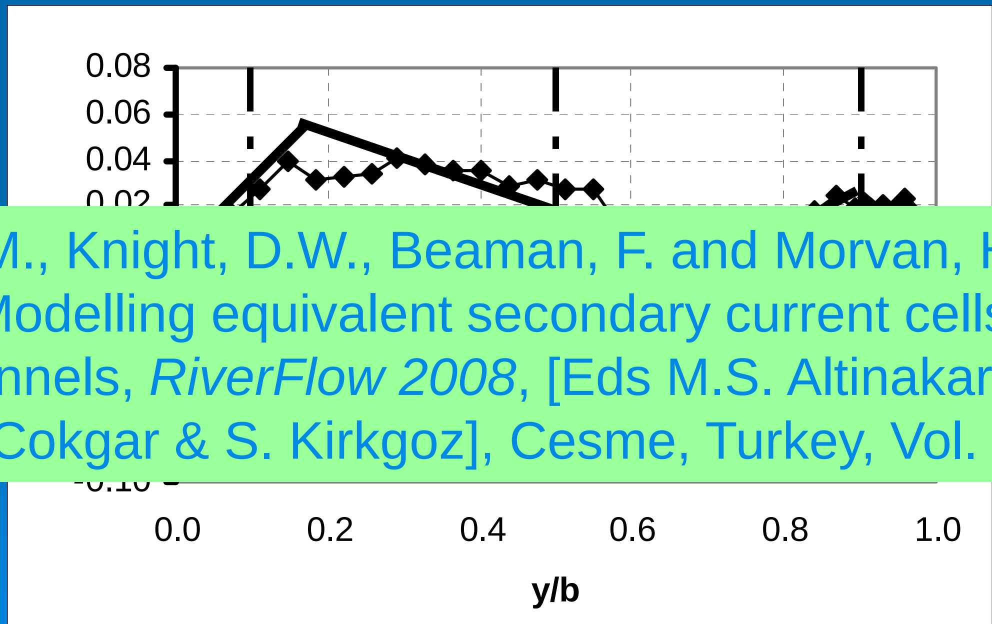

Dr = 1.0

Omran, M., Knight, D.W., Beaman, F. and Morvan, H., 2008, Modelling equivalent secondary current cells in rectangular channels, *RiverFlow 2008*, [Eds M.S. Altinakar, M.A. Kokpinar, I. Aydin, S. Cokgar & S. Kirkgoz], Cesme, Turkey, Vol. 1, 75-82.

Dr = 2.0

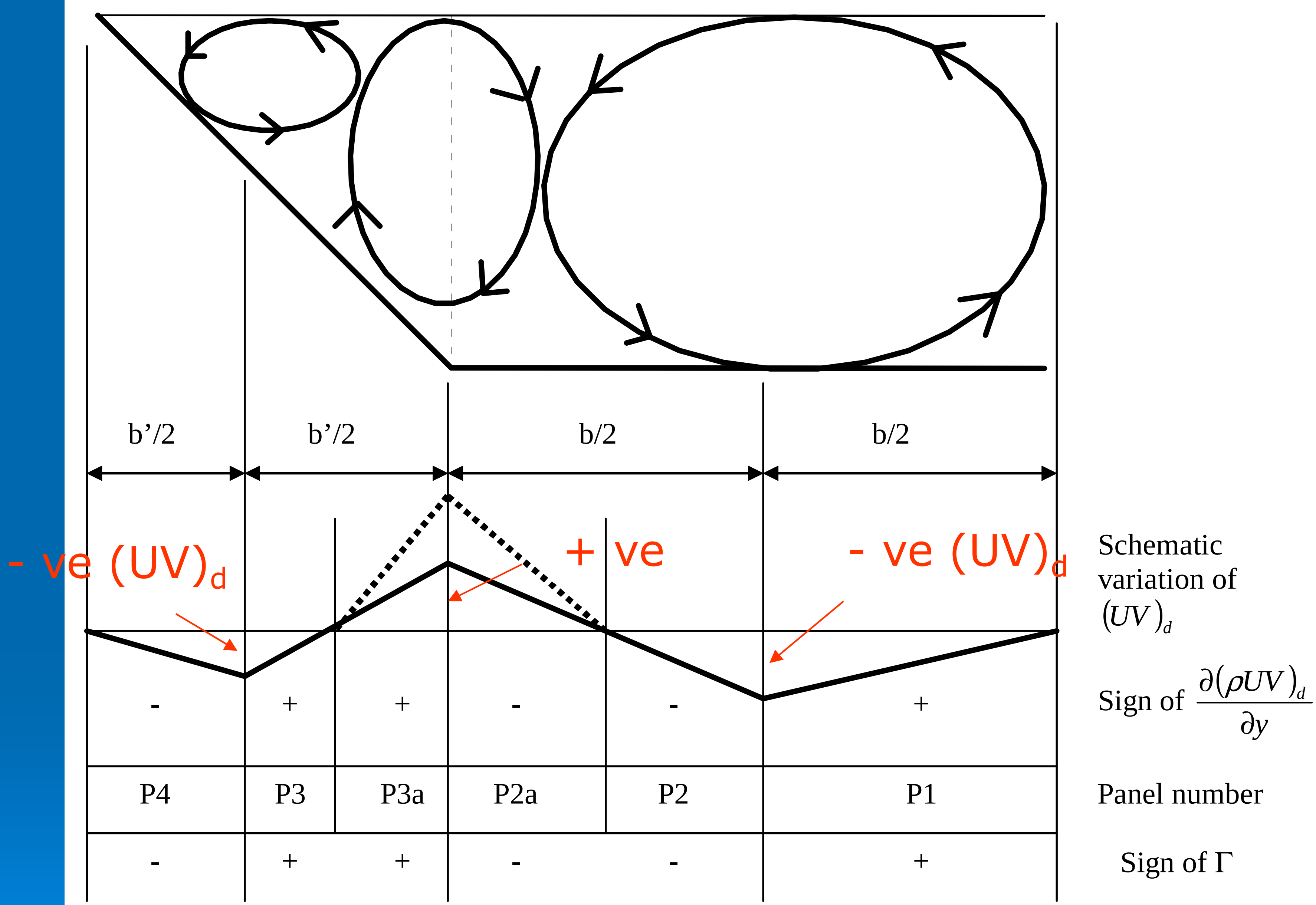

Use of 4 or 6 panels to model flow in a trapezoidal channel, and signs of secondary current term, Γ

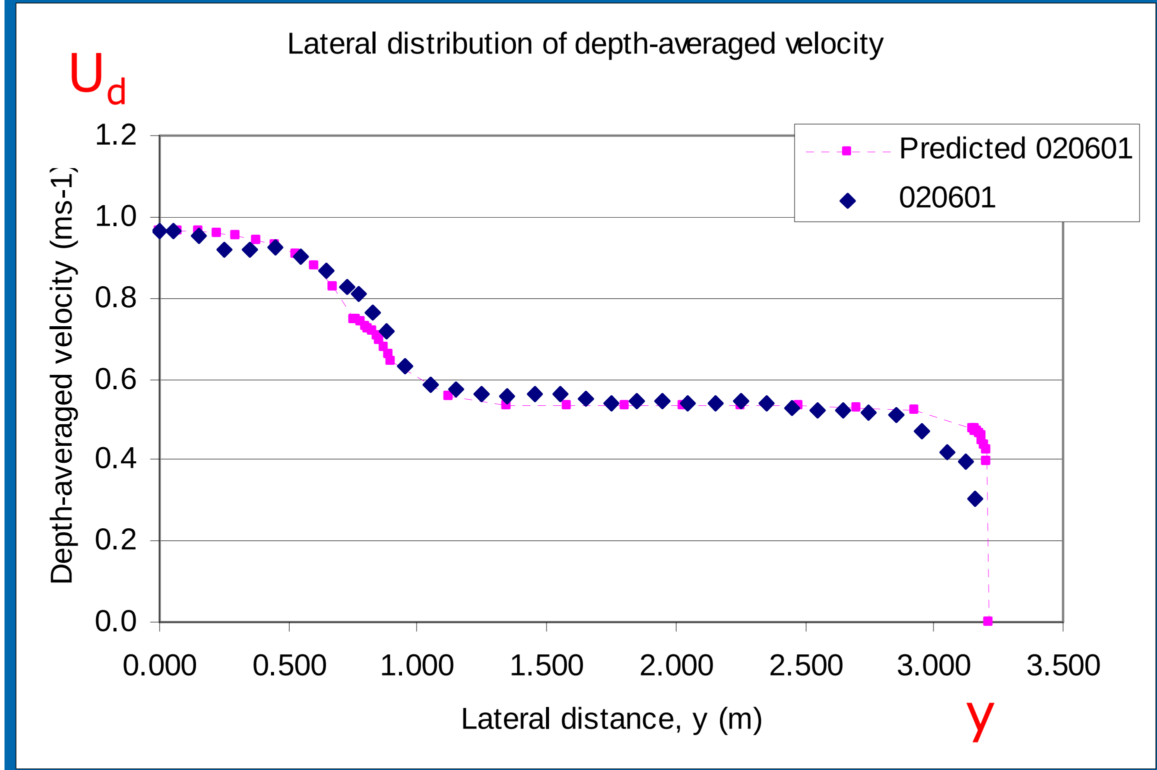

and so a model was constructed ....

Initial model simulations

Fig. 11 Measured and predicted *Ud* v *y*

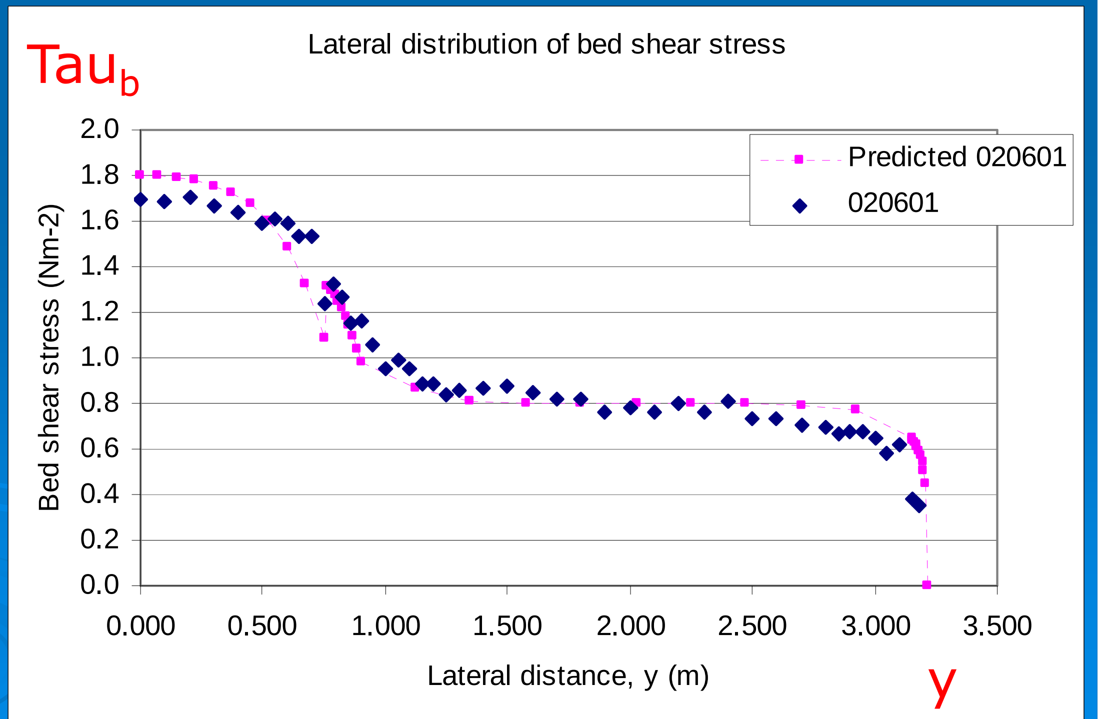

.... and reasonable predictions made of experimental data

Fig. 12 Measured and predicted τb v *y*

For a trapezoidal channel with 3 panels

$$U_d^{(3)}\big|_{\xi_3=0} = 0$$

$$U_d^{(2)}\big|_{\xi_2=0} = 0$$

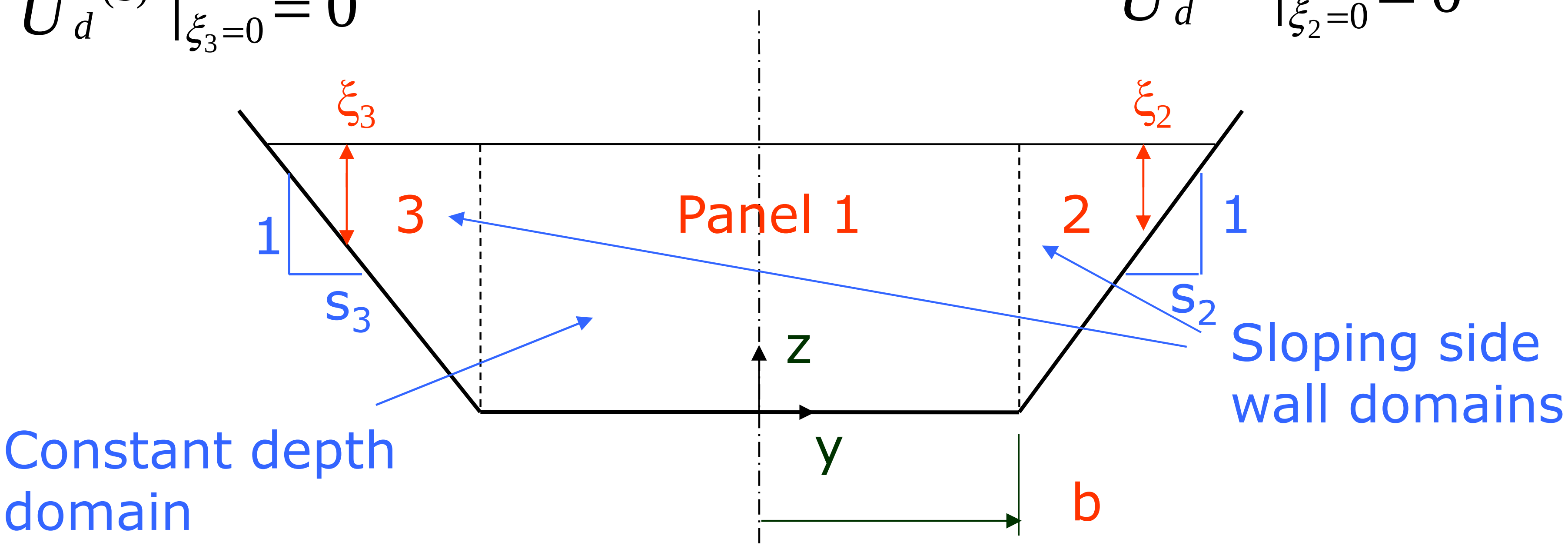

$$U_d^{(1)}\big|_{y=-b} = U_d^{(3)}\big|_{\xi_3=H}$$

$$U_d^{(1)}\big|_{y=b} = U_d^{(2)}\big|_{\xi_2=H}$$

$$\left.\frac{\partial U_d^{(1)}}{\partial y}\right|_{y=-b} = \left.\frac{\partial U_d^{(3)}}{\partial y}\right|_{\xi_3=H}$$

$$\left.\frac{\partial U_d^{(1)}}{\partial y}\right|_{y=b} = \left.\frac{\partial U_d^{(2)}}{\partial y}\right|_{\xi_2=H}$$

Analytical solution for sloping side-wall panel (2)

$$U_d = \left[A_3 \xi^{\alpha} + A_4 \xi^{-\alpha-1} + \omega\xi + \eta\right]^{1/2}$$

where the parameters α, η and ω are given by the following:

$$\alpha = -\frac{1}{2} + \frac{1}{2}\sqrt{1 + \frac{s\left(1+s^2\right)^{1/2}}{\lambda}\left(8f\right)^{1/2}}$$

and the local depth is ξ

$$\xi = H - \frac{y-b}{s}$$

$$\eta = -\frac{\Gamma}{\frac{\left(1+s^2\right)^{1/2}}{s}\rho\left(\frac{f}{8}\right)}$$

$$\omega = \frac{gS_o}{\frac{\left(1+s^2\right)^{1/2}}{s}\left(\frac{f}{8}\right) - \frac{\lambda}{s^2}\left(\frac{8}{f}\right)^{1/2}}$$

Analytical solution

$$U_d = \left[A_1 e^{\gamma y} + A_2 e^{-\gamma y} + k\right]^{1/2}$$

Panel 1 (flat bed)

$$U_d = \left[A_3 \xi^{\alpha} + A_4 \xi^{-\alpha-1} + \omega\xi + \eta\right]^{1/2}$$

Panel 2 (side slope s_2)

$$\xi_2 = H - \frac{y-b}{s_2}$$

$$U_d = \left[A_5 \xi^{\alpha} + A_6 \xi^{-\alpha-1} + \omega\xi + \eta\right]^{1/2}$$

Panel 3 (side slope s_3)

$$\xi_3 = H + \frac{y+b}{s_3}$$

6 unknown coefficients, A_1 - A_6

$$U_d^{(2)}\big|_{\xi_2=0} = 0 \qquad U_d^{(3)}\big|_{\xi_3=0} = 0 \qquad U_d^{(1)}\big|_{y=b} = U_d^{(2)}\big|_{\xi_2=H} \qquad U_d^{(1)}\big|_{y=-b} = U_d^{(3)}\big|_{\xi_3=H}$$

$$\left.\frac{\partial U_d^{(1)}}{\partial y}\right|_{y=b} = \left.\frac{\partial U_d^{(2)}}{\partial y}\right|_{\xi_2=H} \qquad \left.\frac{\partial U_d^{(1)}}{\partial y}\right|_{y=-b} = \left.\frac{\partial U_d^{(3)}}{\partial y}\right|_{\xi_3=H}$$

6 boundary conditions give 6 equations for 6 unknowns

$$A_1 = \frac{[(\alpha_2-1)\omega_2 H - k_1\alpha_2 + \alpha_2\eta_2](\alpha_3+\gamma_1 s_3 H)e^{\gamma_1 b} - [(\alpha_3-1)\omega_3 H - k_1\alpha_3 + \alpha_3\eta_3](\alpha_2-\gamma_1 s_2 H)e^{-\gamma_1 b}}{(\alpha_2+\gamma_1 s_2 H)(\alpha_3+\gamma_1 s_3 H)e^{2\gamma_1 b} - (\alpha_3-\gamma_1 s_3 H)(\alpha_2-\gamma_1 s_2 H)e^{-2\gamma_1 b}}$$

Back substitute coefficients into panel equations to give U_d as function of y

5. Testing a theoretical model

THE UNIVERSITY OF BIRMINGHAM

5.1 Overall integrity

5.2 Number of panels

5.3 Boundary conditions

International School of Hydraulics
May 2012
Lochow, Poland

Discharges (total & zonal)

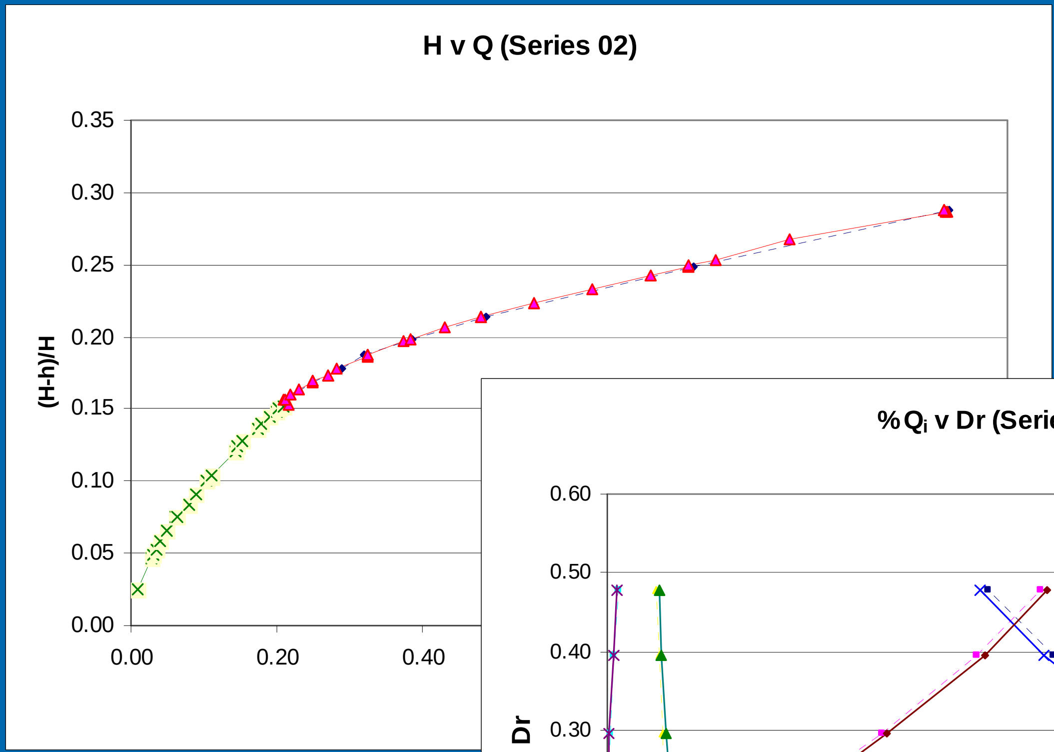

Fig. 15 *H* v *Q* simulation (FCF series 02)

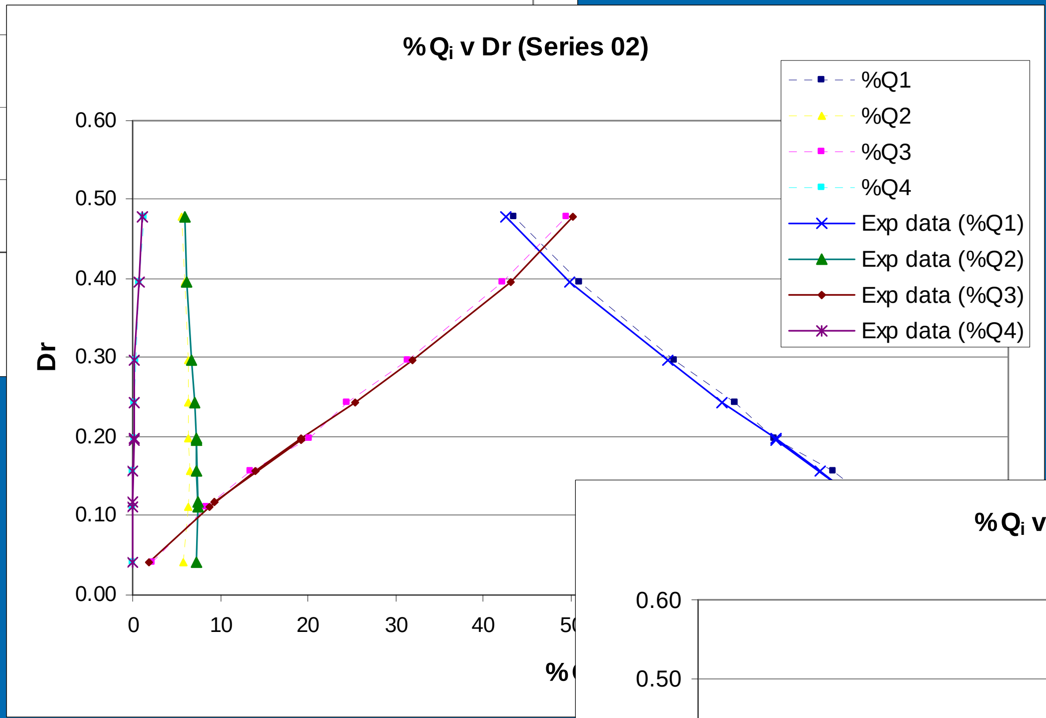

Fig. 16 $\%Q_i$ v Dr

Overall integrity

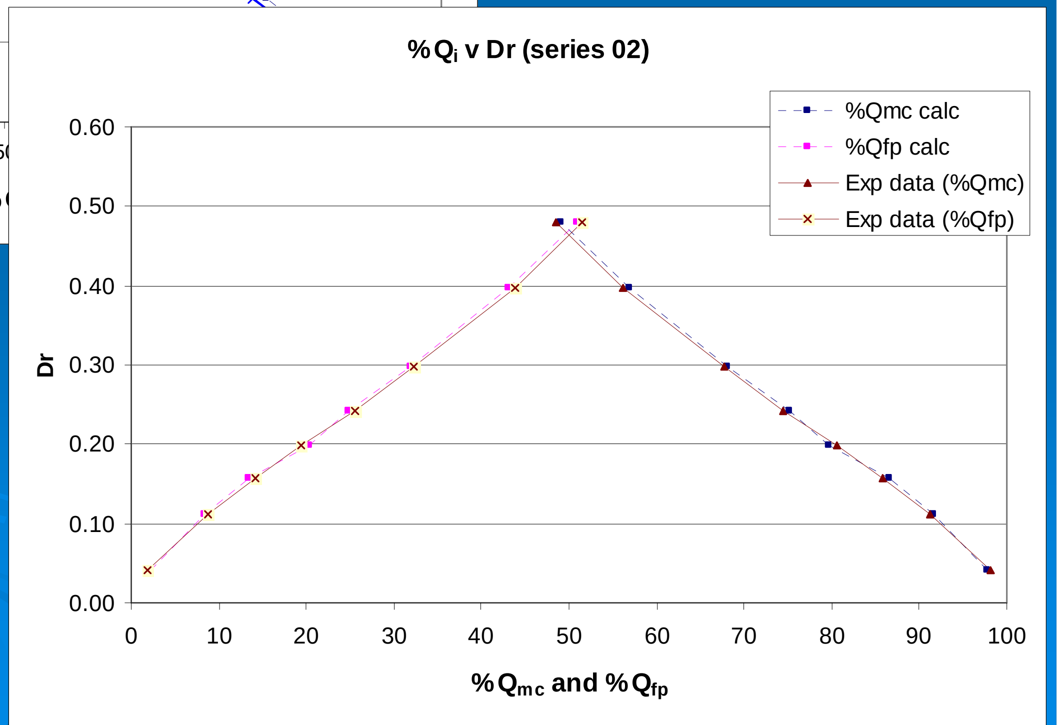

Fig. 17 $\%Q_{mc}$ & $\%Q_{fp}$ v Dr

Shear forces on different boundary elements

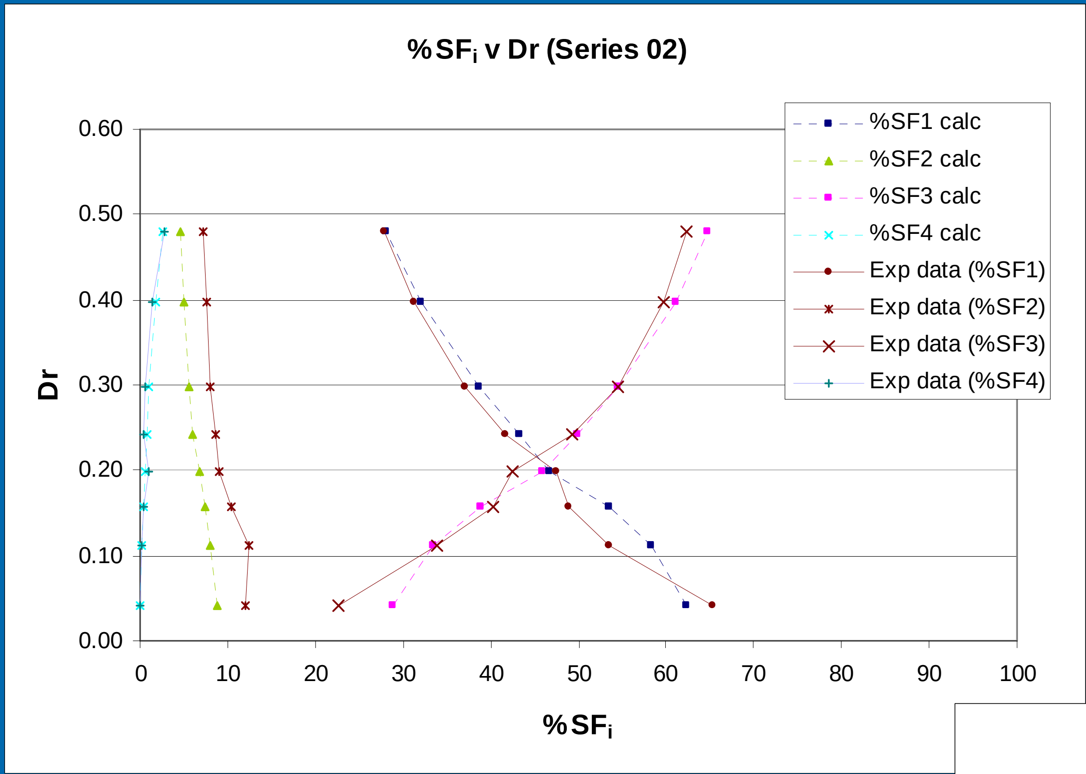

Fig. 18 %SF$_i$ v *Dr*

Overall integrity

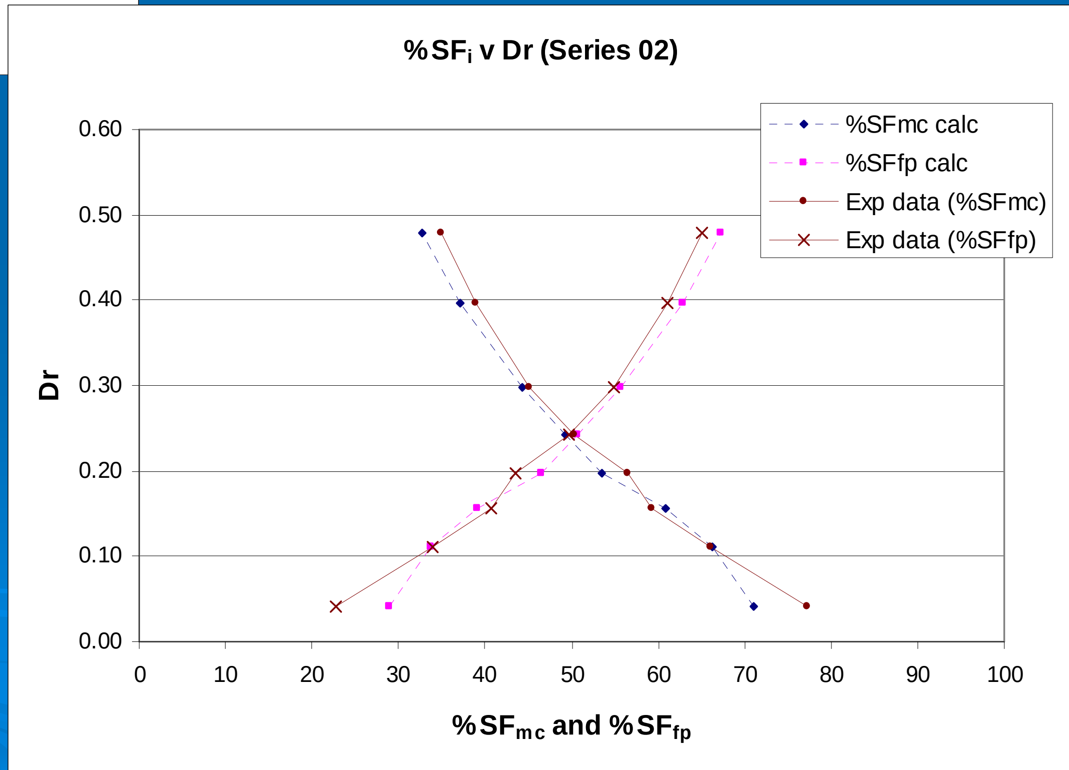

Fig. 19 %SF$_{mc}$ & %SF$_{fp}$ v *Dr*

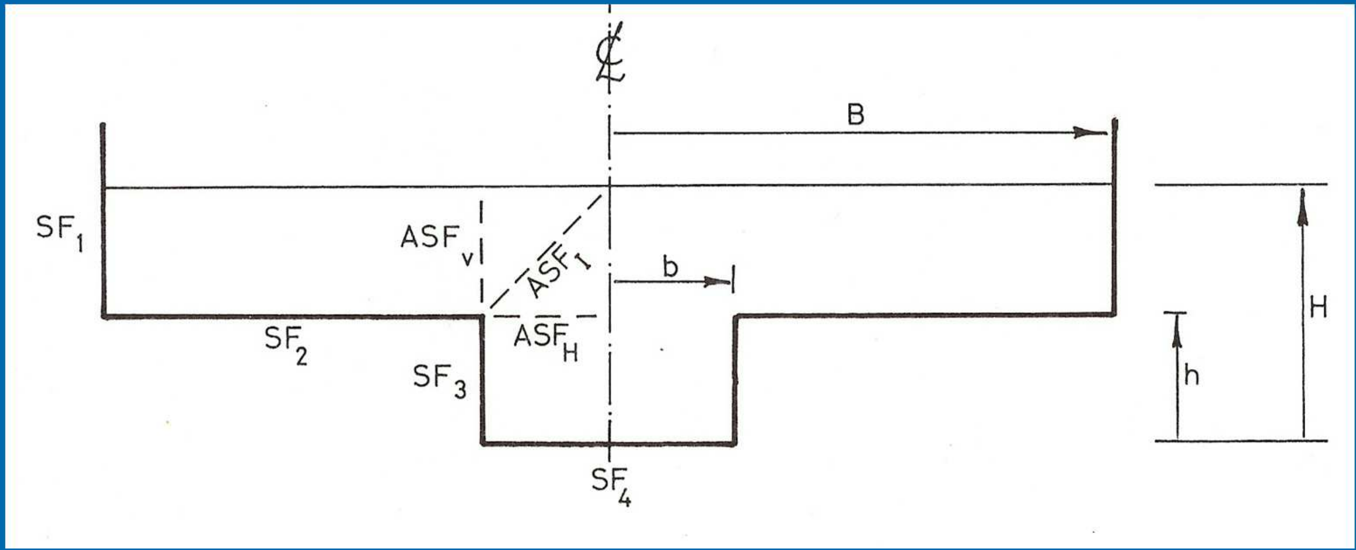

Apparent shear forces on different interfaces

Overall integrity

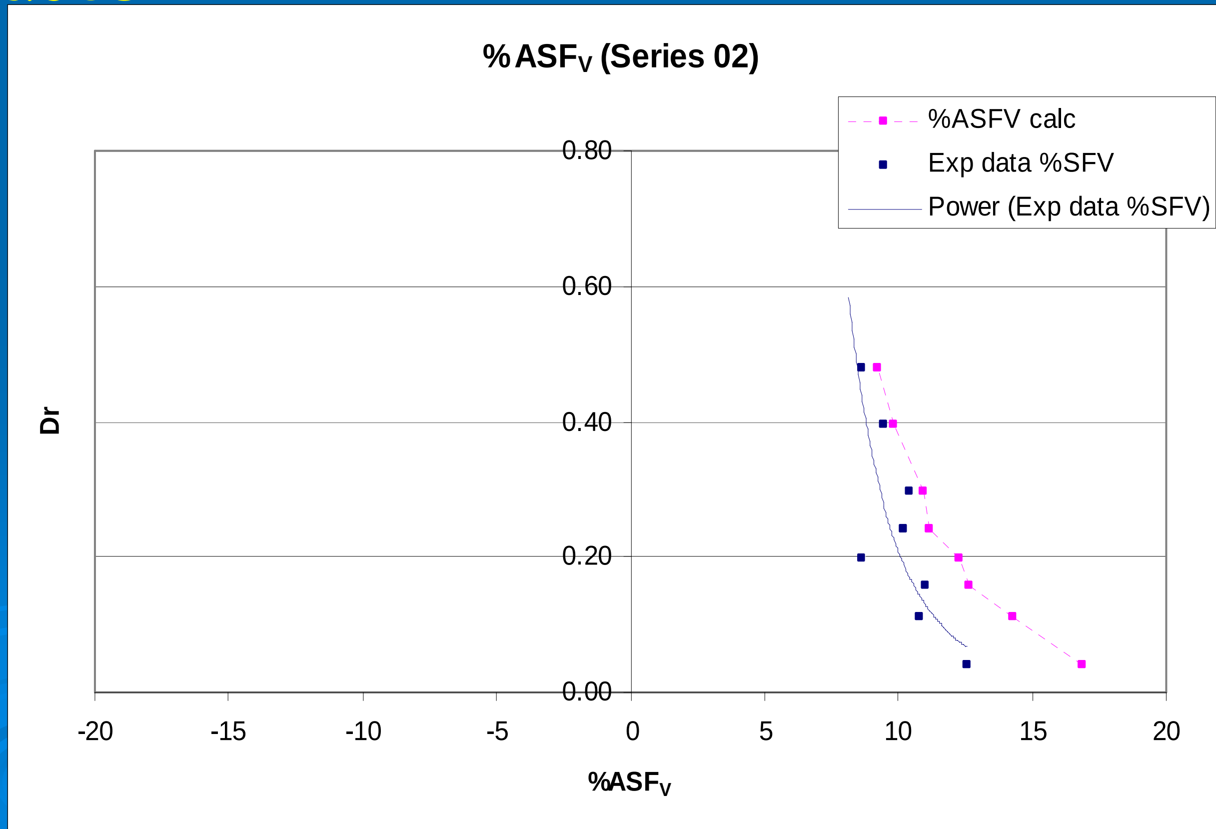

Fig. 20 $\%ASF_V$ v Dr

Apparent shear forces on different interfaces

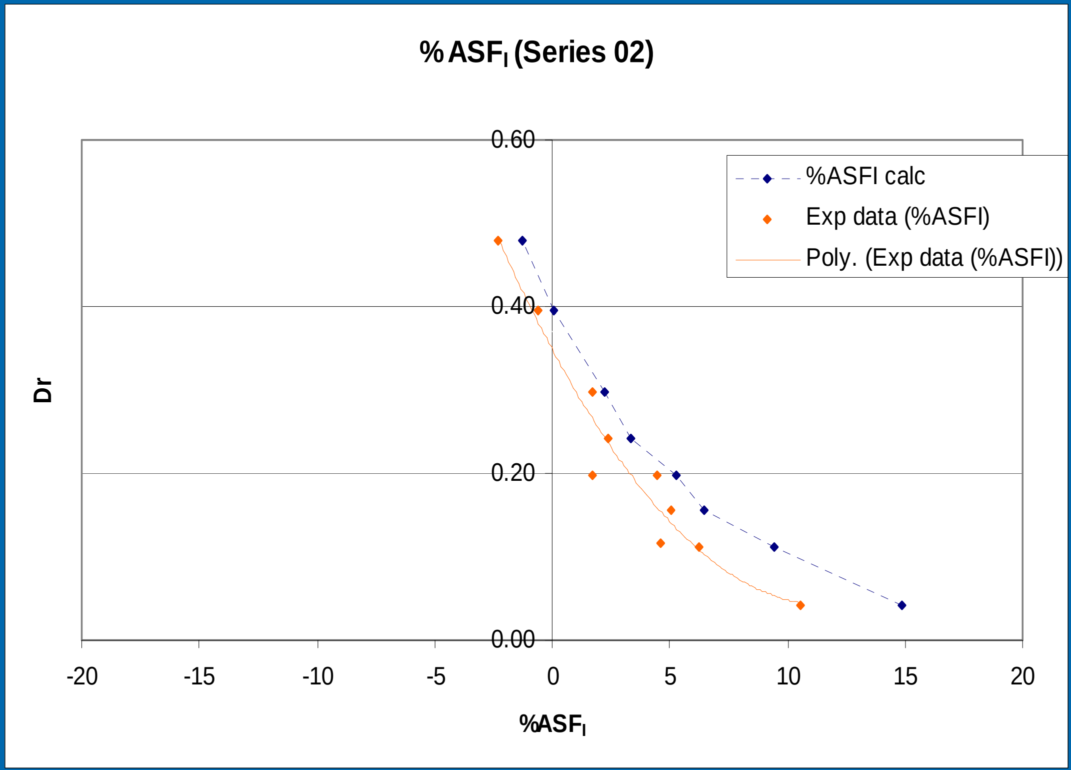

Fig. 21 %ASF_I v *Dr*

Overall integrity

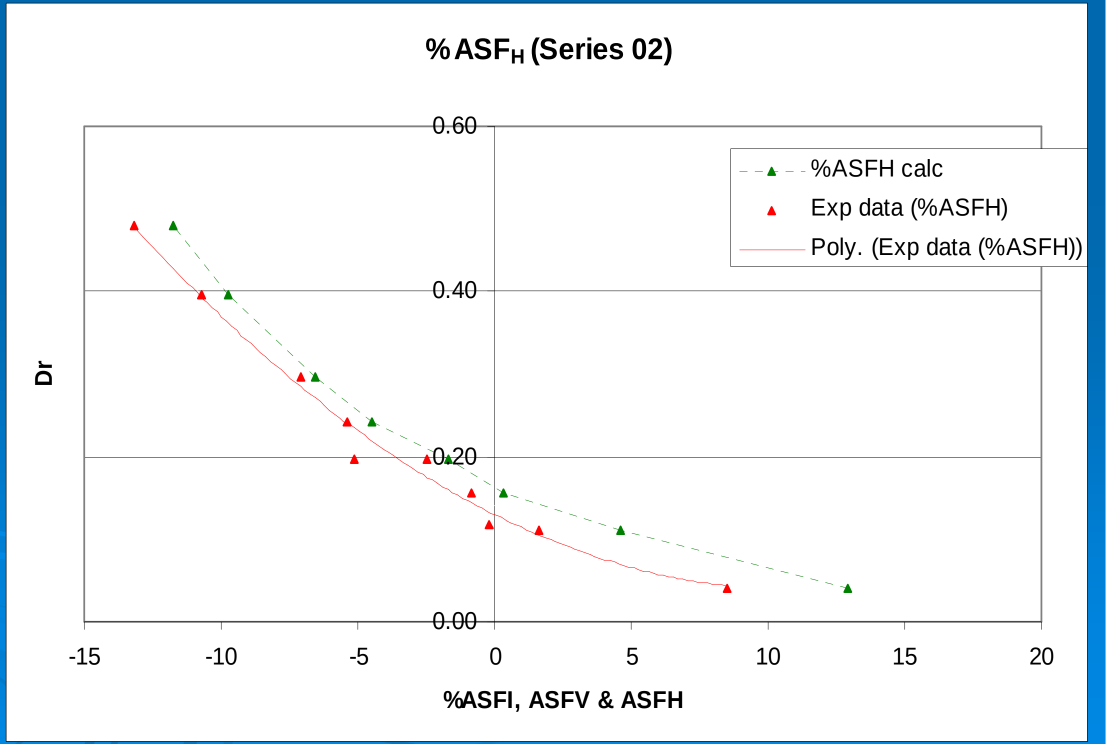

Fig. 22 %ASF_H v *Dr*

	Parameter	Error (%)
	Q total	**-0.11**
	SF total	**1.80**
Panel 1	$\mathbf{Q_1}$	**0.43**
Panel 2	Q_2	-7.40
Panel 3	$\mathbf{Q_3}$	**-0.02**
Panel 4	Q_4	51.98
Panels 1 & 2 (mc)	$\mathbf{Q_{mc}}$	**-0.35**
Panels 3 & 4 (fp)	$\mathbf{Q_{fp}}$	**0.39**
Panel 1	$\mathbf{SF_1}$	**0.89**
Panel 2	SF_2	-3.69
Panel 3	$\mathbf{SF_3}$	**1.63**
Panel 4	SF_4	194.78
Panels 1 & 2 (mc)	$\mathbf{SF_{mc}}$	**0.09**
Panels 3 & 4 (fp)	$\mathbf{SF_{fp}}$	**3.40**

Table 1 Errors in simulation for FCF experiment 020601

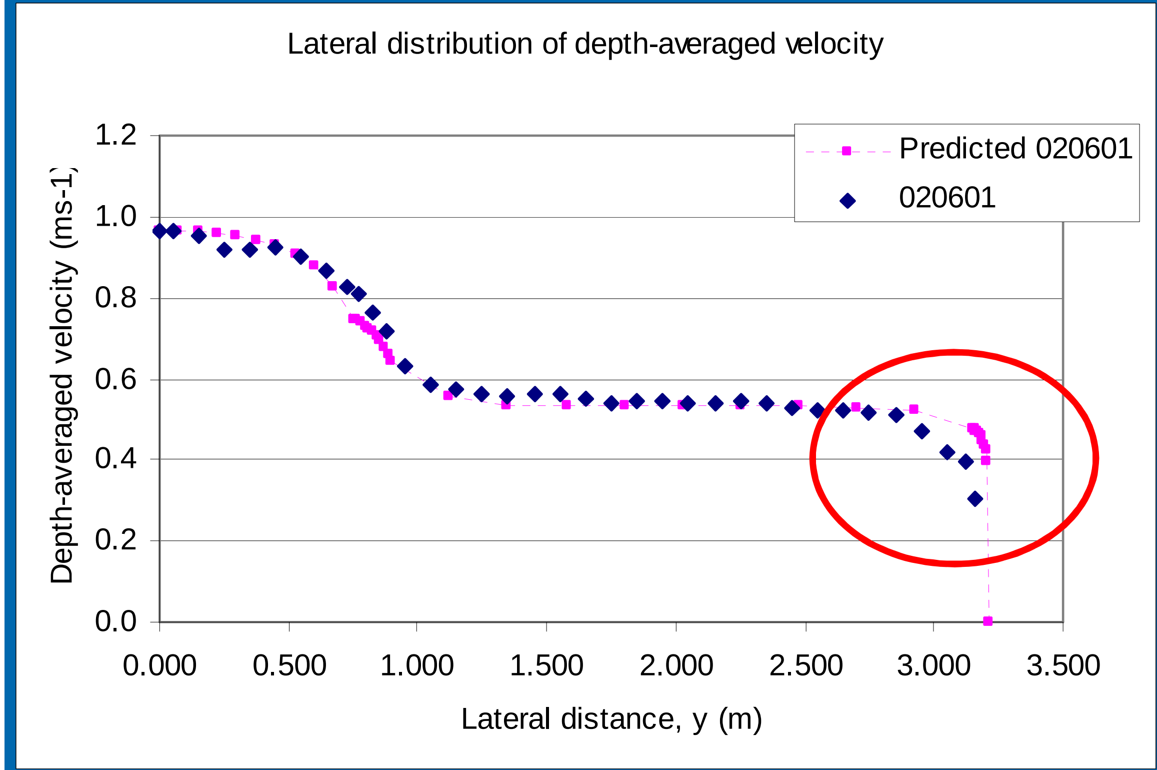

Lack of precision on edge of floodplain, due to only two panels being used for whole of floodplain

Fig. 11 Measured and predicted U_d v y

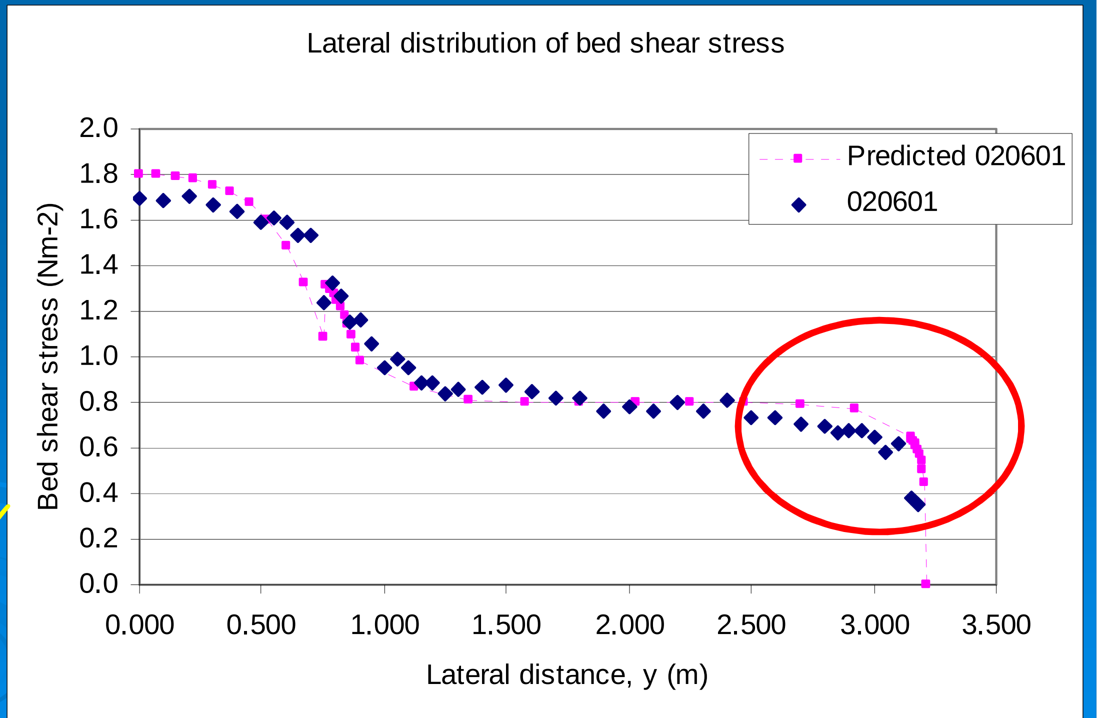

Fig. 12 Measured and predicted Tau_b v y

SKM approach

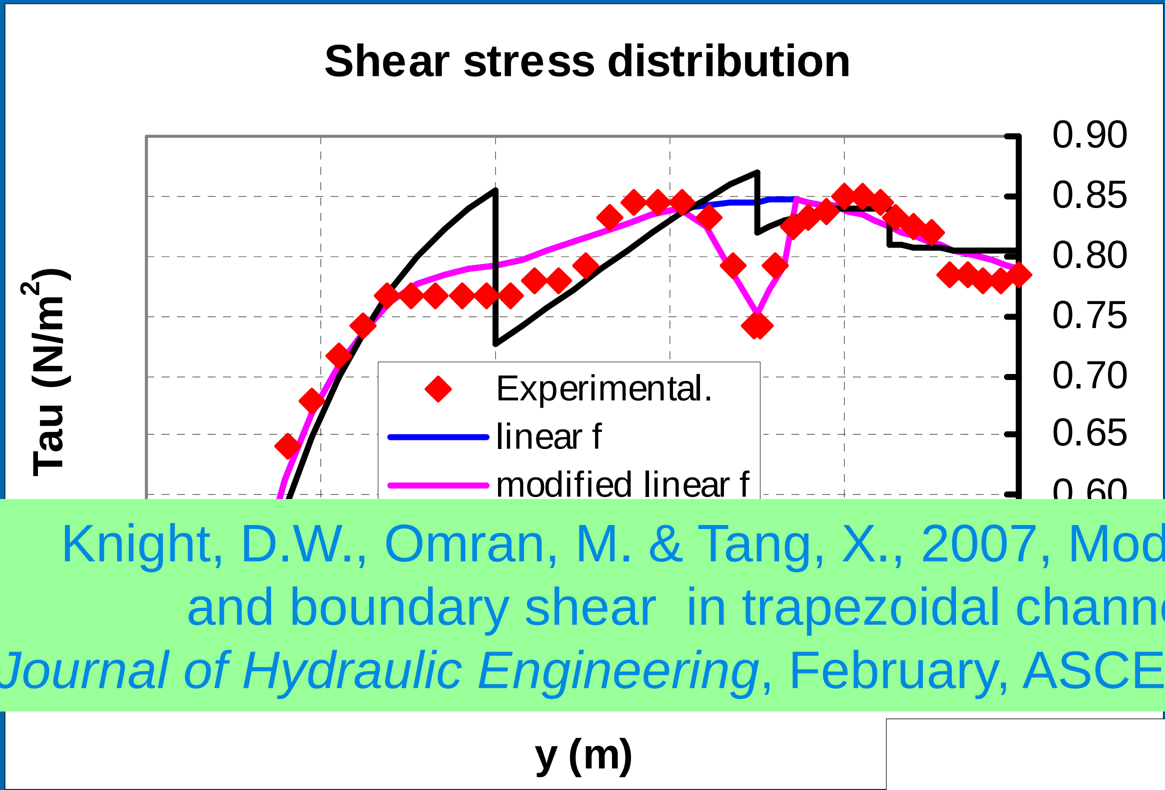

(a) Predicted τ_b using 6 panels (constant λ)

Knight, D.W., Omran, M. & Tang, X., 2007, Modelling depth-averaged velocity and boundary shear in trapezoidal channels with secondary flows, *Journal of Hydraulic Engineering*, February, ASCE, Vol. 133, No. 1, January, 39-47.

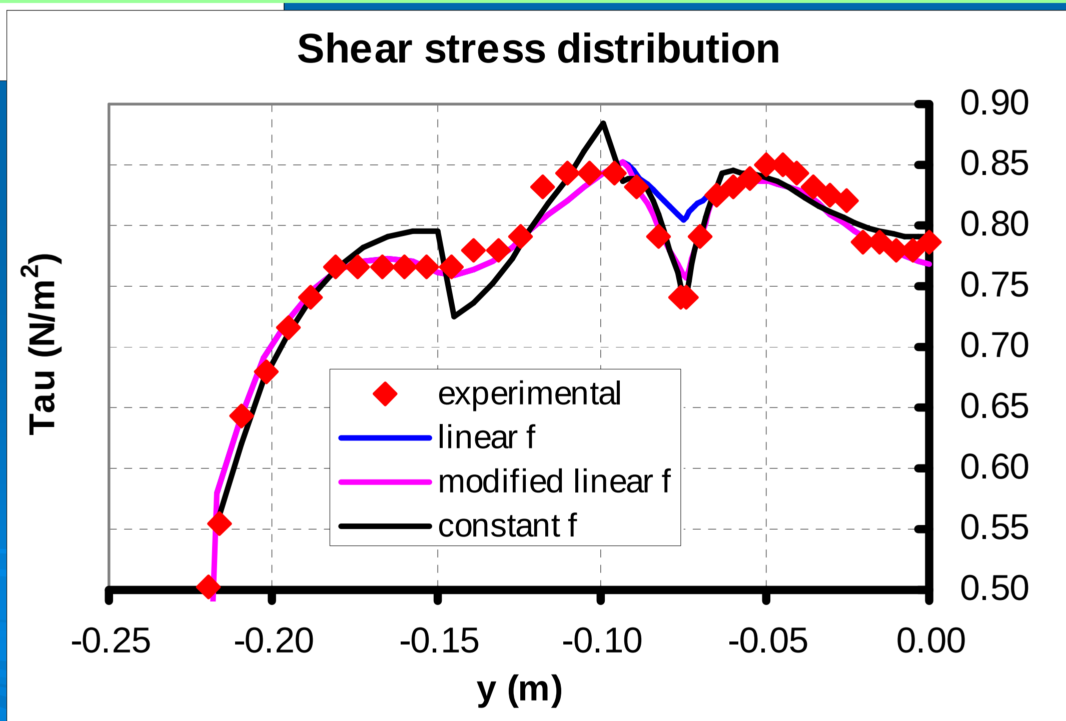

(b) Predicted τ_b using 6 panels (variable λ)

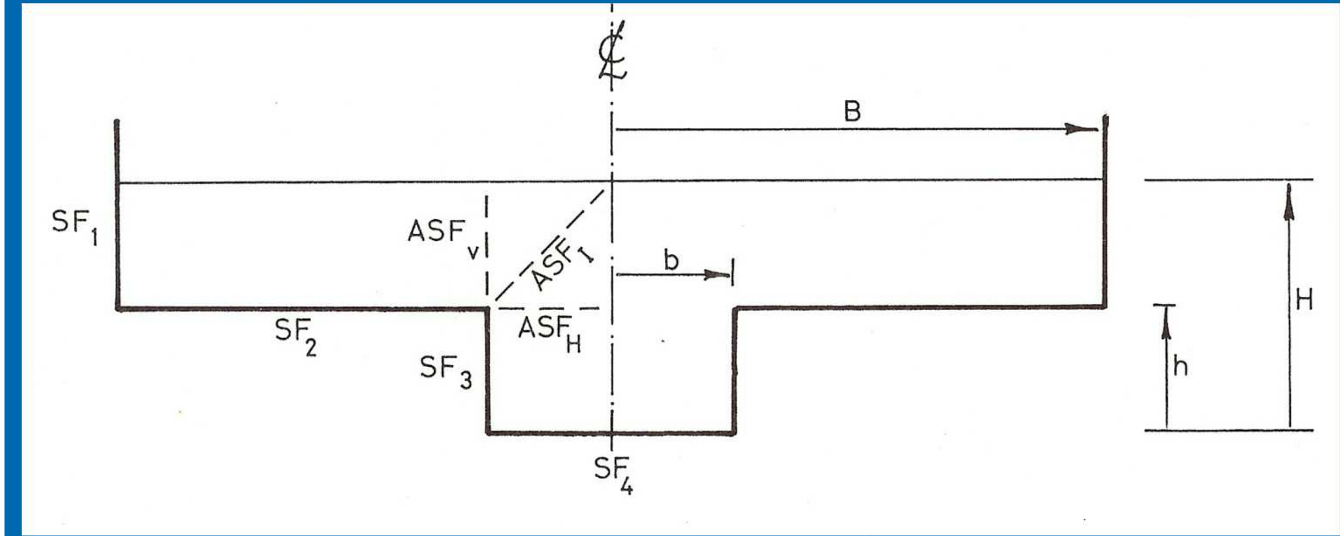

Further testing using different sets of data

(rectangular compound channel)

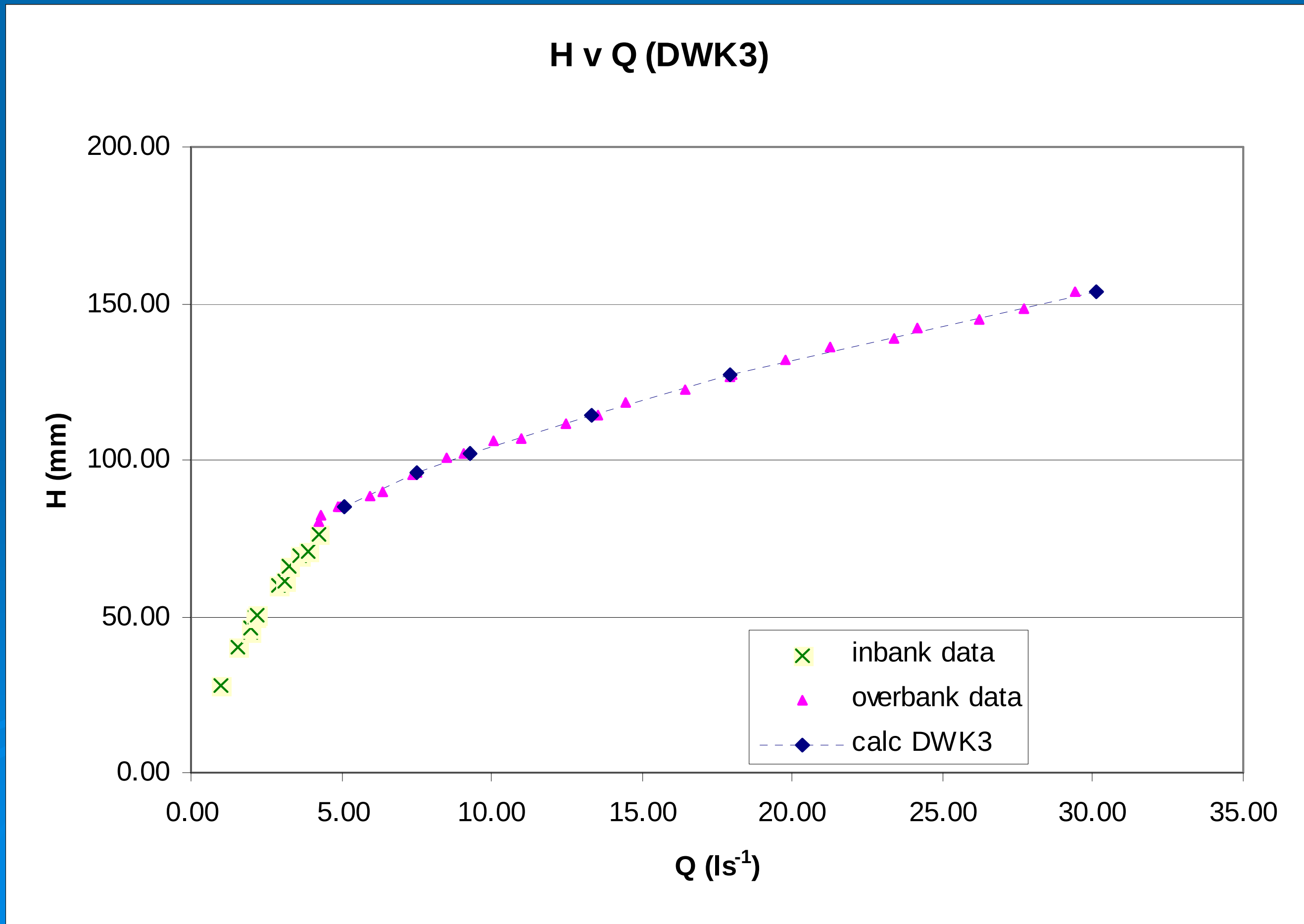

Fig. 24 H v Q (Series DWK3)

Discharges & shear forces (zonal & elements)

Fig. 25 %Q_{mc} v *Dr*

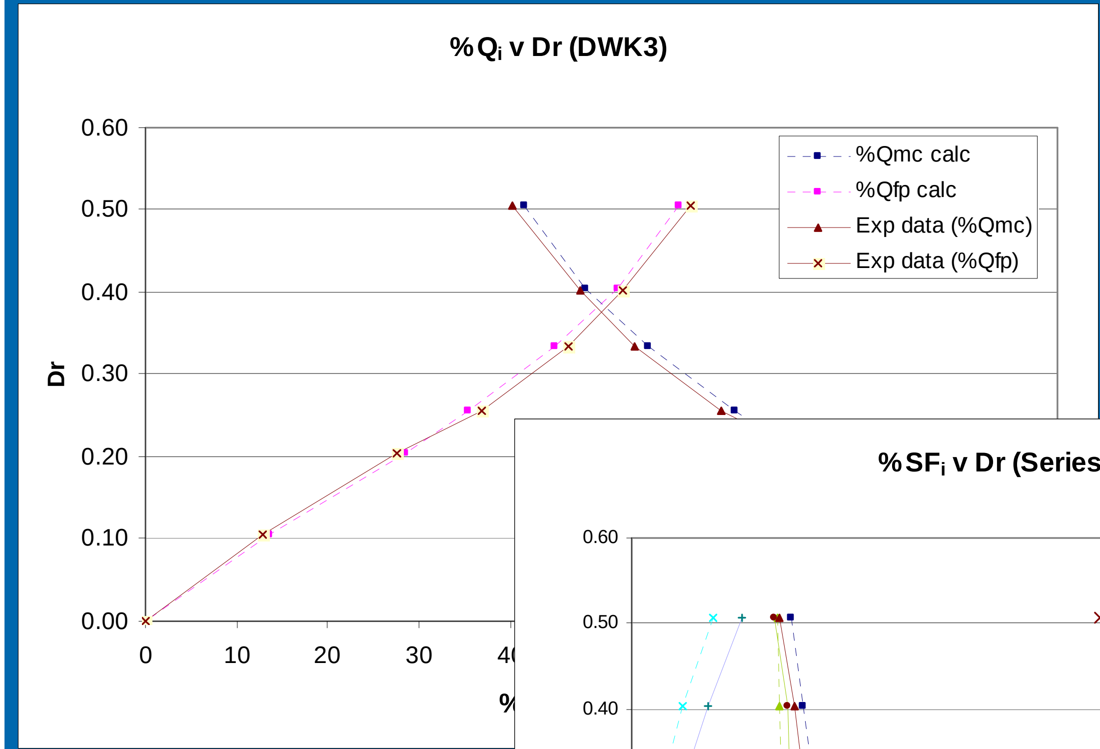

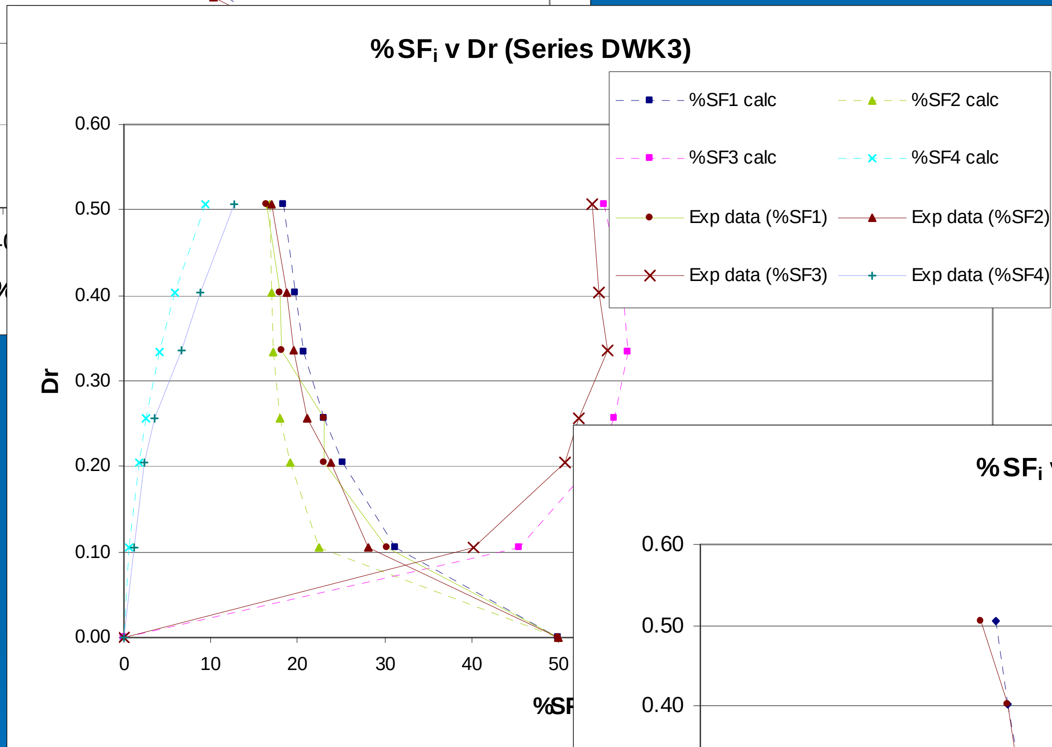

Fig. 26 %SF_i v *Dr*

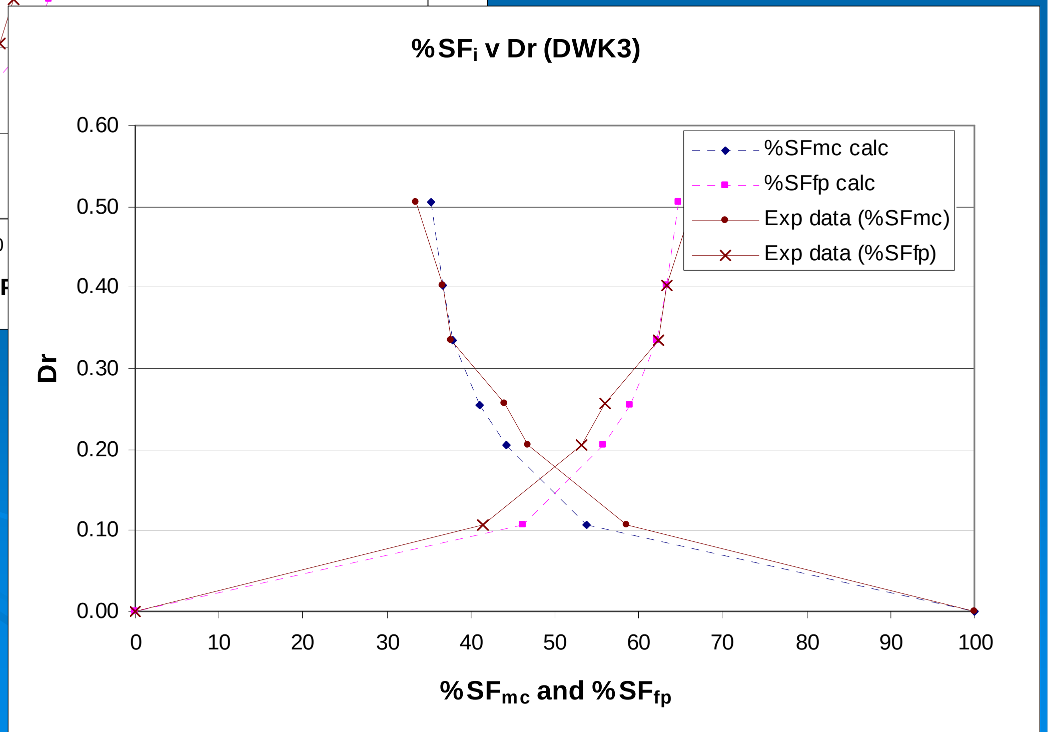

Fig. 27 %SF_v *Dr*

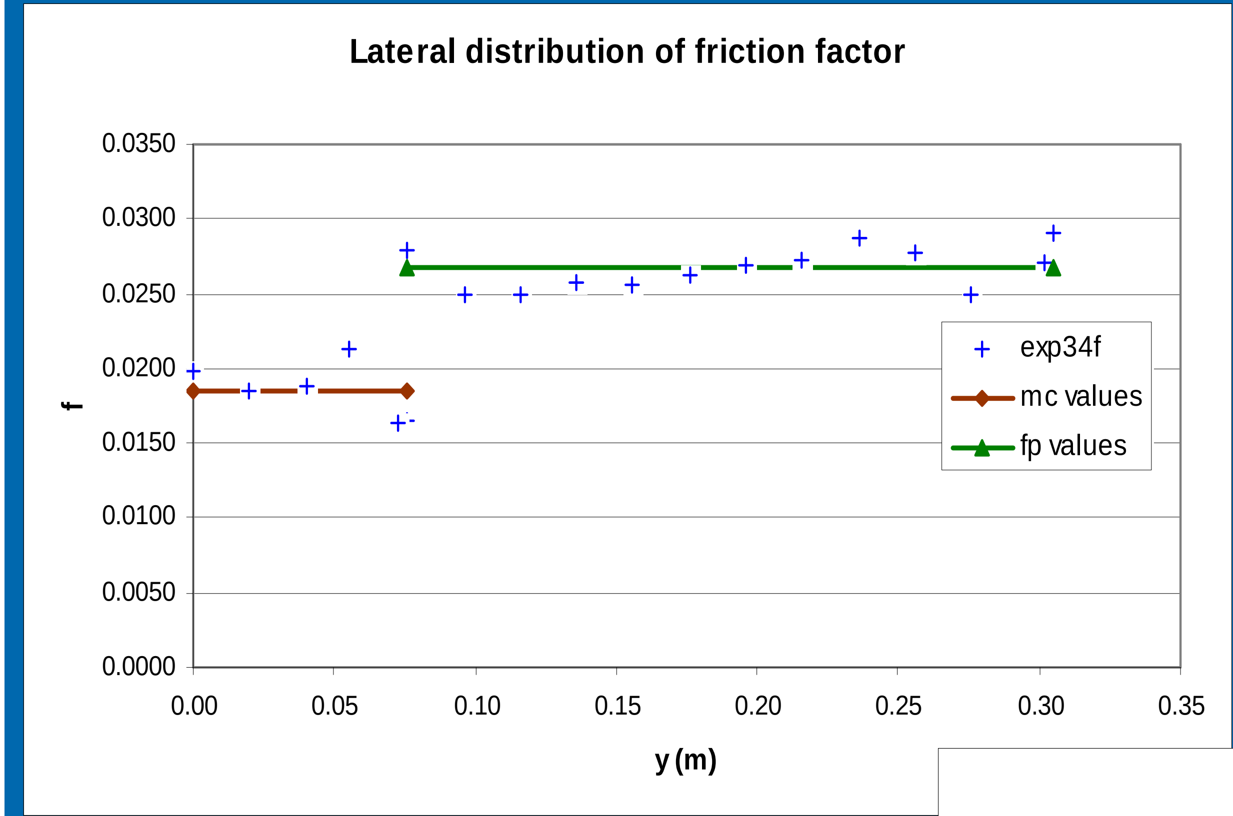

Fig. 28 f_{fp} and f_{mc} v y

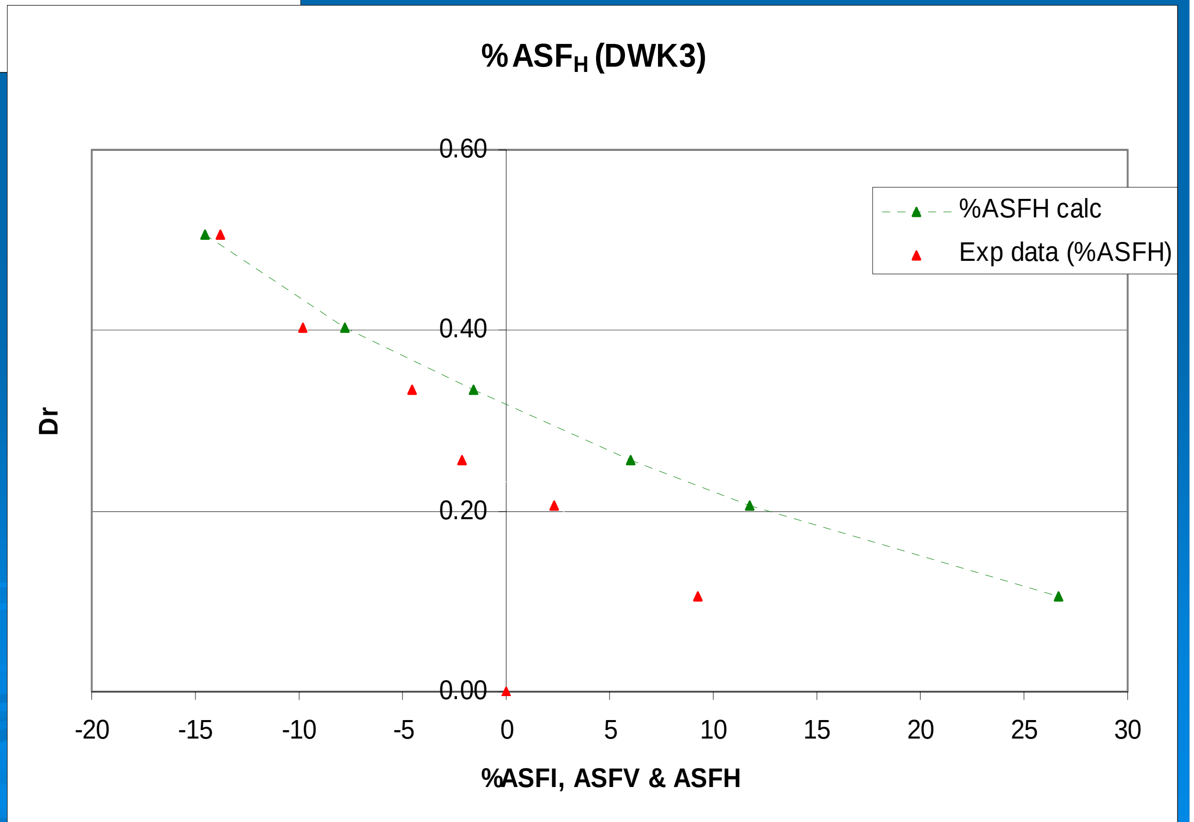

Fig. 29 %ASF$_H$ v Dr

Model simulations

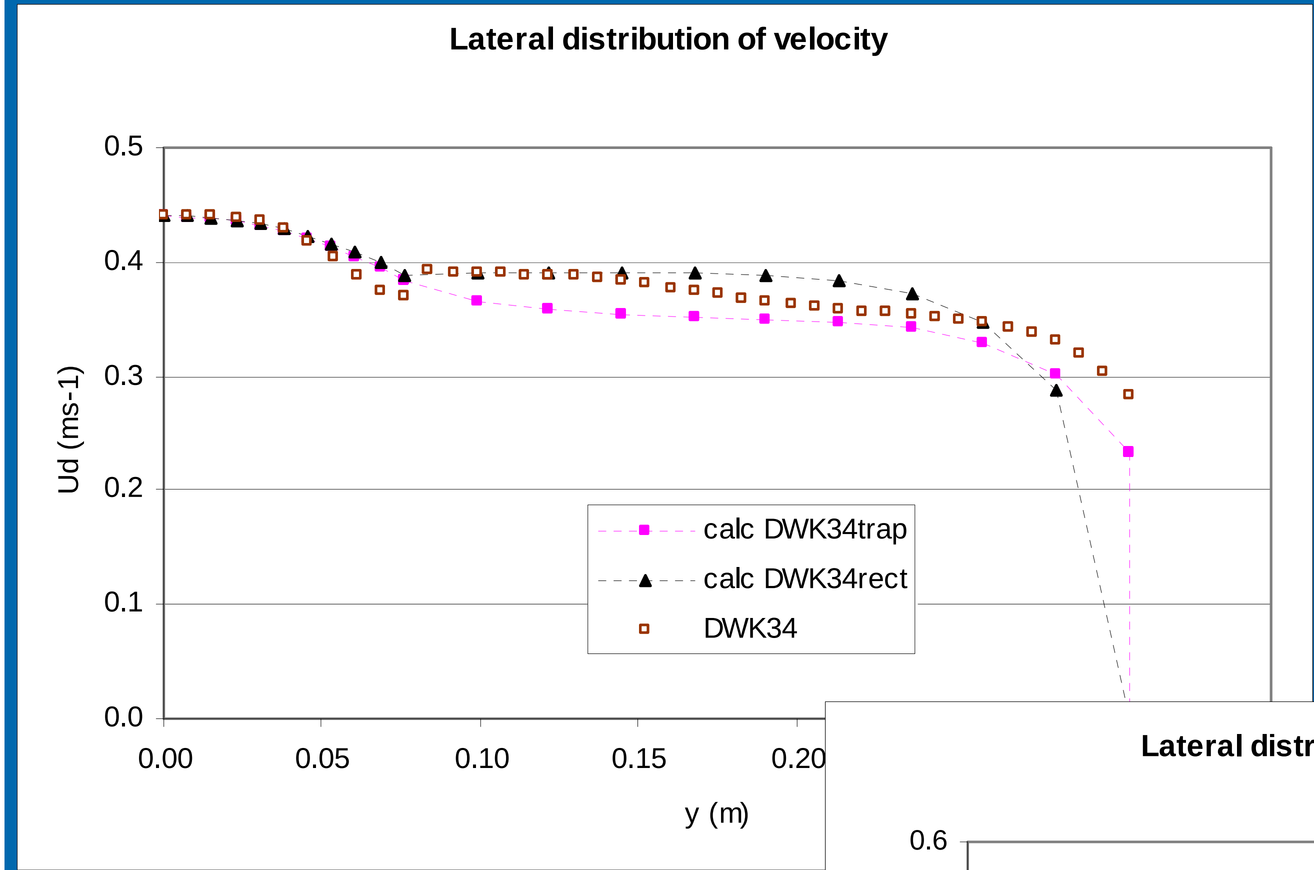

Fig. 30 Calculated and Experimental distributions of U_d (DWK34)

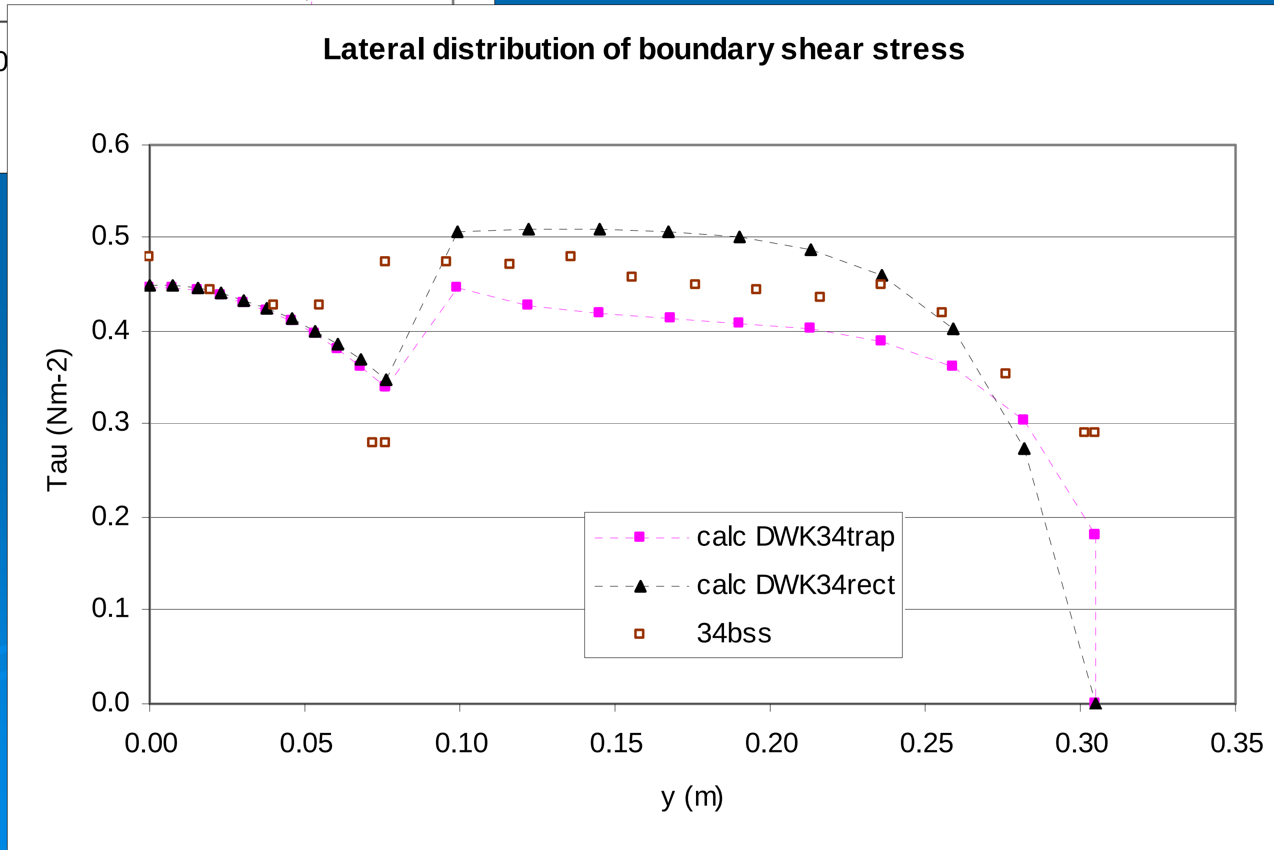

Fig. 31 Calculated and experimental distributions of boundary shear stress (DWK34)

Boundary conditions

For symmetric flow:

$$\left.\frac{\partial U_d^{(1)}}{\partial y}\right|_{y=0} = 0 \quad \text{(centerline) ;} \quad \left. U_d^{(2)}\right|_{y=B} = 0 \quad \text{(floodplain edge)}$$

For vertical internal interfaces

$$\left(H\bar{\tau}_{yx}\right)_{y=b}^{(i)} + h\tau_W = \left(H\bar{\tau}_{yx}\right)_{y=b}^{(i+1)}$$

$$\left(\phi\frac{\partial U_d^2}{\partial y}\right)_{y=b}^{(1)} = \left(\phi\frac{\partial U_d^2}{\partial y}\right)_{y=b}^{(2)} - h\tau_w \quad \text{where} \quad \phi = \frac{1}{2}\rho\lambda H^2\sqrt{f/8}$$

and $\quad \tau_w = \rho f_w U_d^2(y=b)/8$

Boundary condition	U_d or *q* continuity	U_d gradient or unit force continuity	Notes
[A]	$U_d^{(1)} = U_d^{(2)}$	$\left(\phi \frac{\partial U_d^2}{\partial y}\right)_{y=b}^{(1)} = \left(\phi \frac{\partial U_d^2}{\partial y}\right)_{y=b}^{(2)} - h\tau_w$	$\phi = \frac{1}{2}\rho\lambda H^2\sqrt{f/8}$ $\tau_w = \rho f_w U_d^2(y=b)/8$
[B]	$U_d^{(1)} = U_d^{(2)}$	$\left(\mu \frac{\partial U_d}{\partial y}\right)_{y=b}^{(1)} = \left(\varphi\mu \frac{\partial U_d}{\partial y}\right)_{y=b}^{(2)}$	$\mu = H^2\lambda\sqrt{f}$ with an adjust-ment factor, phi
[C]	$[HU_d]^{(1)} = [HU_d]^{(2)}$	$\left(\frac{\partial U_d}{\partial y}\right)_{y=b}^{(1)} = \left(\frac{\partial U_d}{\partial y}\right)_{y=b}^{(2)}$	
[D]	$U_d^{(1)} = U_d^{(2)}$	$\left(\mu \frac{\partial U_d}{\partial y}\right)_{y=b}^{(1)} = \left(\mu \frac{\partial U_d}{\partial y}\right)_{y=b}^{(2)}$	$\mu = H^2\lambda\sqrt{f}$
[E]	$U_d^{(1)} = U_d^{(2)}$	$\left(\frac{\partial U_d}{\partial y}\right)_{y=b}^{(1)} = \left(\frac{\partial U_d}{\partial y}\right)_{y=b}^{(2)}$	

Tang X and Knight DW (2008) Lateral depth-averaged velocity distributions and bed shear in rectangular compound channels. *Journal of Hydraulic Engineering*, ASCE, 134, No. 9, September, 1337-1342

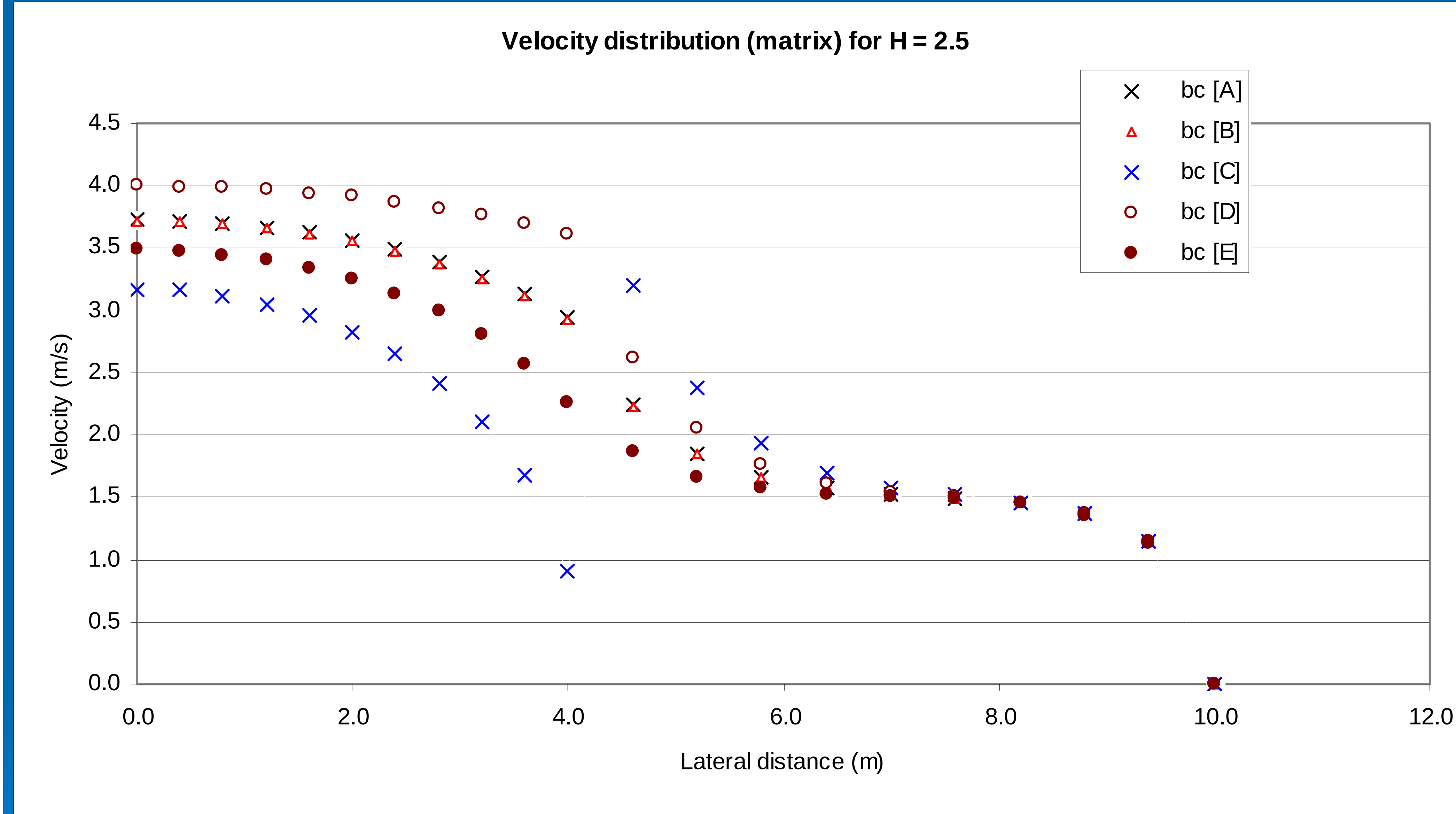

Fig. 32 Effect of different boundary conditions on U_d for a symmetric rectangular compound channel for H = 2.5m (So = 0.001, b = 4m, B =10m, h = 2m; $f_1 = f_w$ =0.01 & f_2 =0.02; λ_1 =0.01 & λ_2 = 0.2; Γ_1 = 1.0 & Γ_2= -0.75)

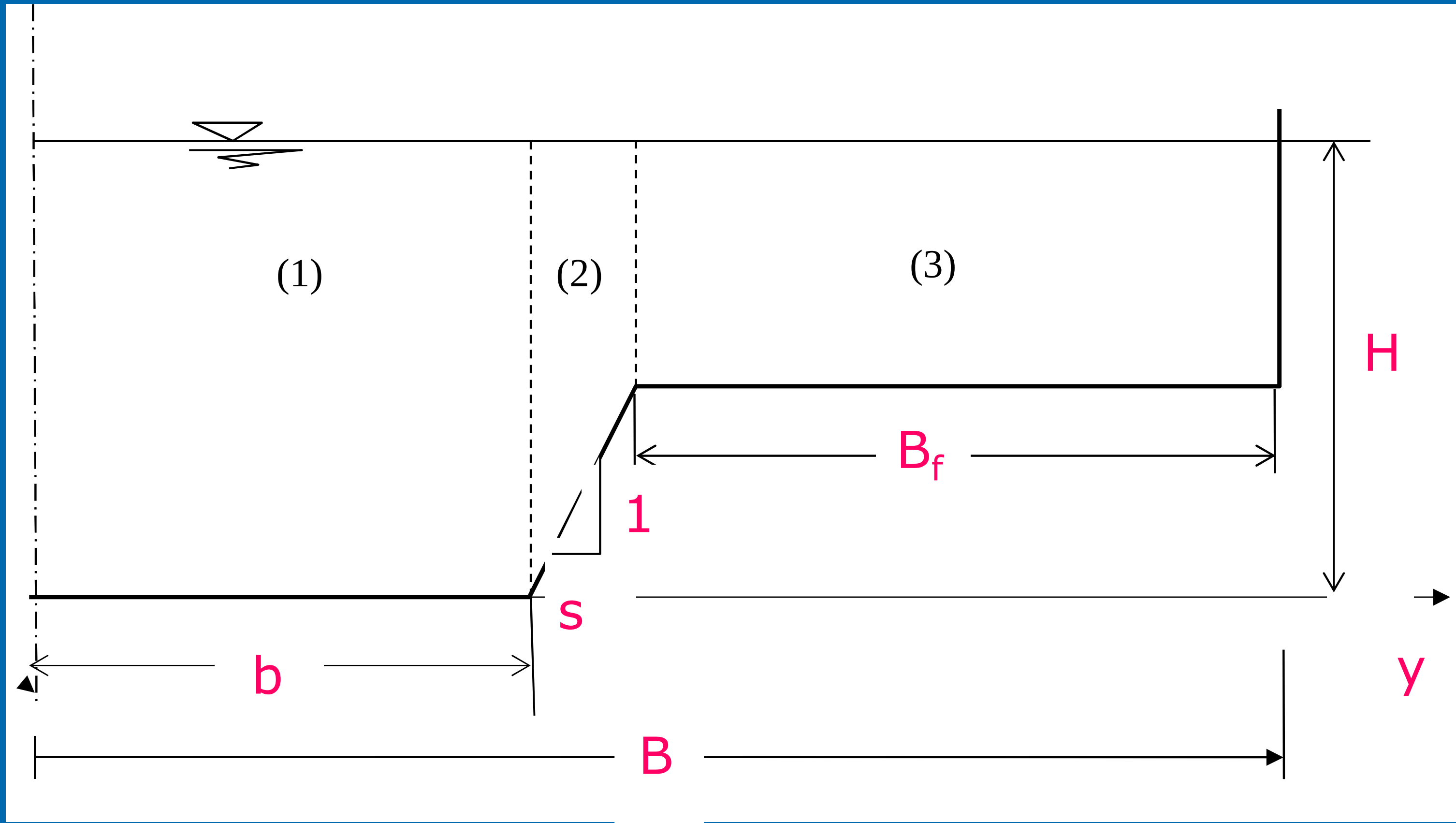

Fig. 33 Symmetric compound channel with a very steep internal wall

Comparisons (H=2.5, 3.0 & 4.0m)

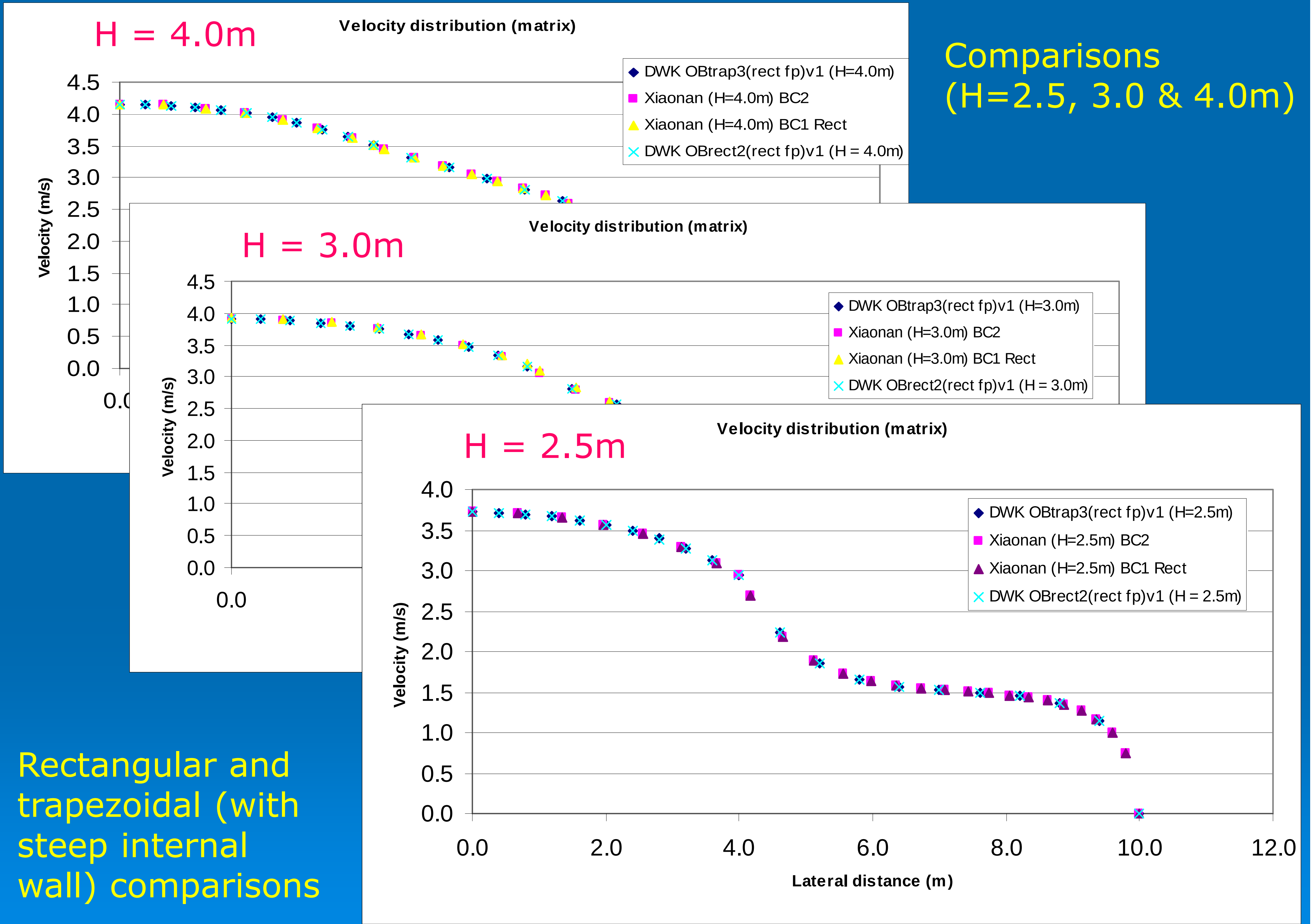

Rectangular and trapezoidal (with steep internal wall) comparisons

6. Using a model in practice

THE UNIVERSITY OF BIRMINGHAM

6.1 Getting a software company

6.2 Setting the technical objectives for solution

6.3 Testing against a wider spectrum of data

6.4 Introducing new technical capabilities & tools

International School of Hydraulics
May 2012
Lochow, Poland

CES predicted flows v measured flows

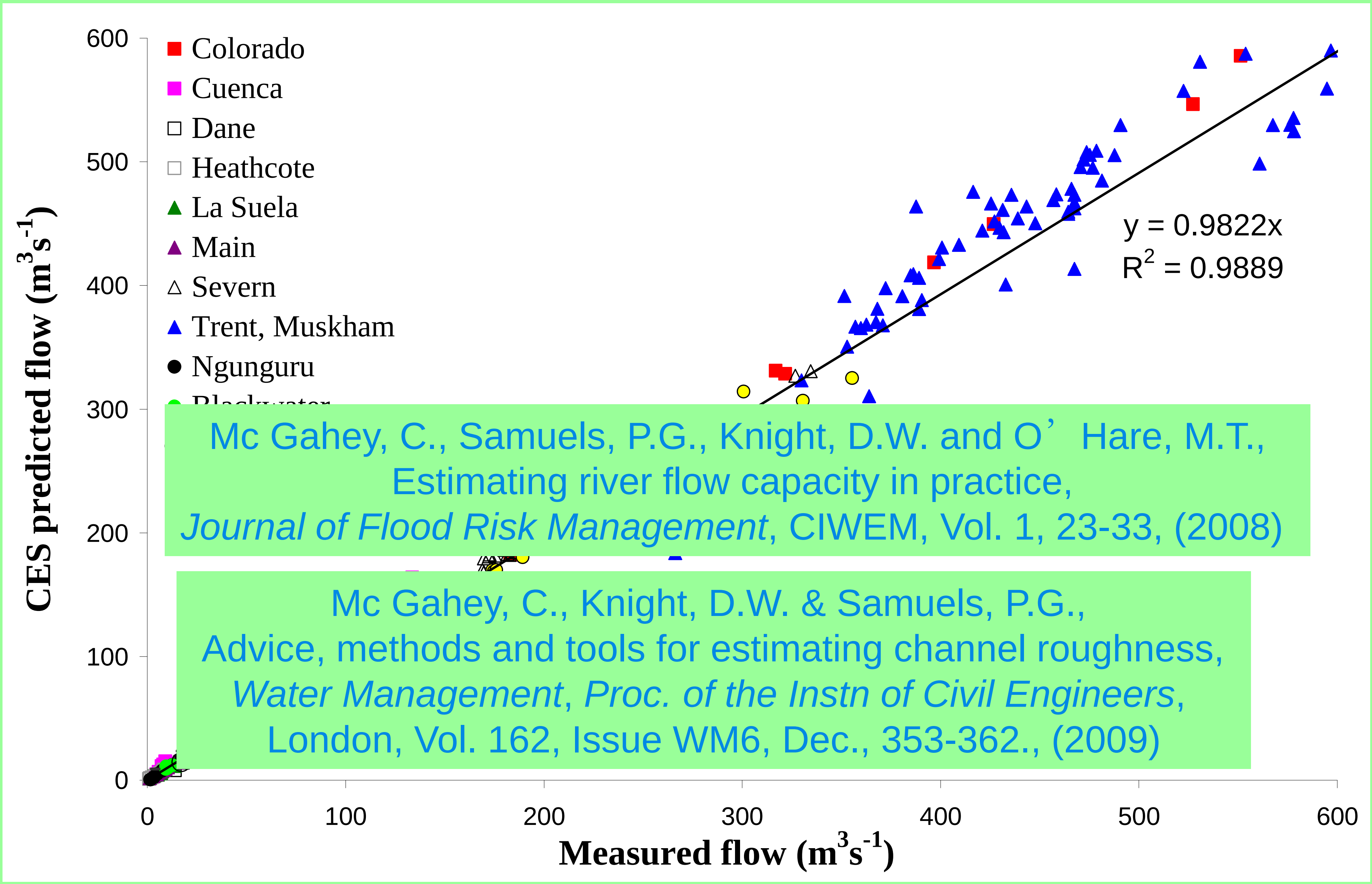

Mc Gahey, C., Samuels, P.G., Knight, D.W. and O'Hare, M.T., Estimating river flow capacity in practice, *Journal of Flood Risk Management*, CIWEM, Vol. 1, 23-33, (2008)

Mc Gahey, C., Knight, D.W. & Samuels, P.G., Advice, methods and tools for estimating channel roughness, *Water Management*, *Proc. of the Instn of Civil Engineers*, London, Vol. 162, Issue WM6, Dec., 353-362., (2009)

River Waiwakaiho (New Zealand) and River Tomebamba (Ecuador)
(boulder sizes ~ 1-2 m)

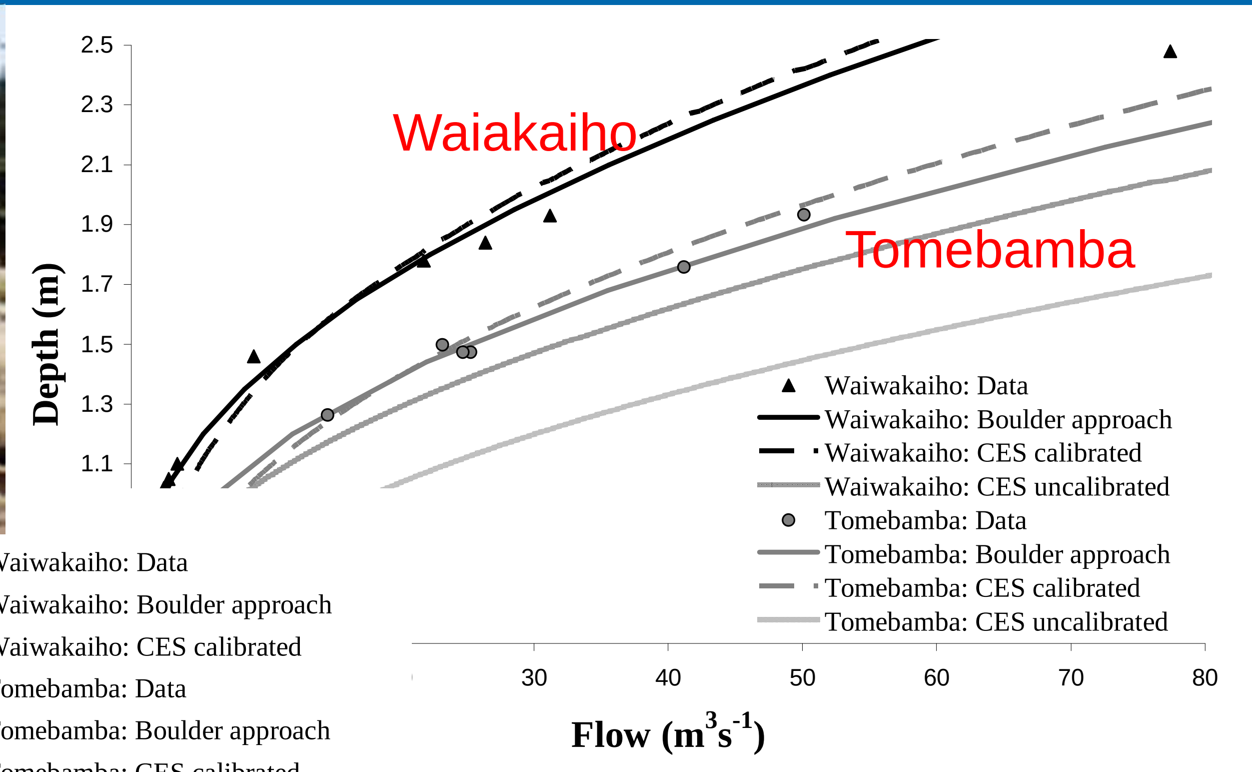

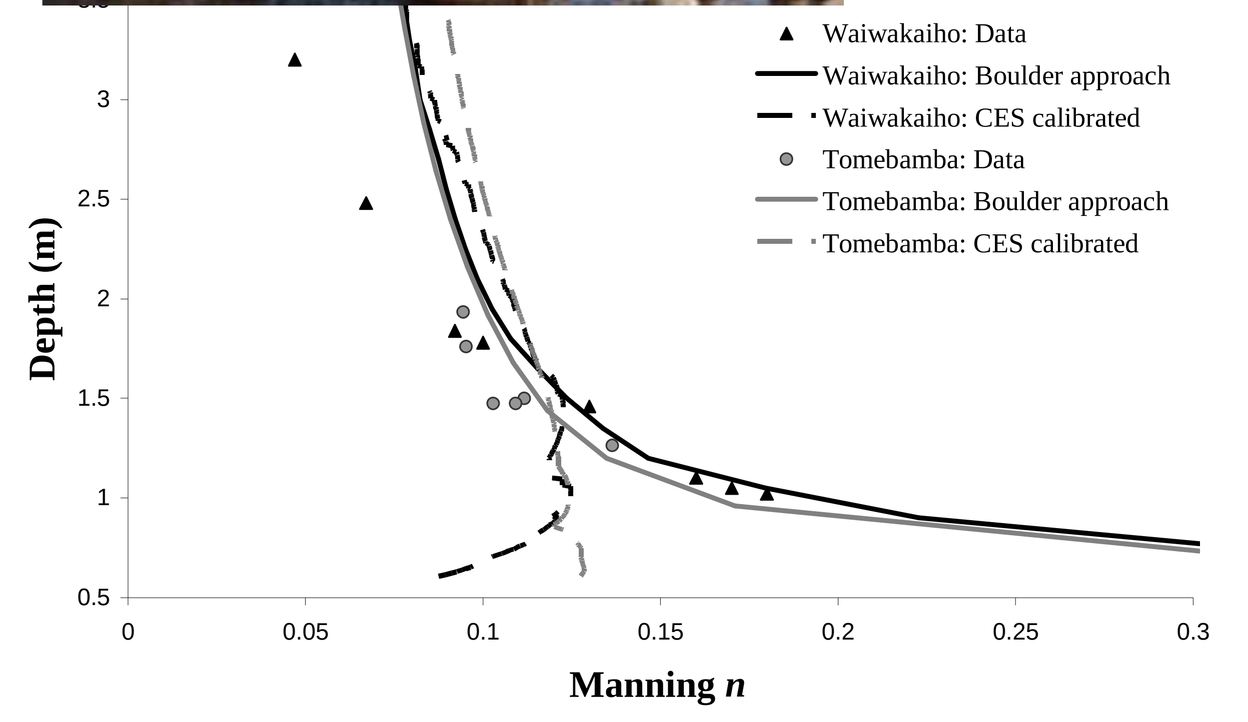

Variation of roughness with depth

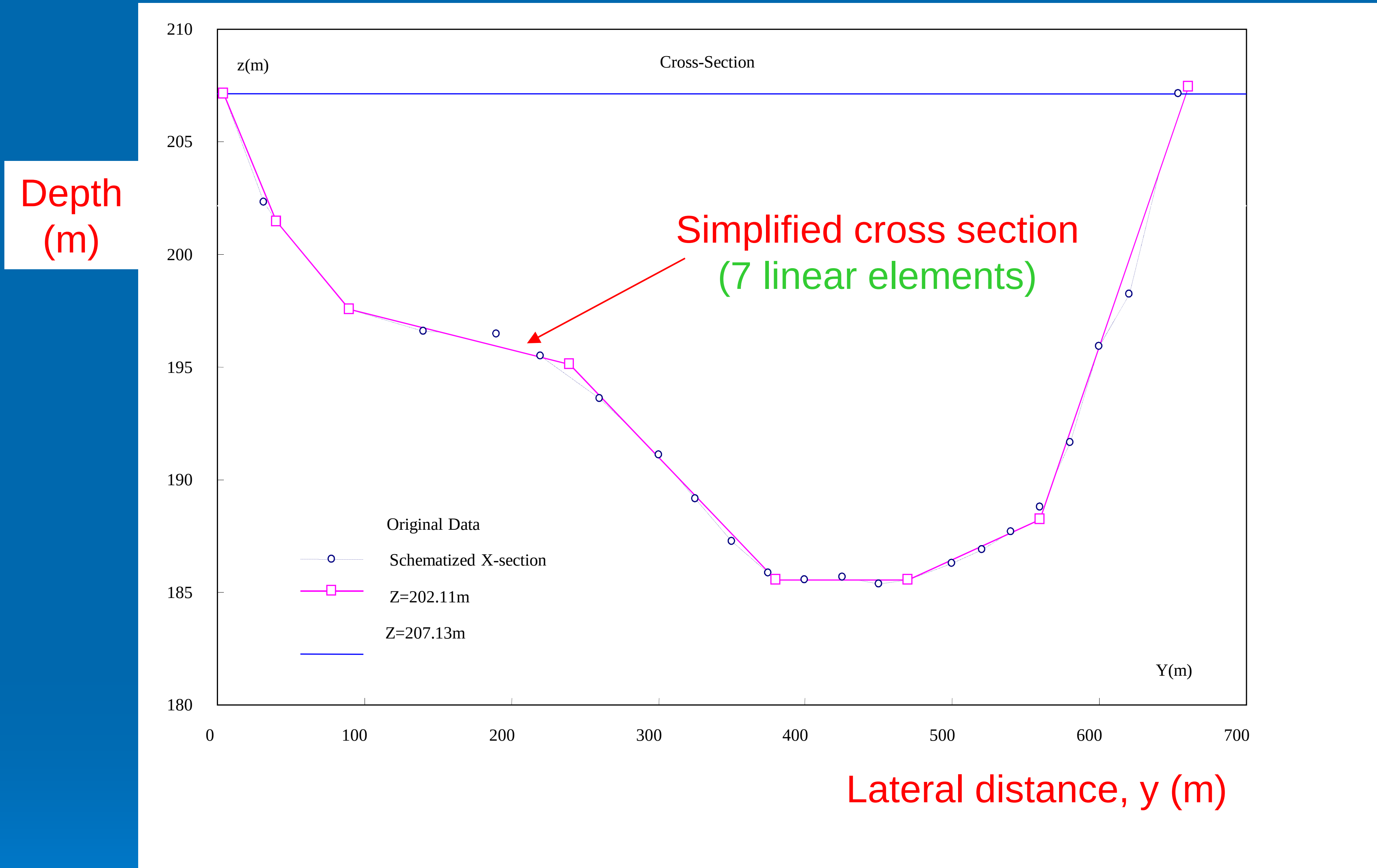

Fig. 7 Schematized and actual cross-section of River Yangtze at ZhuTuo gauging station (7 panels)

U_d (ms^{-1})

Measured $Q = 23{,}127\ m^3s^{-1}$

Predicted $Q = 22{,}924\ m^3s^{-1}$

Difference = - 0.9%

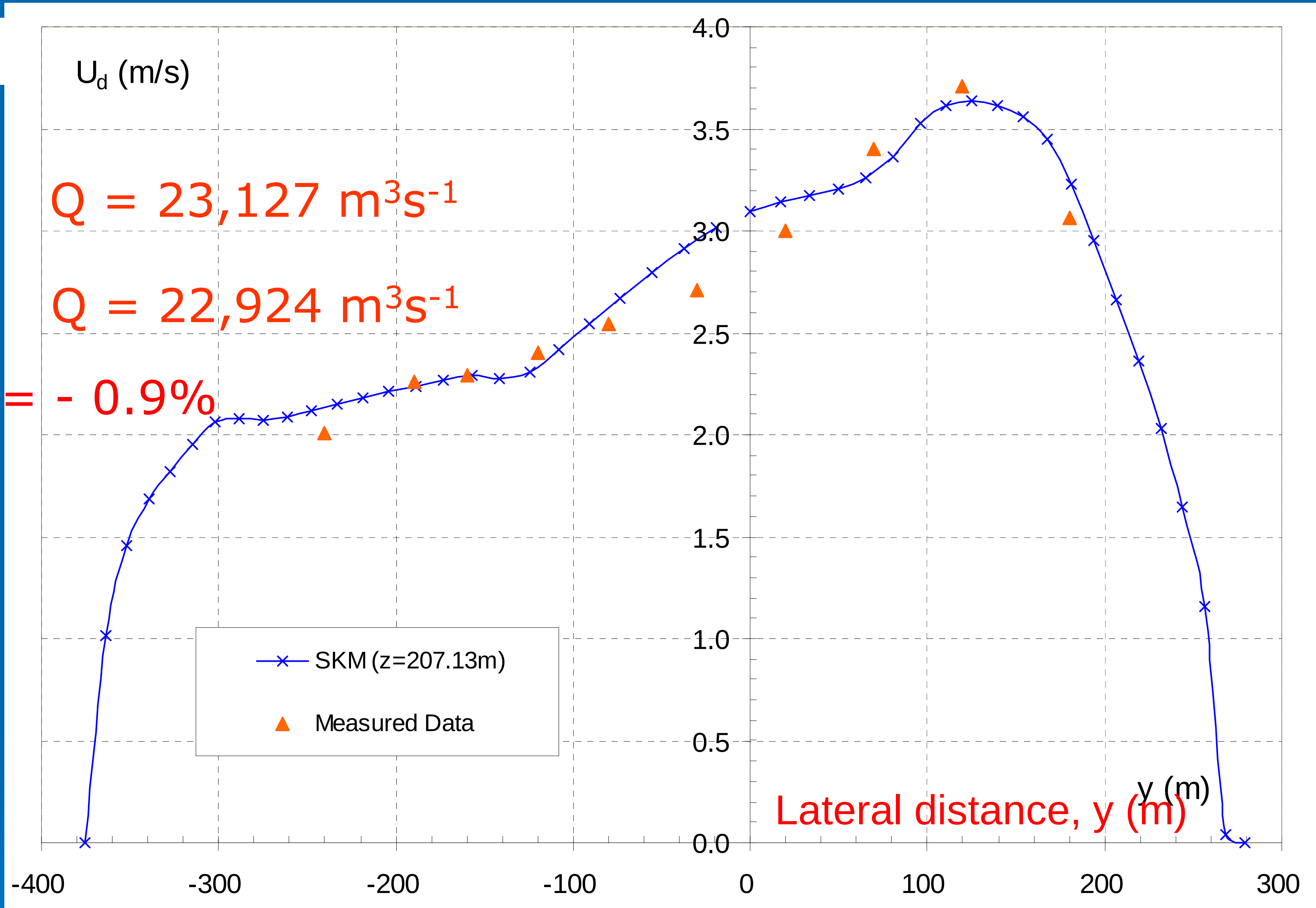

Lateral distance, y (m)

Fig. 9 Predicted and measured velocity distribution in River Yangtze at Zhu Tuo gauging station for a water level, z = 207.13m

2. Analytic Discharge Formula for Case II

Liao, H. and Knight, D.W. 2007a. Analytic stage-discharge formulas for flow in straight prismatic channels, *Journal of Hydraulic Engineering*, ASCE, Vol. 133, No. 10, October, 1111-1122.

Liao, H. and Knight, D.W. 2007b. Analytic stage-discharge formulae for flow in straight trapezoidal open channels, *Advances in Water Resources*, Elsevier, Vol. 30, Issue 11, November, 2283-2295.

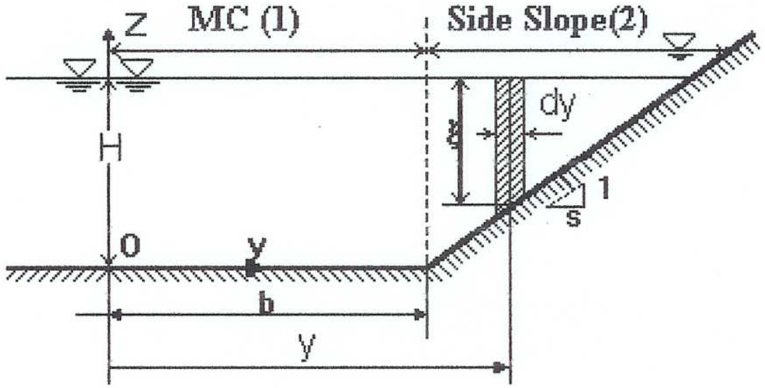

Fig.8 Trapezoidal Channel

$$Q = H\int_0^b \sqrt{2A_1\cosh(\gamma_1 y) + C_1}\,dy - s\int_H^0 \sqrt{A_3\xi^\alpha + \omega_2\xi}\cdot\xi d\xi$$

$$\begin{cases} D=\sqrt{A_3H^\alpha}, & q=\frac{2}{A_3H^{\alpha-1}}, & D'=\frac{}{2n(1-\alpha)+\alpha+4} & \text{when } \alpha<1 \\ D=\sqrt{\omega_2 H}, & q=\frac{A_3H^{\alpha-1}}{\omega_2}, & D'=\frac{2}{2n(\alpha-1)+5} & \text{when } \alpha>1 \end{cases}$$

Analytic H v Q relationships

3. Analytic Discharge Formula of Case III

$$Q = \int U_d dA = \int_0^b U_d^{(1)} H dy + \int_b^B U_d^{(2)}(H-h)dy$$
$$= I_1 + I_2$$

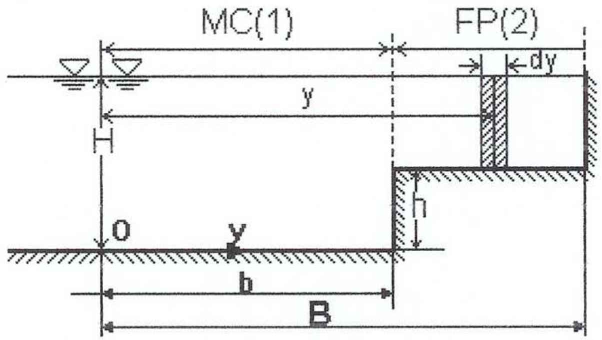

Thus

Predictions of lateral distributions of depth-averaged velocity (cont.)

River Blackwater, Hampshire, UK

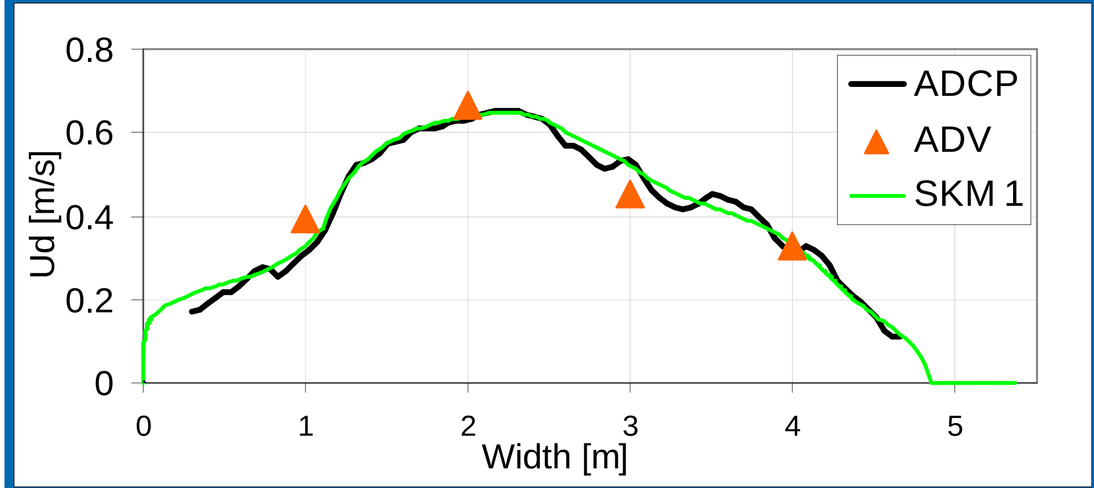

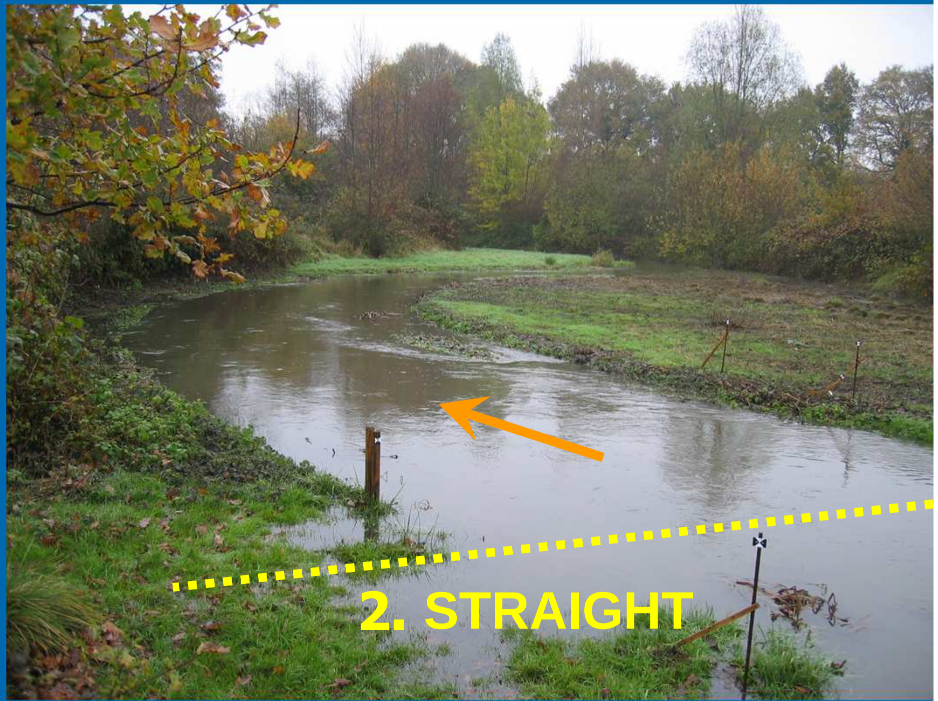

Inbank flow (looking downstream)

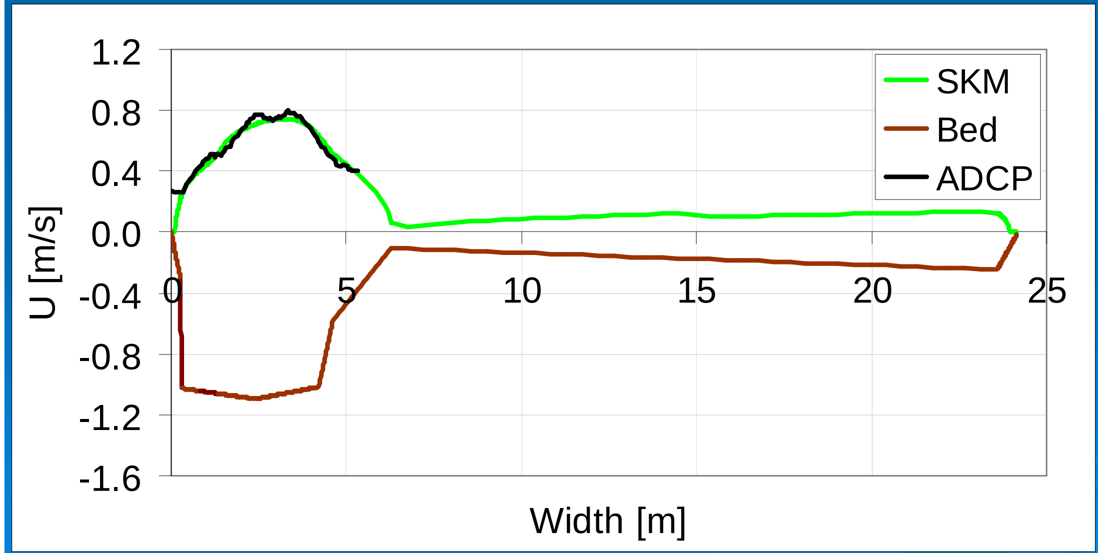

Overbank flow (looking downstream)

ADCP traverse

Submerged vegetation (Winter)

3. Seasonal growth patterns

River Blackwater, showing seasonal growth (Winter to Summer) in a narrow reach

River Blackwater, showing seasonal growth (Winter to Summer) in a meandering reach

Adapted governing SKM equation, including additional drag term

$$\rho \frac{\partial H(UV)_d}{\partial y} = \rho g H S_o + \frac{\partial H \overline{\tau}_{yx}}{\partial y} - \tau_b \sqrt{1 + \frac{1}{s^2}} \boxed{- \frac{1}{2\delta} \rho (C_D \beta A_v') H U_d^2}$$

or, in terms of velocity

$$\rho g H S_o - \rho \frac{f}{8} U_d^2 \sqrt{1 + \frac{1}{s^2}} \boxed{- \frac{1}{2\delta} \rho (C_D \beta A_v') H U_d^2}$$
$$+ \frac{\partial}{\partial y} \left\{ \rho \lambda H^2 \left(\frac{f}{8} \right)^{1/2} U_d \frac{\partial U_d}{\partial y} \right\} = \Gamma$$

Tang, X., Sterling, M. and Knight, D.W., 2010. A general analytical model for lateral velocity distributions in vegetated channels,
Proceedings of RiverFlow 2010, Braunschweig, 469-477.

Inbank flow with non-uniform roughness (rectangular channel)

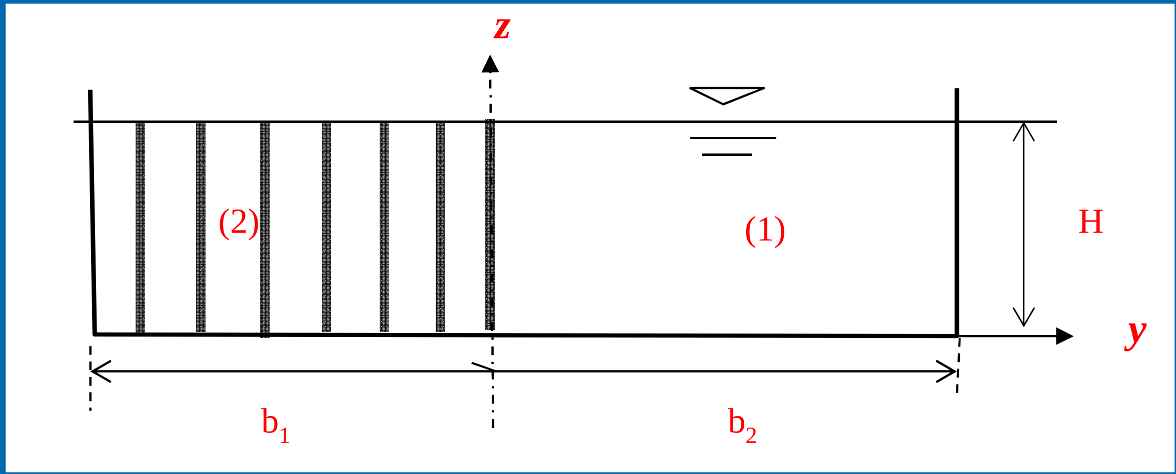

Cross section of partially vegetated rectangular channel (after White & Nepf, 2008).

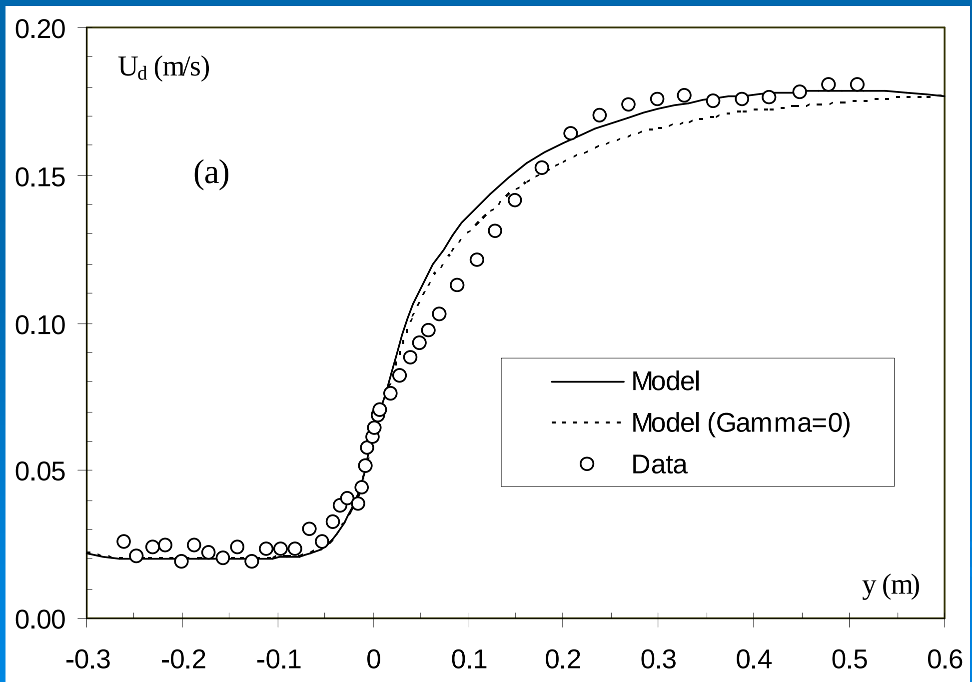

Comparison of predicted U_d with data, simulated using SKM (after Tang *et al*., 2010)

River Flow 2010

Overbank flow with uniform floodplain roughness

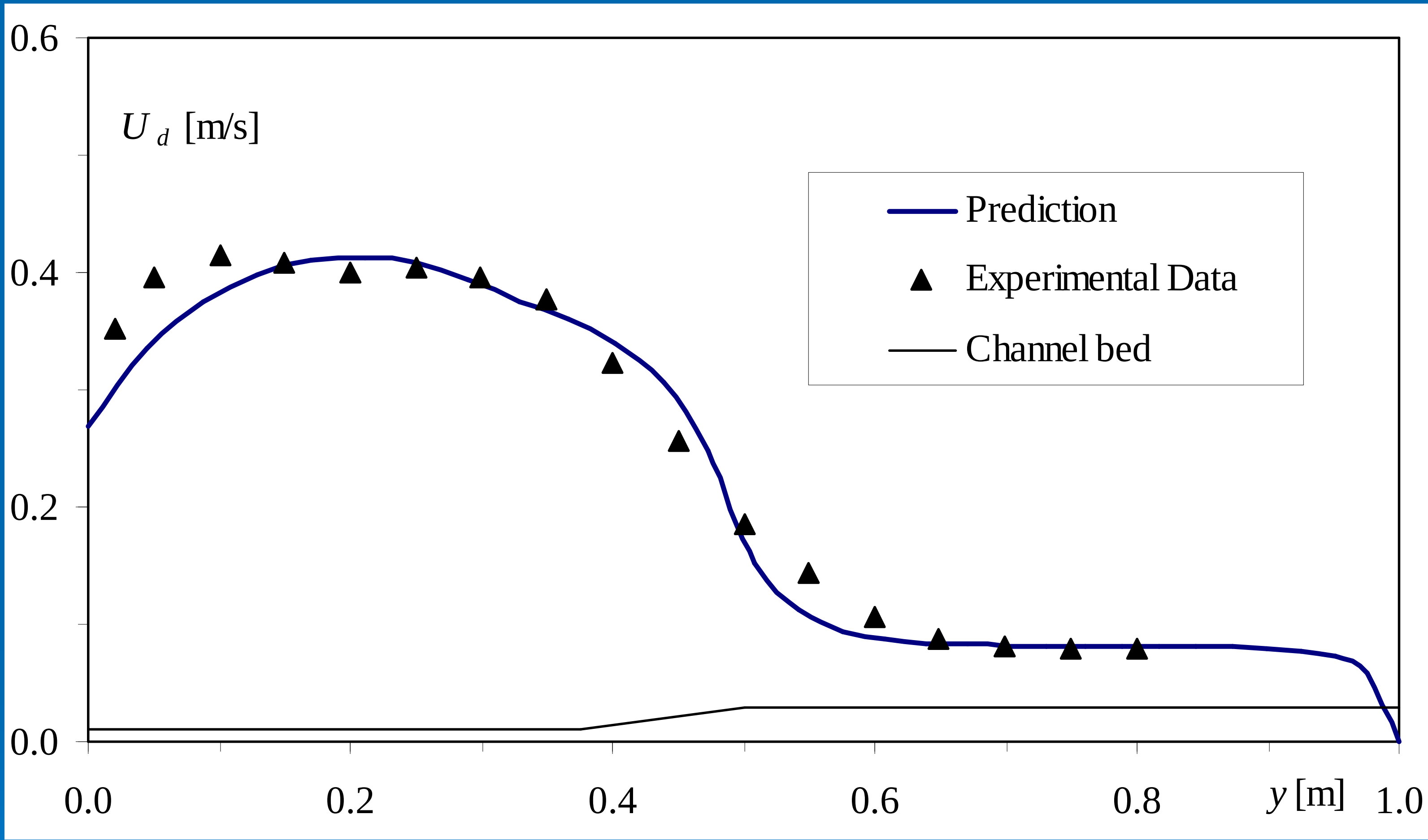

Comparison of modelled U_d distributions with experimental data for φ = 1.26% (Pasche & Rouve, 1985).

Overbank flow with non-uniform floodplain roughness

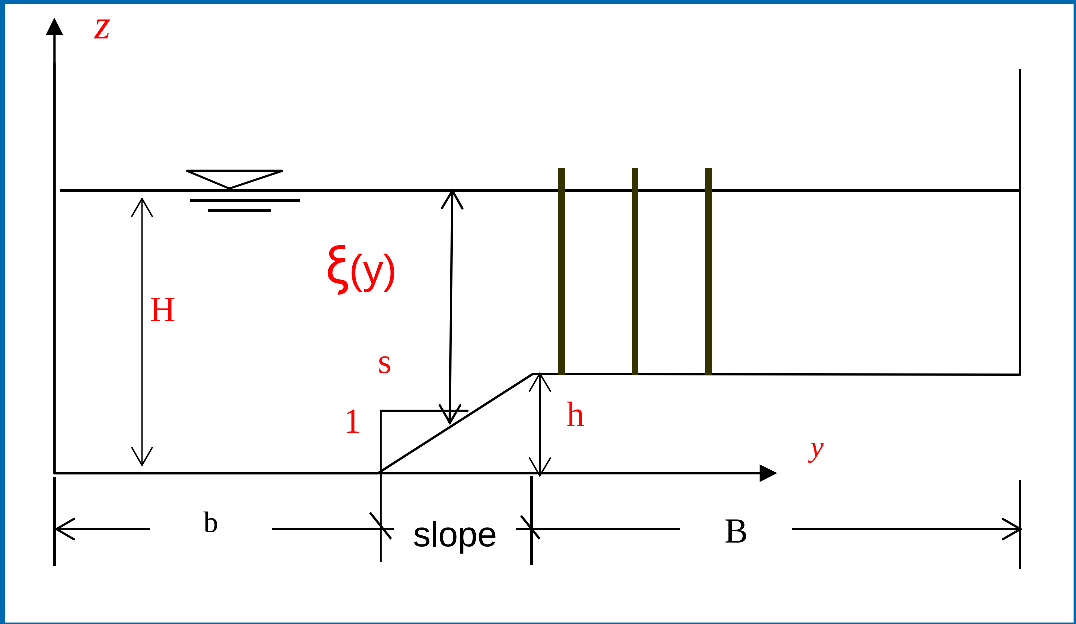

Emergent tree line vegetation

Cross section of partially vegetated compound channel (after Sun & Shiono, 2009).

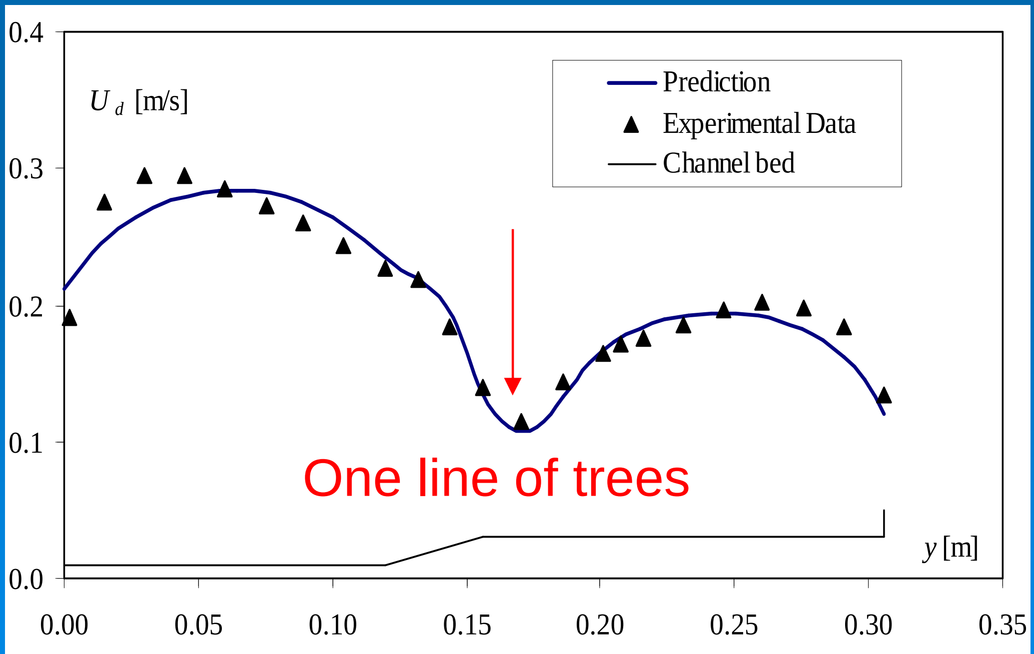

Comparison of predicted U_d with data (Run 2b), simulated using SKM (after Tang *et al*., 2009)

Submerged vegetation

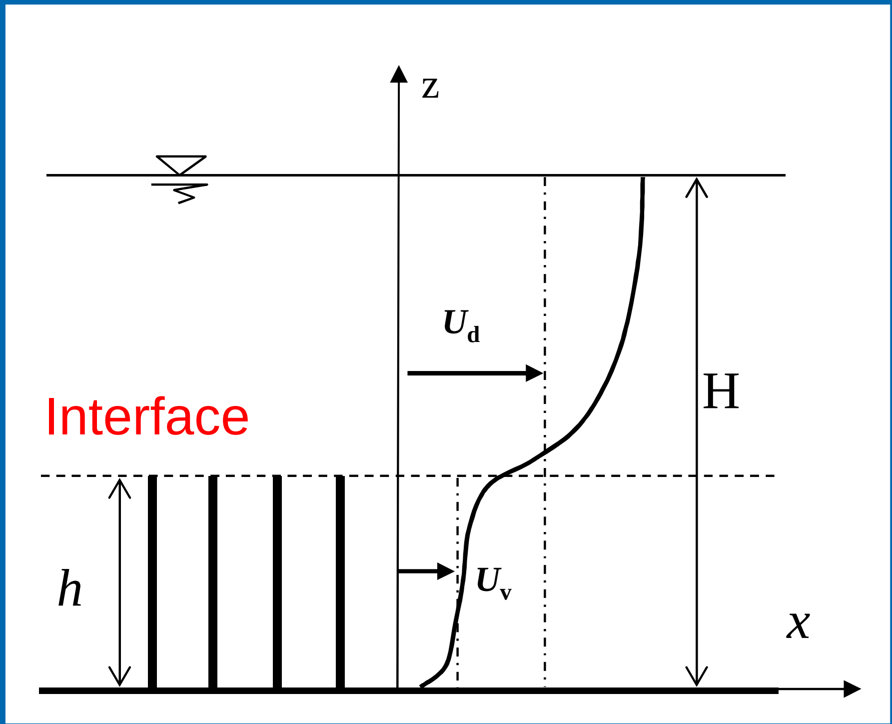

Compound channel data
(Knight & Demetriou, 1983)

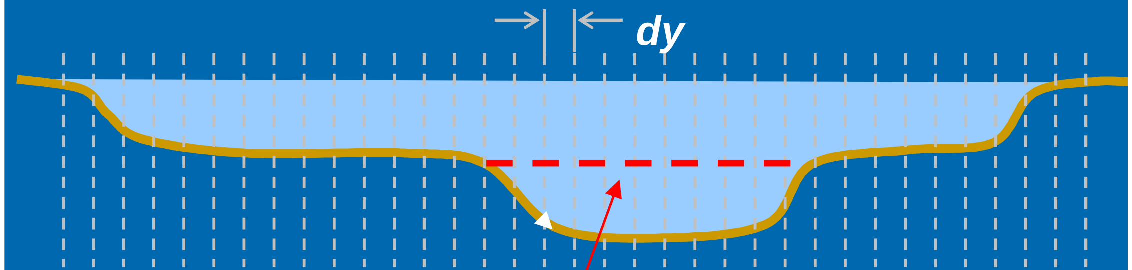

Apparent shear force on this interface

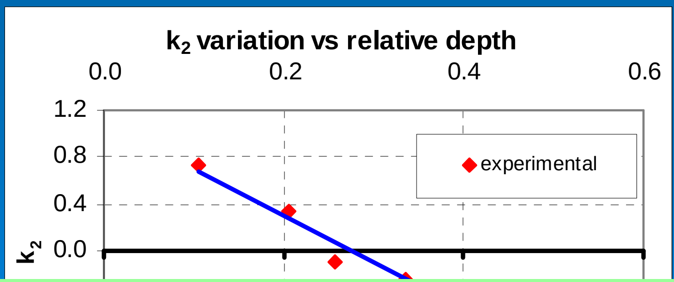

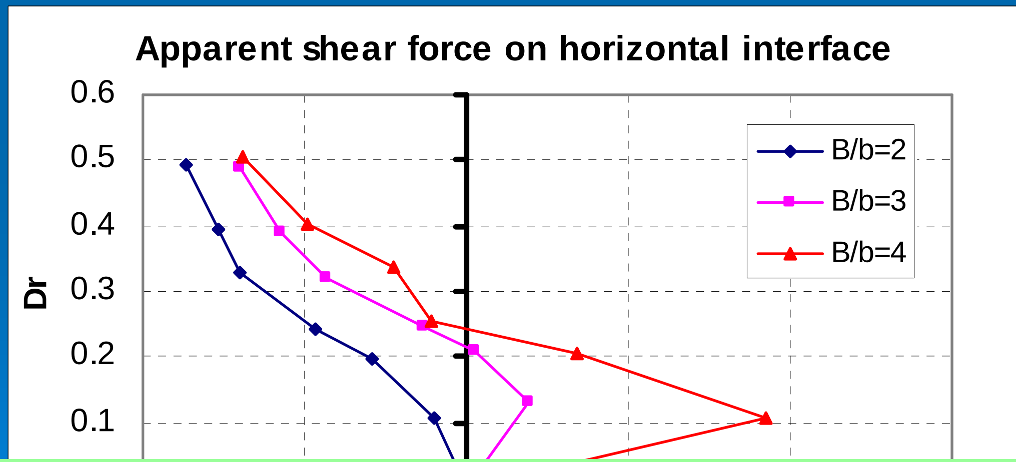

Omran, M., Modelling stage-discharge curves, velocity and boundary shear stress distributions in natural and artificial channels using a depth-averaged approach, PhD thesis, University of Birmingham, 2005

ADCP vs. PIV

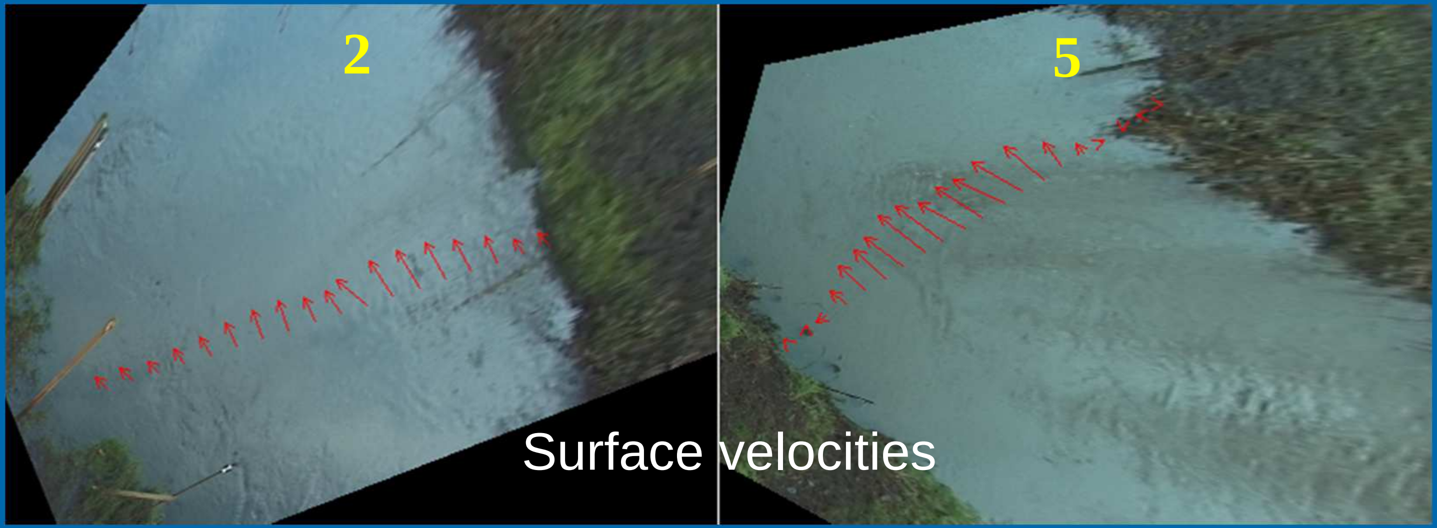

2
5
Surface velocities

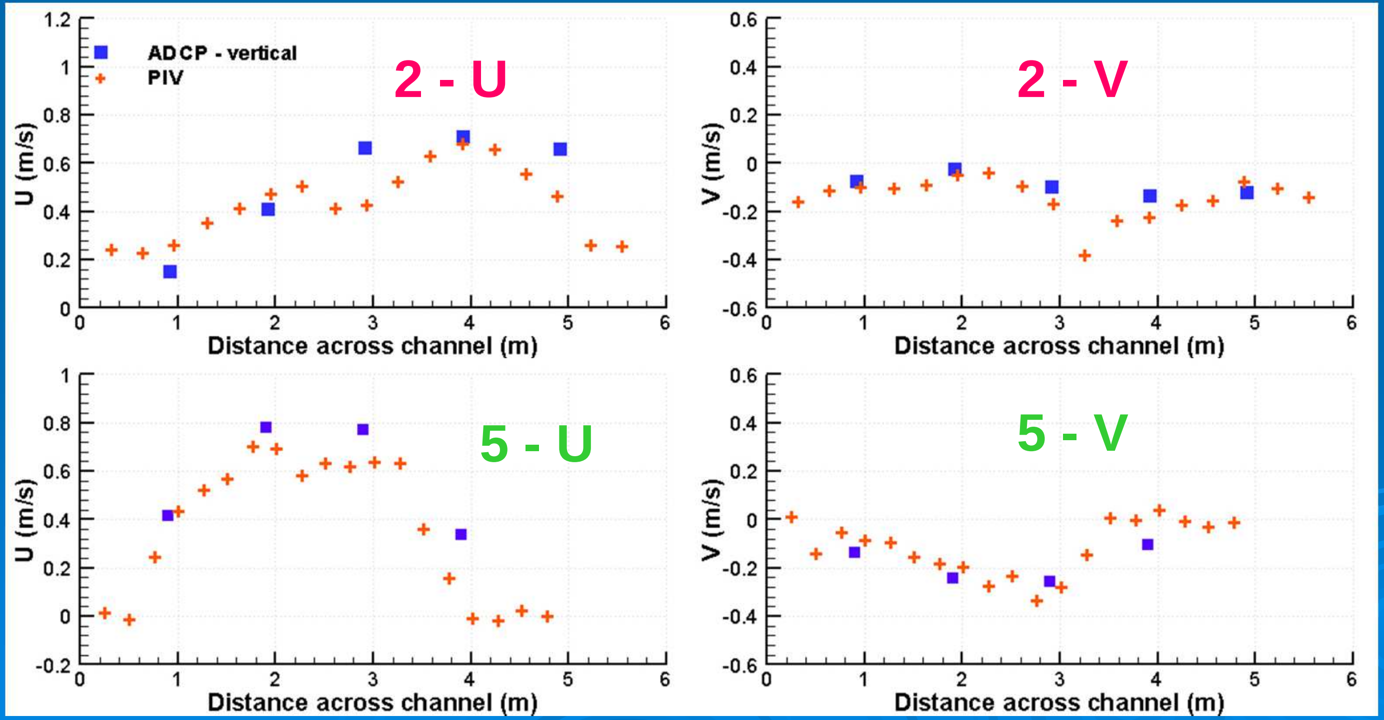

ADCP - vertical
PIV
2 - U
2 - V
5 - U
5 - V
U (m/s)
V (m/s)
Distance across channel (m)

100 m
5
2

7. Conclusions

THE UNIVERSITY OF BIRMINGHAM

1. Simplicity has some advantages – ease of use, knowing inner working of all algorithms, meaning of key coefficients, computational speed, reasonable accuracy, etc.

2. The SKM or CES can predict lateral distributions of U_d and τ_b in straight prismatic channels and low sinuosity channels for both inbank and overbank flows.

3. CES/SKM can be used to estimate stage-discharge relationships, extend rating curves, velocity distributions and sediment transport rates in straight prismatic channels.

4. The software is available at www.river-conveyance.net . Further information is contained in an accompanying book 'Practical Channel Hydraulics' (Knight *et al*., CRC Press, 2009)


University of Birmingham
Department of Civil Engineering
PER AD
ARDUA ALTA
The End

over .....

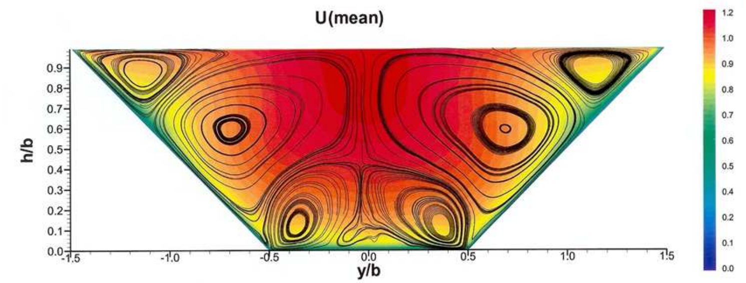

Figure 4. Streamlines from Thorsten's LES results.

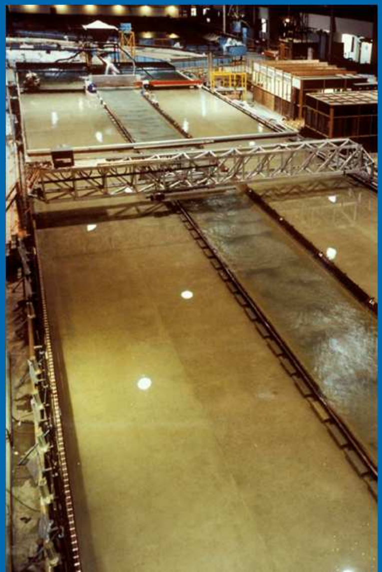

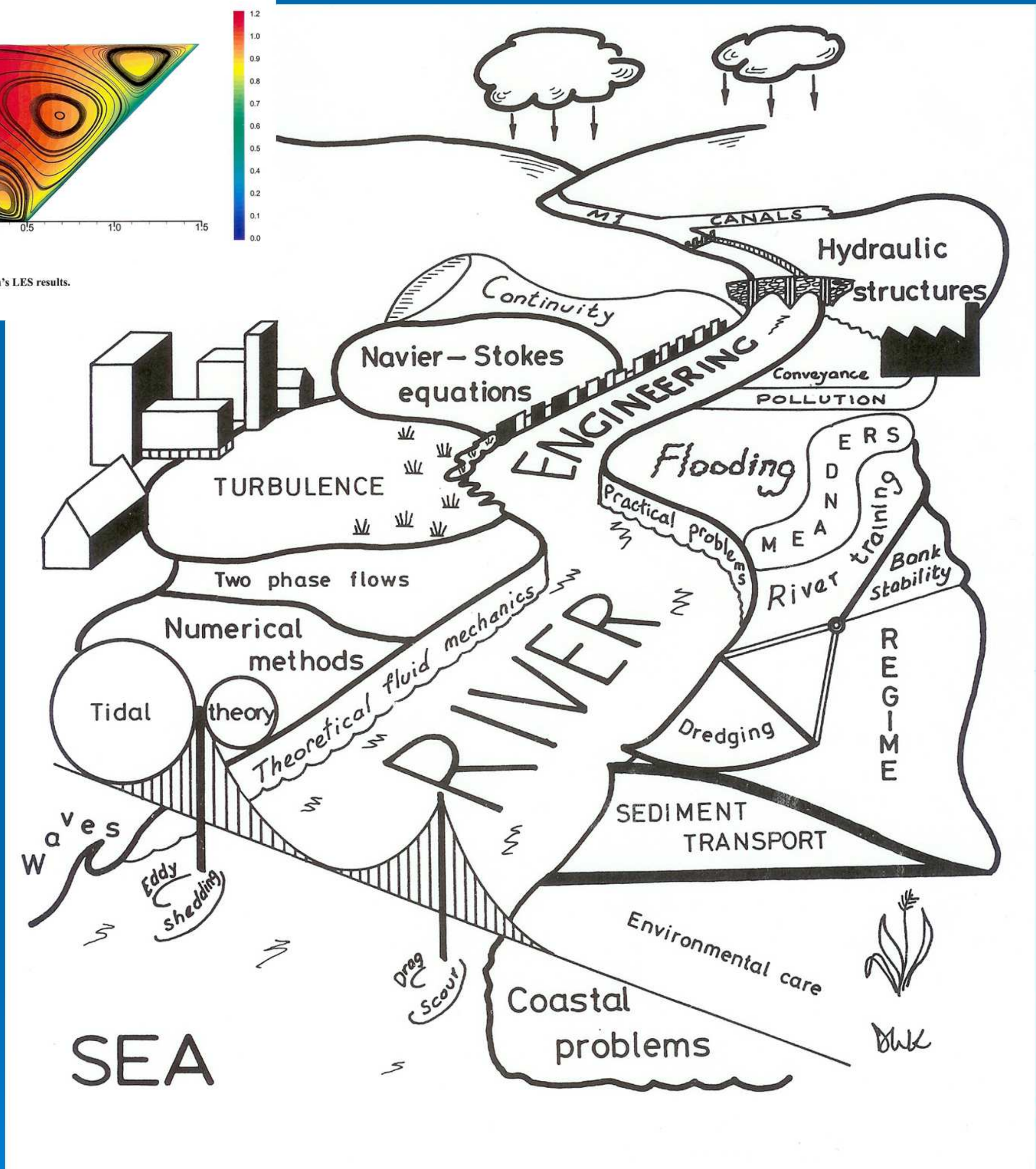

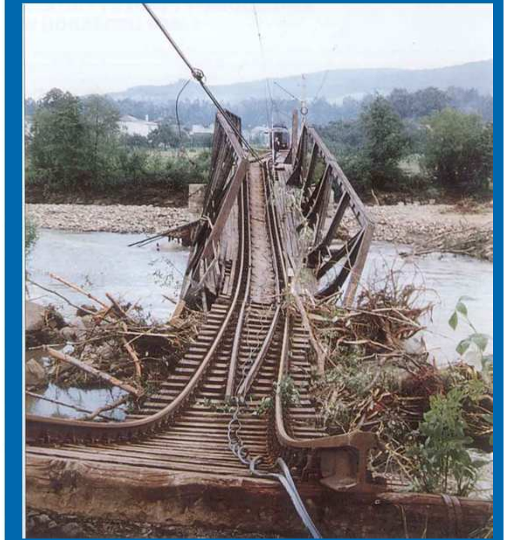

The art and science of river engineering (after Knight)
[reproduced from Nakato & Ettema, (1996), page 448]

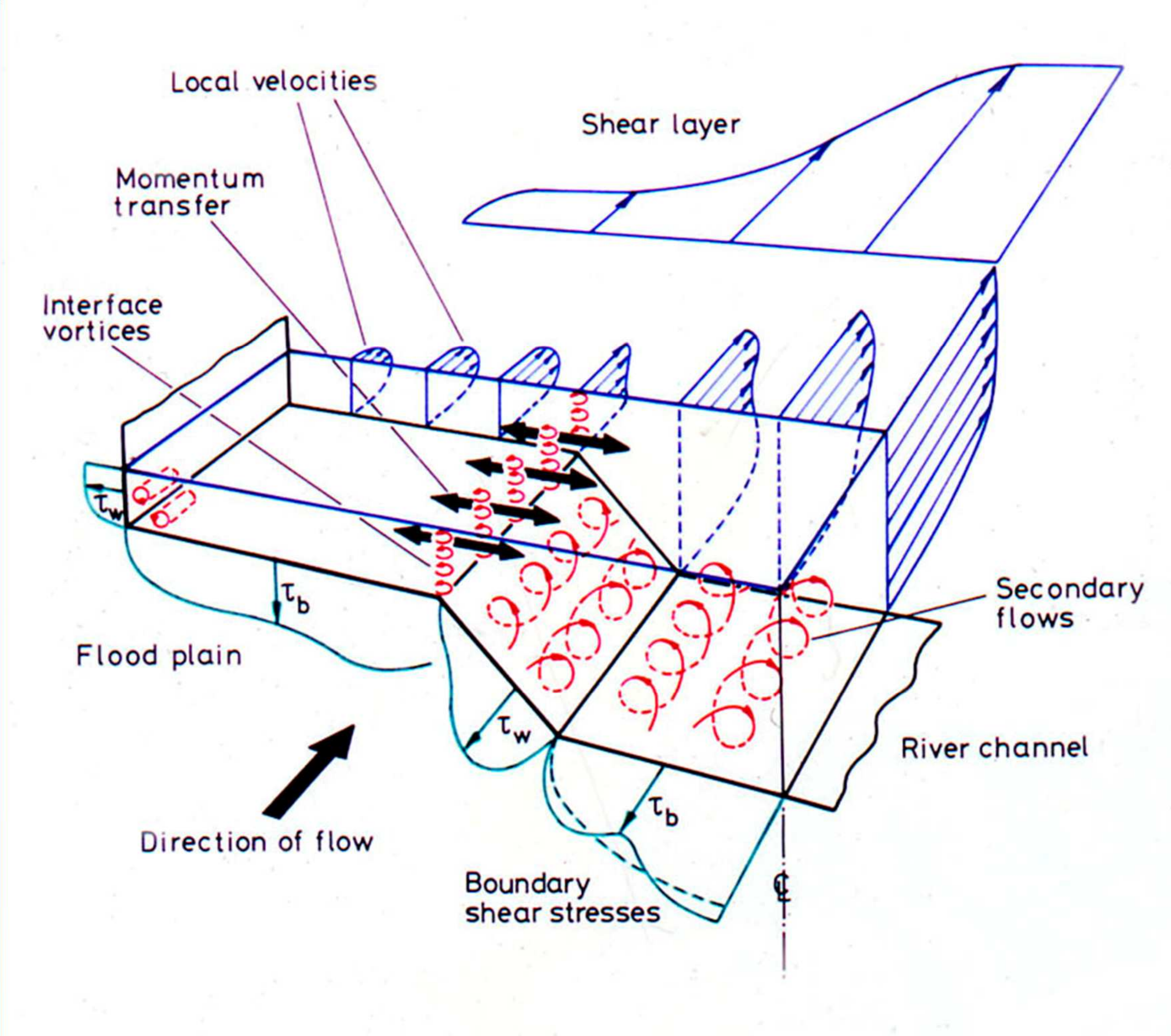

Flow structures in a straight two-stage channel (after Knight)

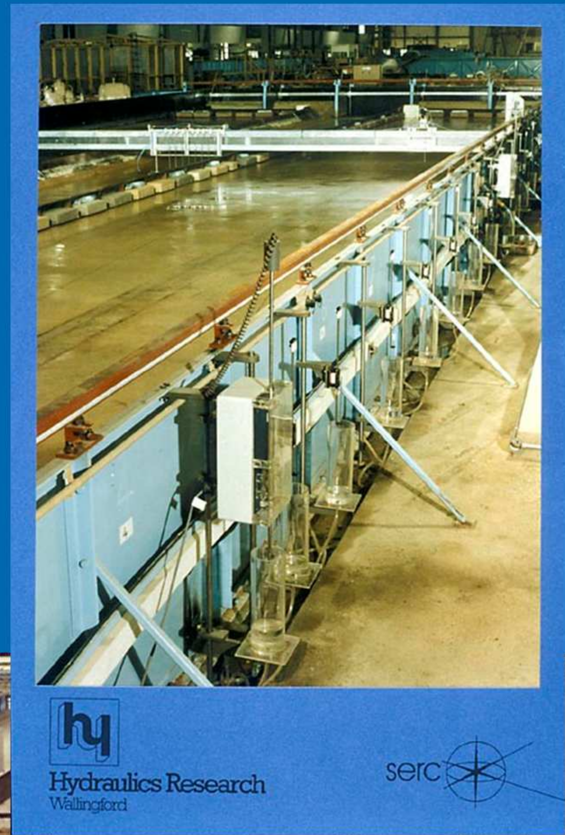

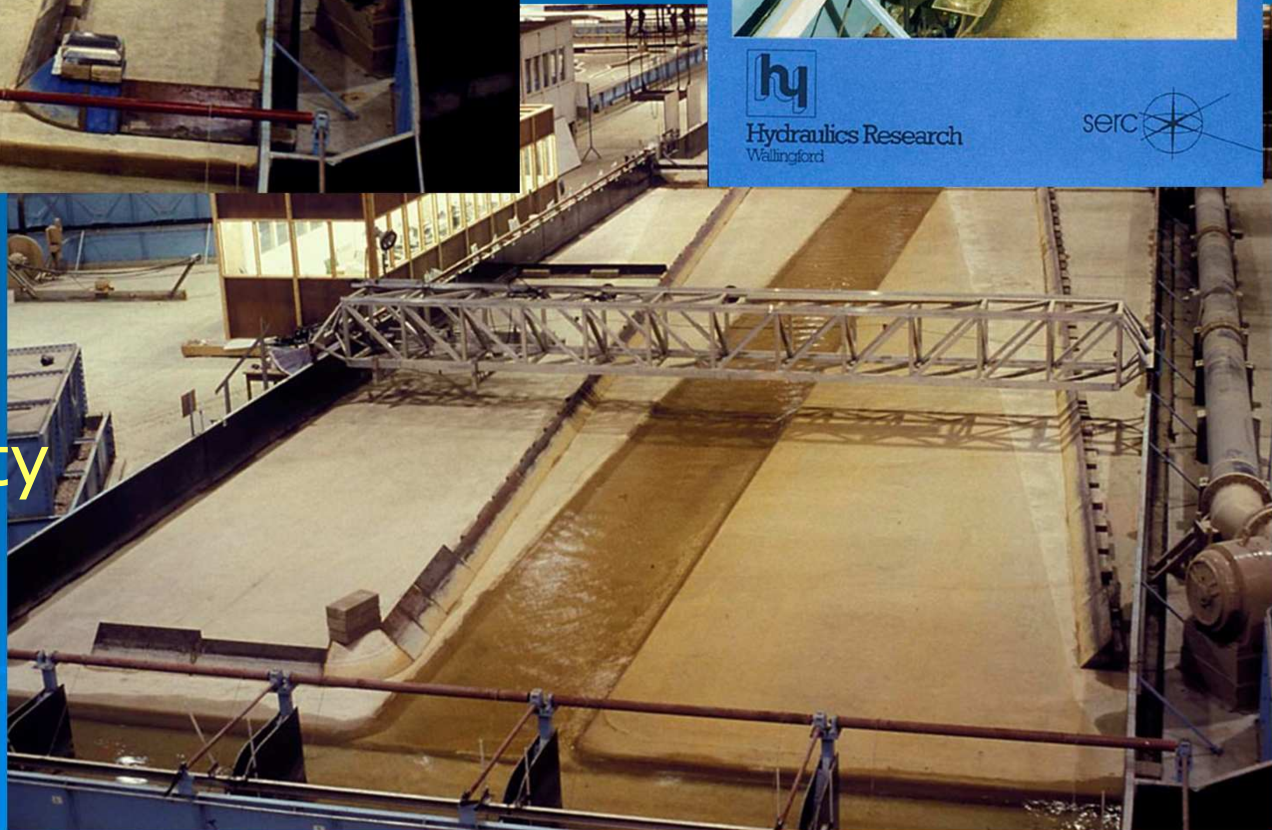

Flood Channel Facility
(FCF) data

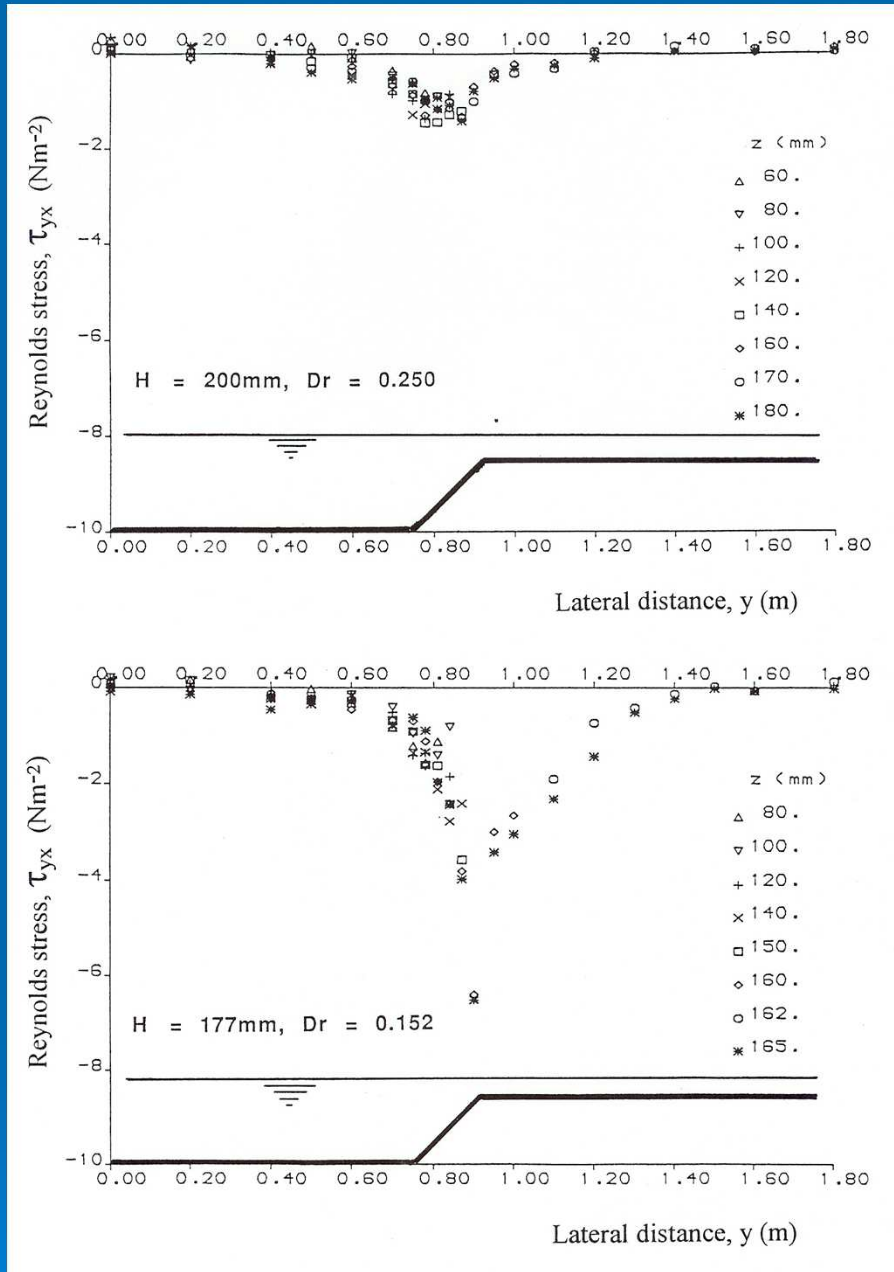

Medium floodplain depth

Dr = 0.250

Low floodplain depth

Dr = 0.152

Lateral variation of Reynolds stress, τ_{yx}, near main channel/floodplain interface (FCF Exps 020301 & 020501)

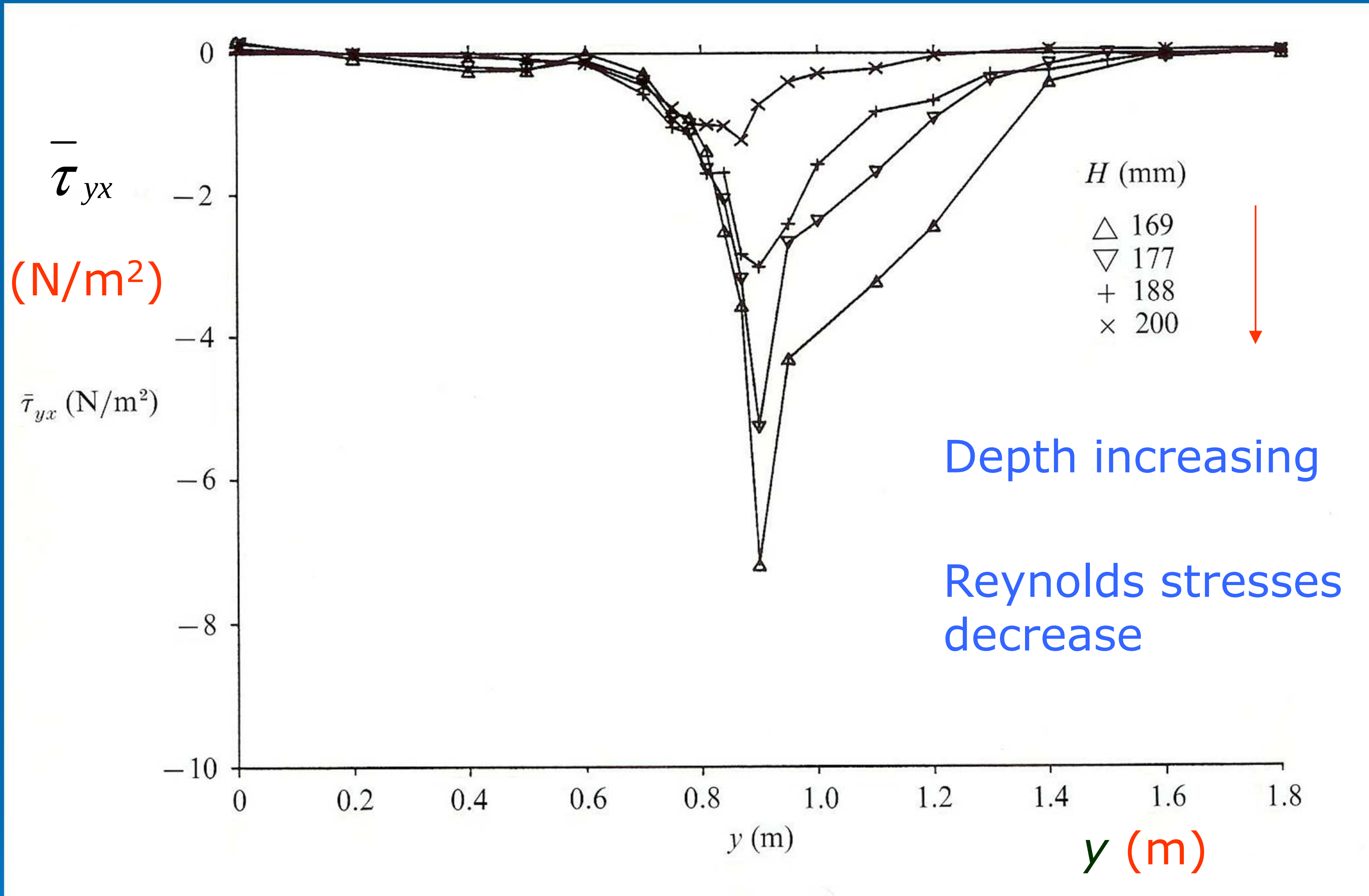

Lateral variation of depth-averaged Reynolds shear stress, τ_{yx} (FCF data, Series 02)

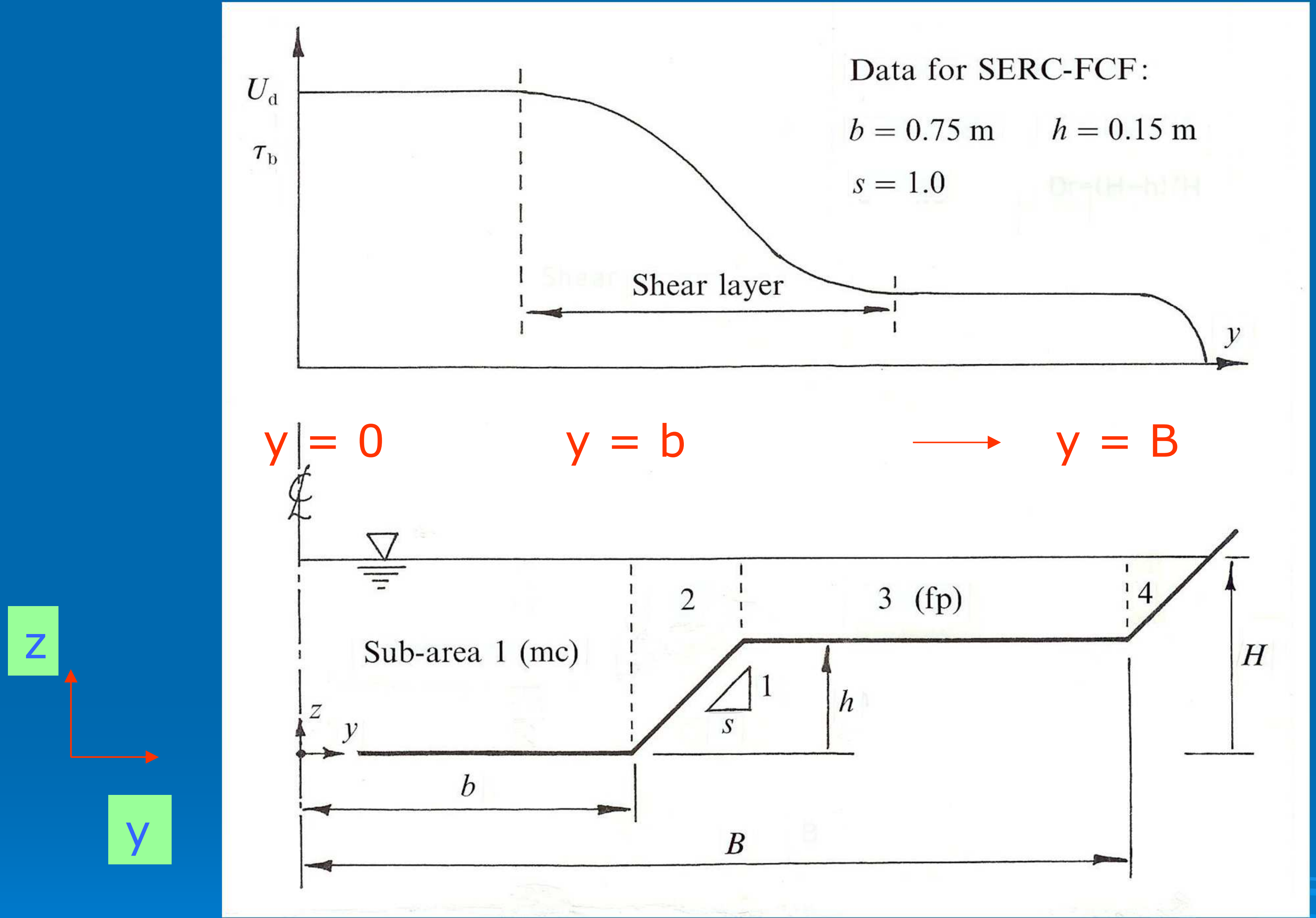

Cross section of a two-stage channel with notation

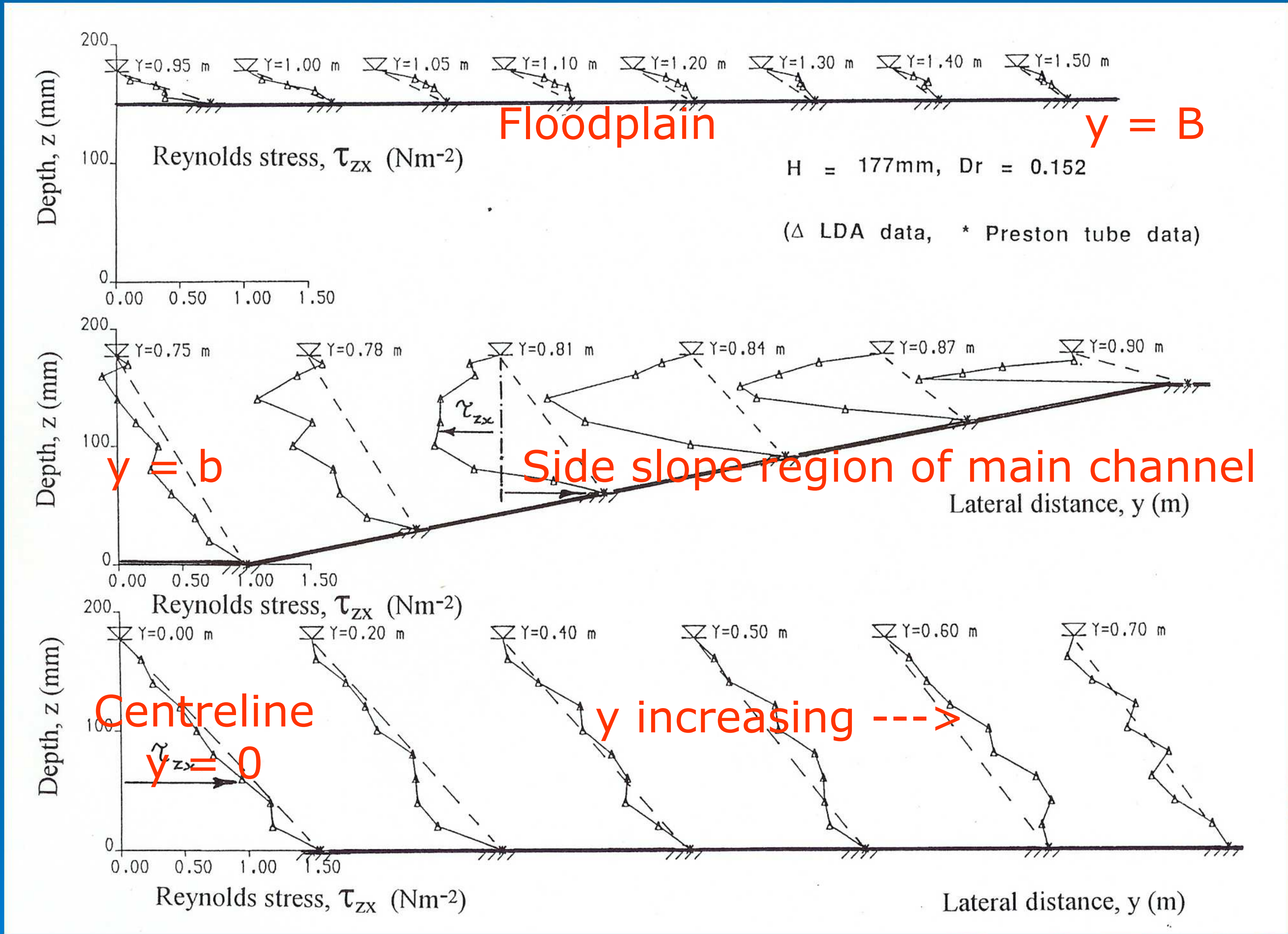

Distribution of Reynolds stress, τ_{zx}, over the depth at various lateral positions (FCF data, Series 02)

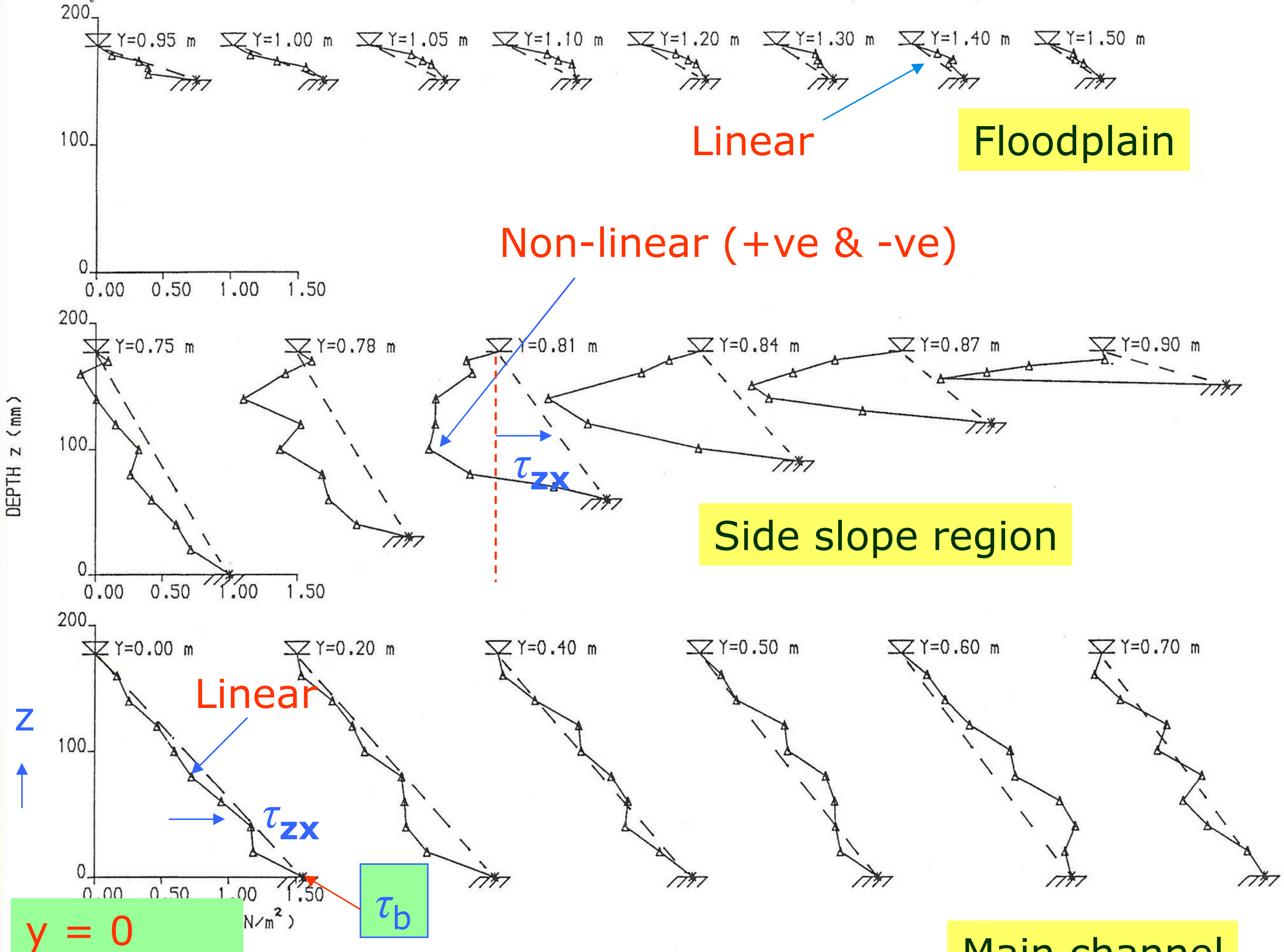

Reynolds stress τ_{zx} data for overbank flow, H = , Dr = 0.152

(Δ LDA data, * Preston tube data)

Cross-section

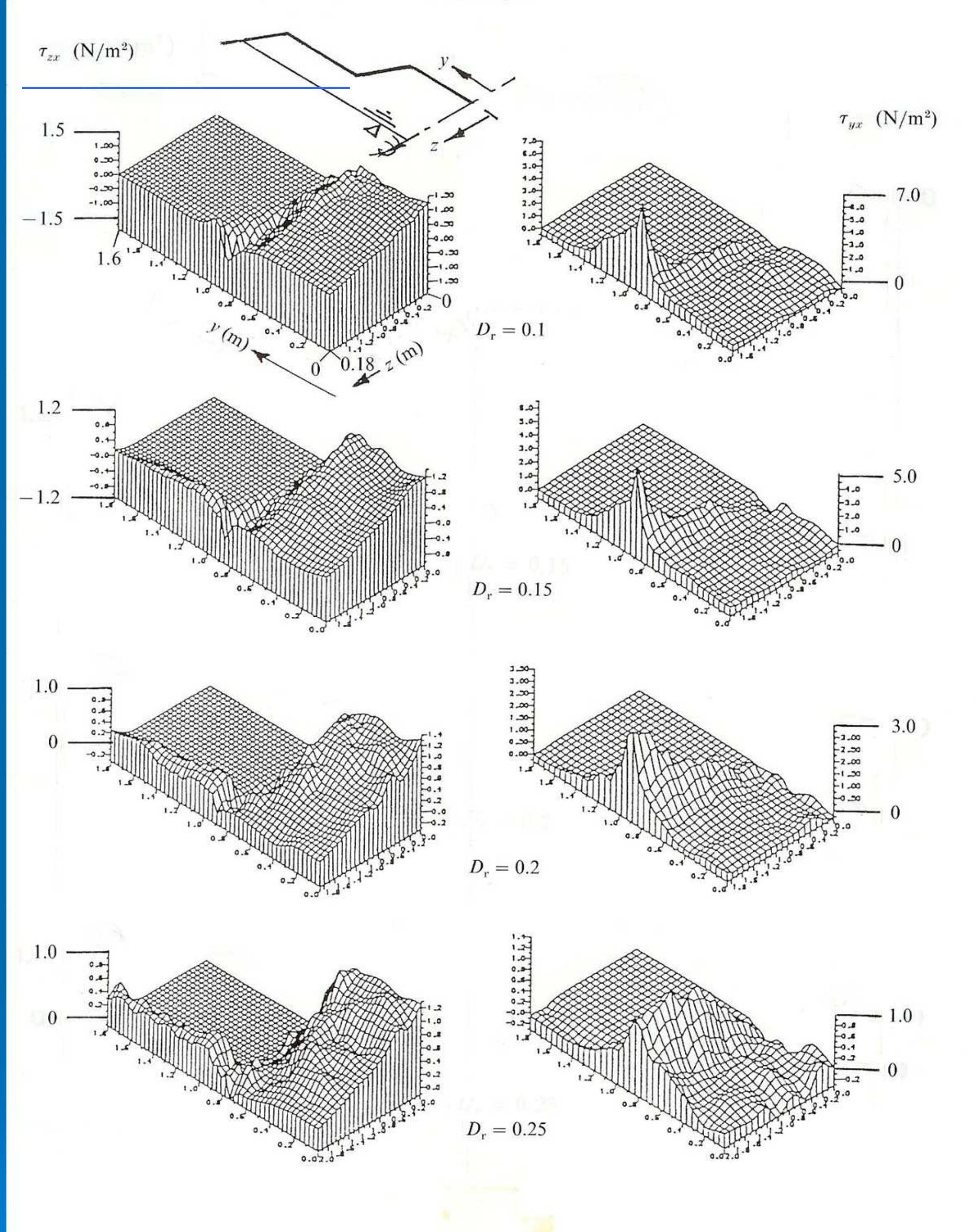

τ_{zx}

τ_{yx}

Dr = (H-h)/H

Dr = 0.10

Dr = 0.15

Dr = 0.20

Dr = 0.25

Isometric views of the Reynolds stresses τ_{zx} and τ_{yx} for 4 relative depths; FCF data, Series 02 (Shiono & Knight, 1991)

Measured distributions of Reynolds stress and secondary flow terms

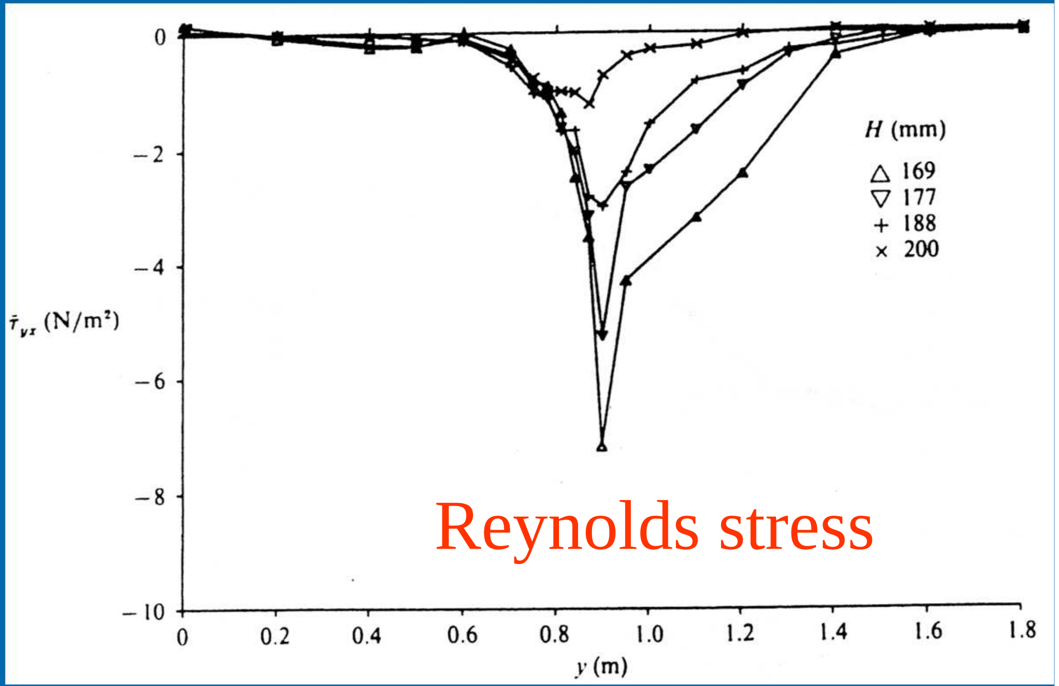

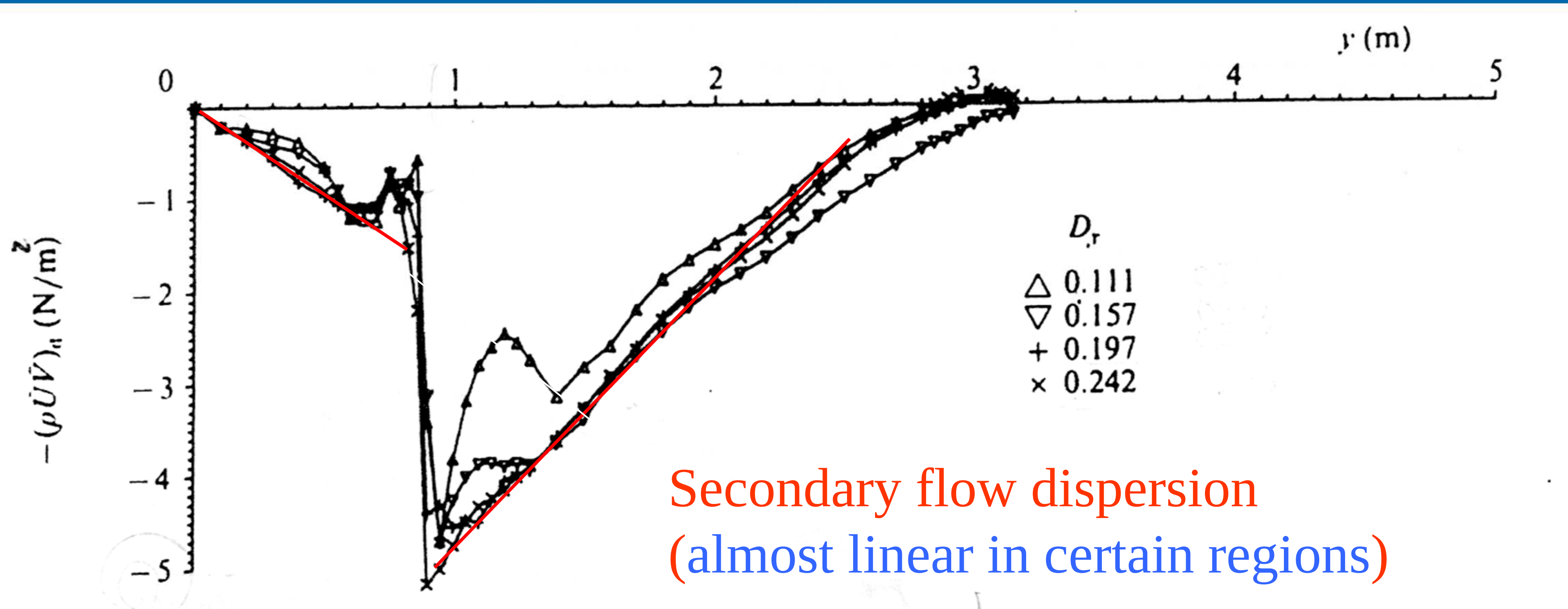

Definition of friction factors

$$\tau_o = \left(\frac{f}{8}\right)\rho U_A^2$$

$$\tau_z = \left(\frac{f_z}{8}\right)\rho U_z^2$$

$$\tau_b = \left(\frac{f_b}{8}\right)\rho U_d^2$$

τ_b = function of k_s or surface roughness

global
(1-D models)

zonal/sub-area
(1-D models)

depth-averaged
(2-D models)

local
(3-D models)

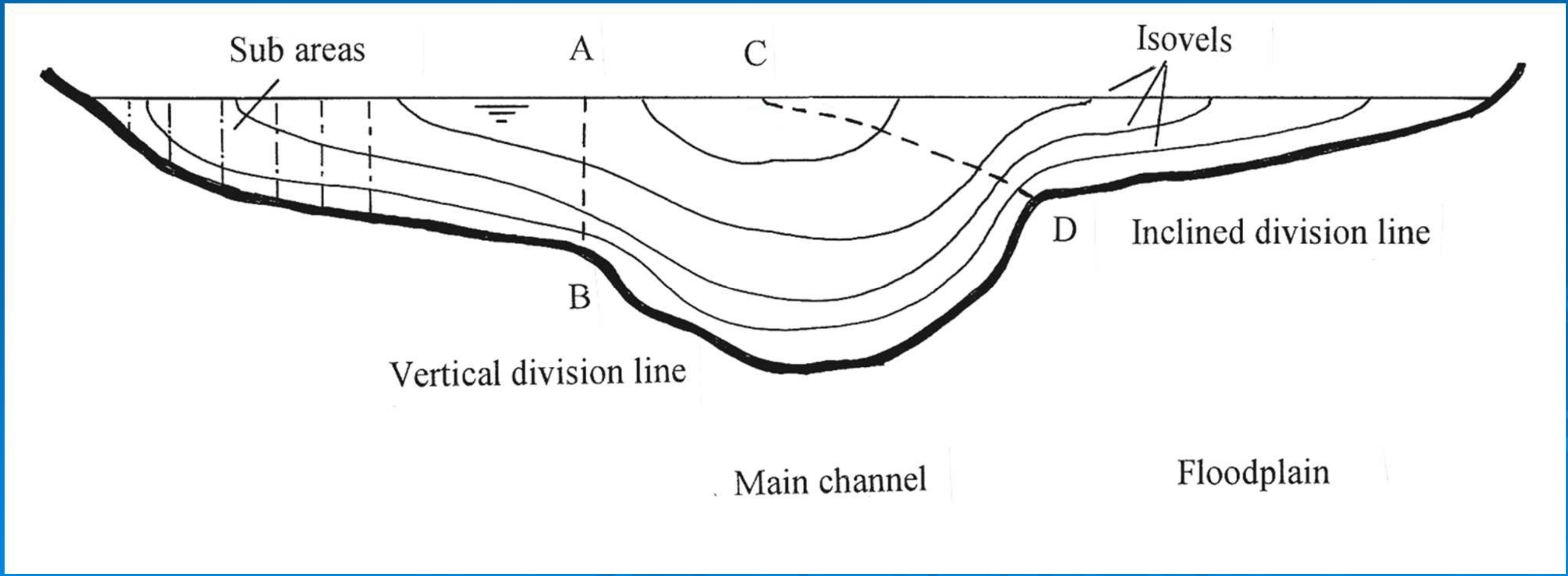

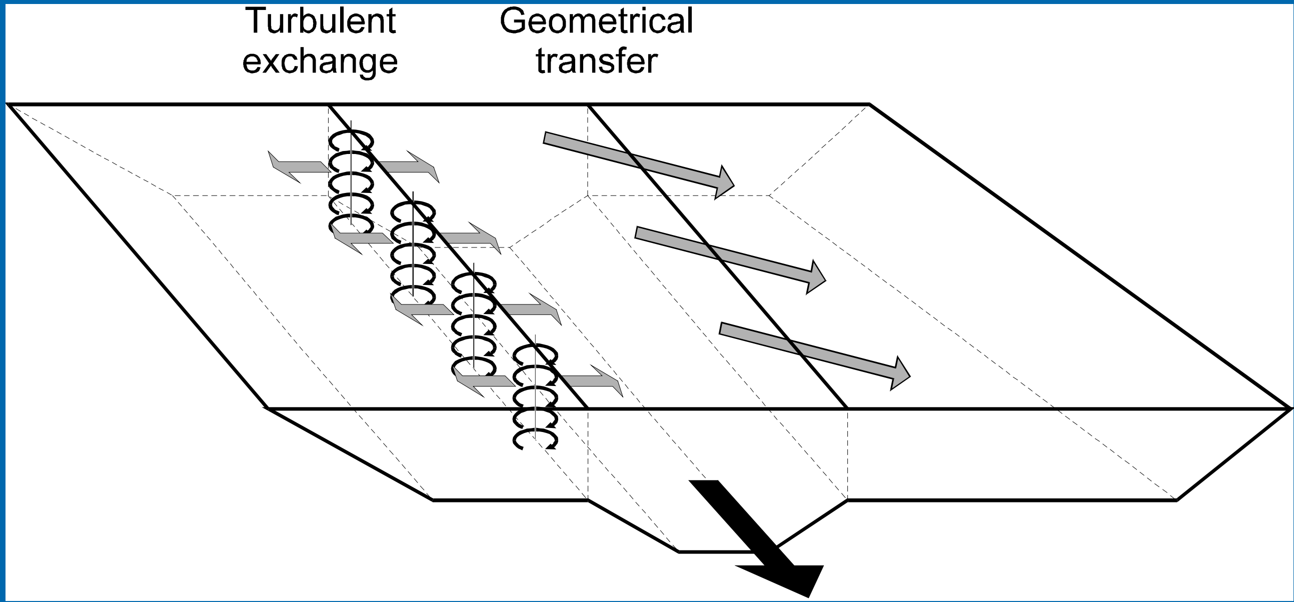

Compound channel
With skewed
floodplains

Channel with
non-prismatic
floodplains
(after Bousmar)

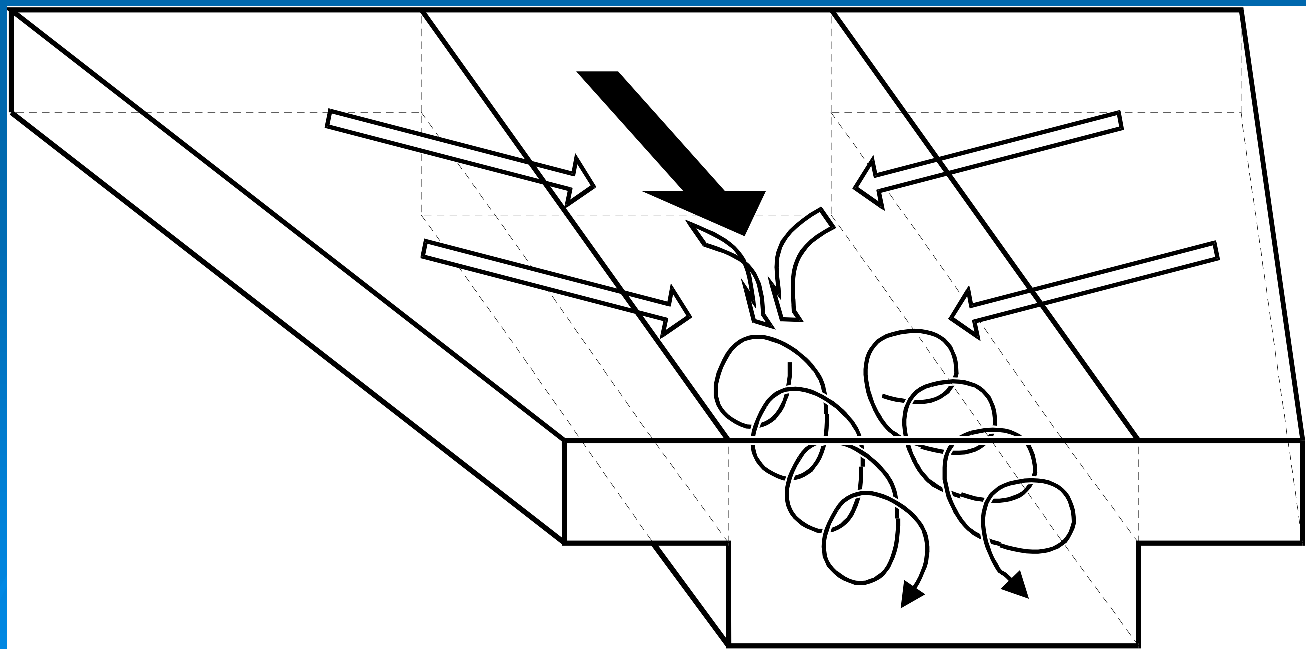

Concepts:

Secondary flows – longitudinal vortices

Large scale eddies – planform vortices

3-D flow structures

Oscillations in free surface

Definition of friction factor

RANS equations not adequate

THE UNIVERSITY OF BIRMINGHAM

Models

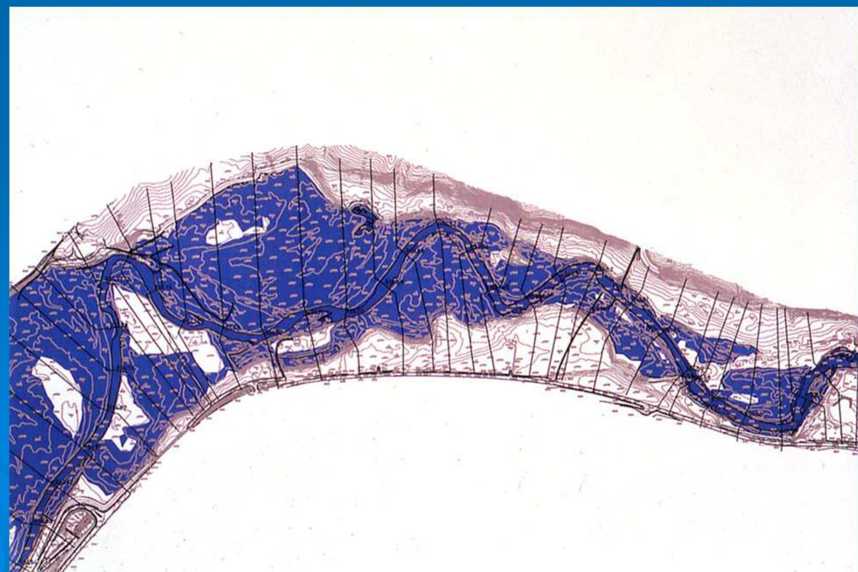

Range of model types

Different types of model

Spatial dimensions: 1-D, 2-D & 3-D
Level of turbulence closure: mixing length, Reynolds stress, etc.
RANS (numerous types, SSG, k-ε, k-ω, etc.)
LES, DNS, etc.
Numerical procedures vary between models

Different types of model according to purpose

Hydrodynamic, flood routing, sediment motion, pollution, etc

Selection of model

Select the right 'tool' for the right 'job'

Depth-averaged form of the Navier–Stokes equation

$$\rho g H S_o - \tfrac{1}{8}\rho f U_d^2\left(1+\frac{1}{s^2}\right)^{1/2} + \frac{\partial}{\partial y}\left\{\rho\lambda H^2\left(\frac{f}{8}\right)^{1/2} U_d \frac{\partial U_d}{\partial y}\right\} = \frac{\partial}{\partial y}\left[H\left(\rho UV\right)_d\right]$$

where $$U_d = \frac{1}{H}\int_0^H U\,dz$$ Depth –averaged velocity

$$\tau_b = \left(\frac{f_b}{8}\right)\rho U_d^2$$ Boundary shear stress

$$\bar{\tau}_{yx} = \bar{\rho}\varepsilon_{yx}\frac{\partial U_d}{\partial y}$$ $$\bar{\varepsilon}_{yx} = \lambda U_* H$$ Depth-averaged Reynolds shear stress

$$\frac{\partial\left(H\rho UV\right)_d}{\partial y} = \Gamma$$ Secondary flow term

Thus in the Shiono & Knight Method (SKM) there are 3 key coefficients, *f*, λ and Γ:

f governing - boundary friction

λ governing - lateral mixing & turbulence

Γ governing - secondary flow

[With additional coefficients for vegetation - C_D, β and δ]

Simplified form of the basic equation used in the Shiono & Knight Method (SKM)

$$\rho g H S_o - \tau_b \left(1 + \frac{1}{s^2}\right)^{1/2} + \frac{\partial}{\partial y}\left\{H \bar{\tau}_{yx}\right\} = \Gamma$$

where s = side slope (1:s, vertical:horizontal)

Note that when the lateral shear and $\Gamma = 0$, for a flat bed with $s = \infty$, the bed shear stress, τ_b, is due to the weight of the water column above it, i.e. $\tau_b = \rho g H S_o$

This illustrates why the boundary shear stress is affected by both lateral shear and secondary flows

Flow in a rectangular channel, modelled with a single panel

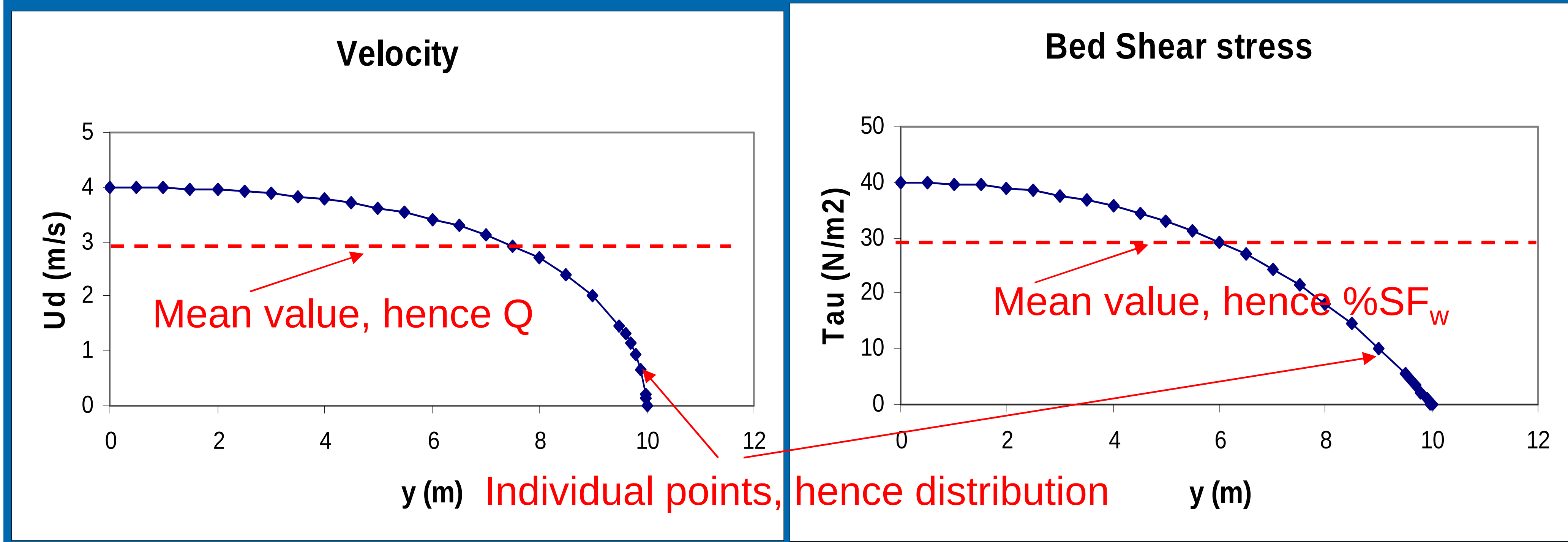

Vary	Fixed	+/-	%SF$_W$	Q
f	λ & Γ	increase f	decrease	decrease
		decrease f	increase	increase
λ	f & Γ	increase λ	increase	decrease
		decrease λ	decrease	increase
Γ	f & λ	increase Γ	increase	decrease
		decrease Γ	decrease	increase

Effect of varying the 3 calibration parameters

River Flow 2010

Comparison of predicted and experimental data

B=70mm, H=103.8mm, Q=1.98l/s %SFw=73.6%

Flow in a rectangular channel, fixed f and gamma, variable lamda

Varying l									
	f	λ	Γ	Q	t_{mean}, τ_b	t_{mean}	%SFw	%Qerror	%SFw error
1	0.024	0.001	0.250	0.0029	0.513	0.526	46.519	45.463	-36.795
2	0.024	0.002	0.250	0.0026	0.432	0.443	54.904	32.972	-25.402
3	0.024	0.003	0.250	0.0024	0.376	0.385	60.802	23.703	-17.389
4	0.024	0.004	0.250	0.0023	0.333	0.341	65.278	16.275	-11.307
5	0.024	0.005	0.250	0.0022	0.299	0.307	68.816	10.098	-6.499
6	0.024	0.006	0.250	0.0021	0.271	0.278	71.691	4.838	-2.594
7	**0.024**	**0.007**	**0.250**	**0.0020**	**0.249**	**0.255**	**74.075**	**0.280**	**0.646**
8	0.024	0.008	0.250	0.0019	0.229	0.235	76.087	-3.722	3.379
9	0.024	0.009	0.250	0.0018	0.213	0.218	77.807	-7.276	5.716
10	0.024	0.010	0.250	0.0018	0.198	0.204	79.296	-10.459	7.739
11	0.024	0.011	0.250	0.0017	0.186	0.191	80.596	-13.334	9.506

Optimisation of parameters, using experimental data (one channel, single depth)

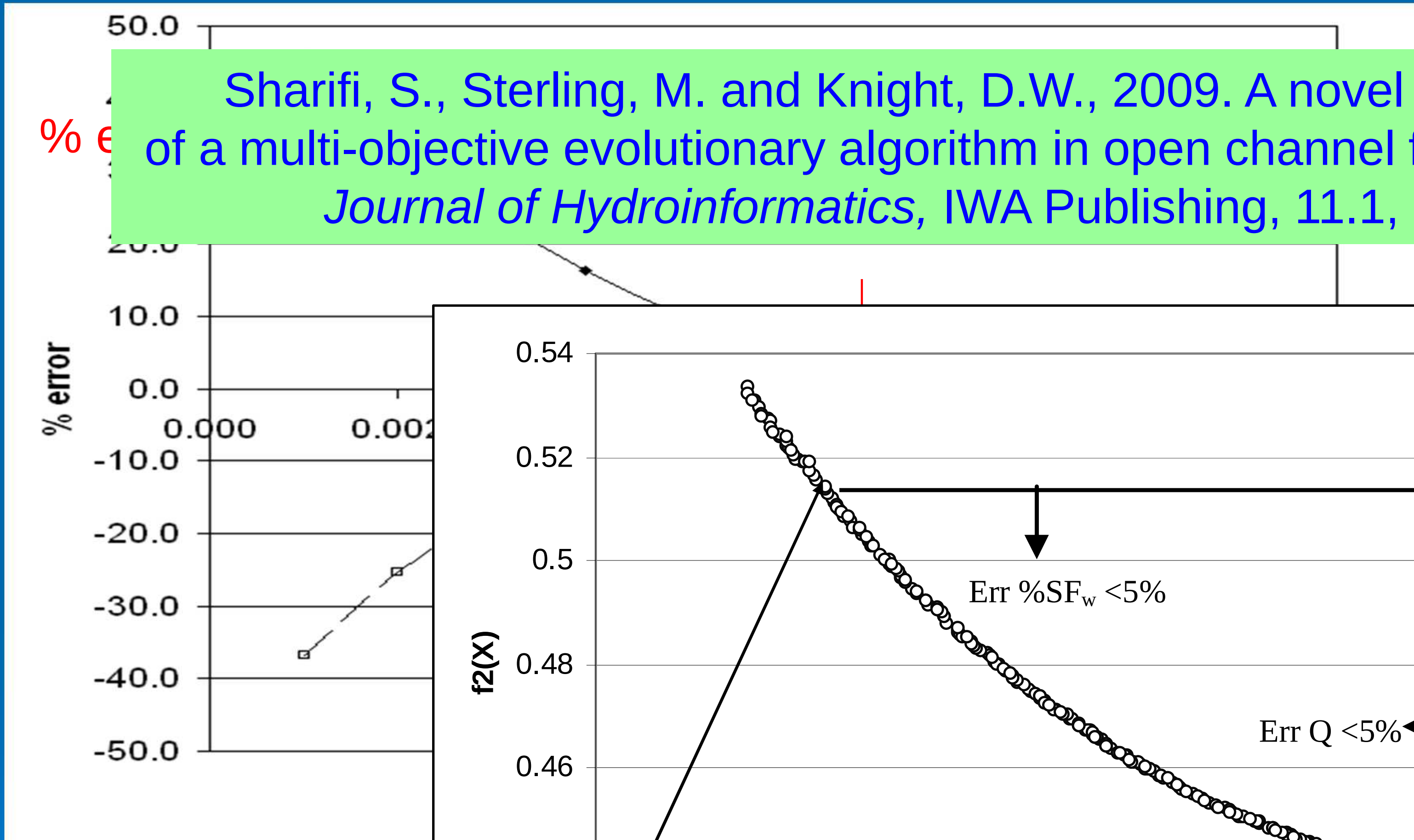

Sharifi, S., Sterling, M. and Knight, D.W., 2009. A novel application of a multi-objective evolutionary algorithm in open channel flow modelling, *Journal of Hydroinformatics,* IWA Publishing, 11.1, 31-50.

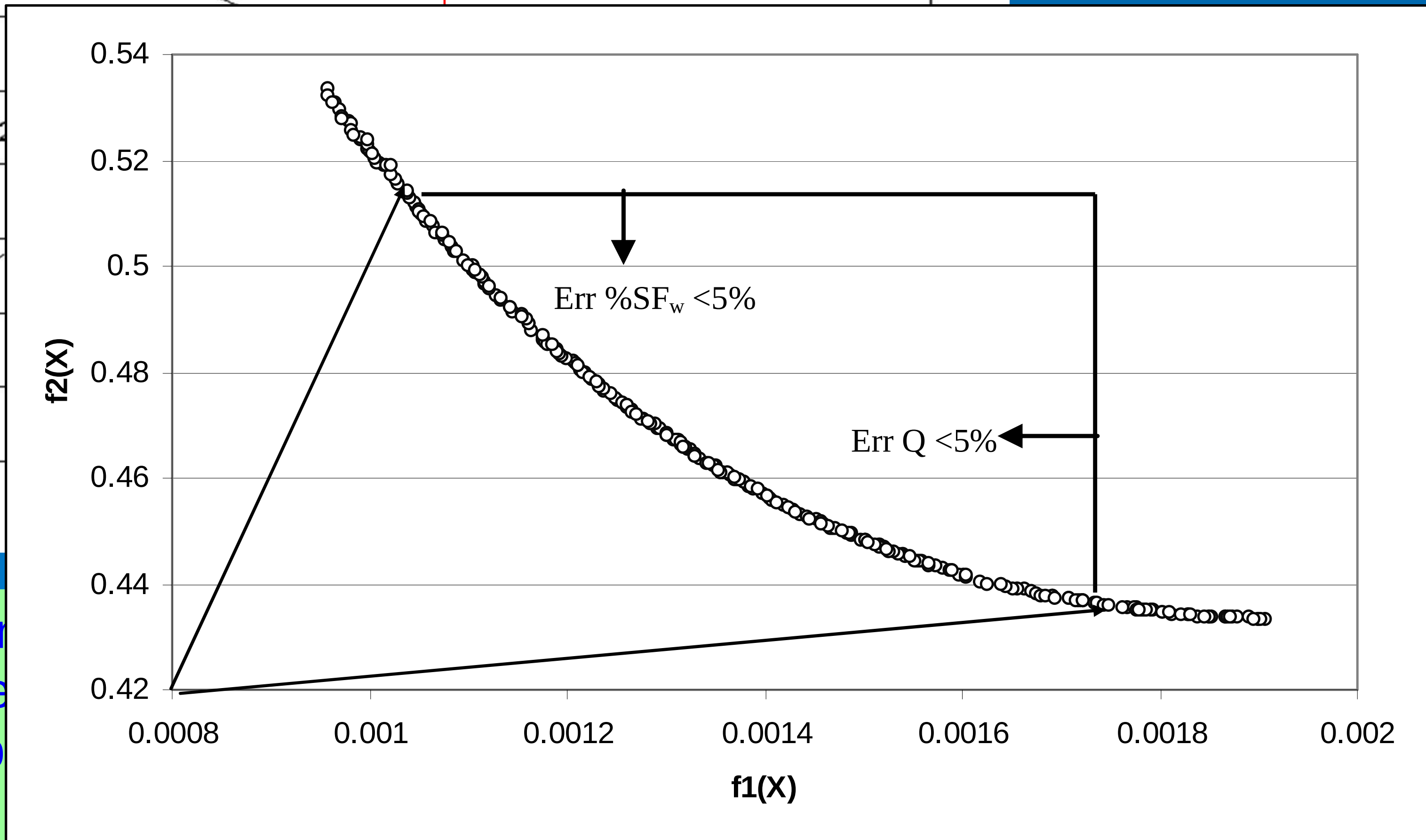

Chlebek, J. ar
on sidewall corre
RiverFlow 2006, Lisb

Trapezoidal channel
(4 panels)

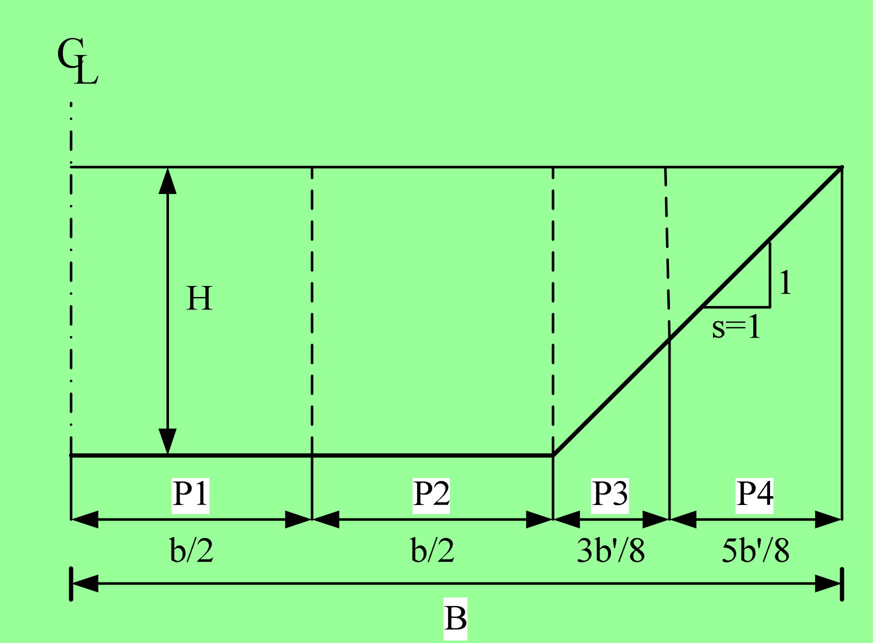

a) Smooth bed and rough walls

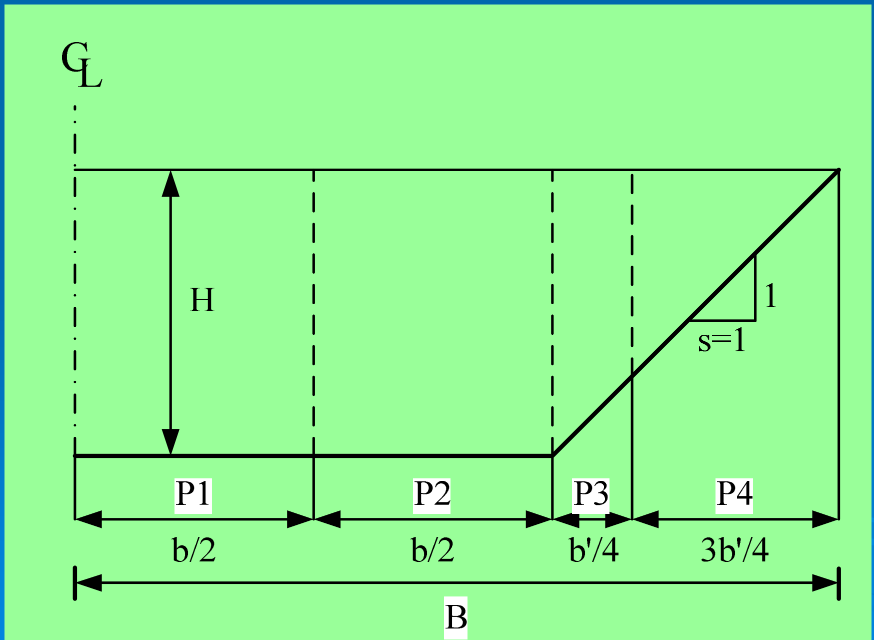

b) Rough bed and rough walls

4 objective functions

$$f_1(X) = \sum_i \left((U_d)_{SKM} - (U_d)_{\exp} \right)^2$$

$$f_2(X) = \sum_i \left((\tau_b)_{SKM} - (\tau_b)_{\exp} \right)^2$$

$$f_3(X) = \left| \frac{Q_t - Q_{SKM}}{Q_t} \right| \times 100$$

$$f_4(X) = \left| \frac{\%(SF_w)_t - \%(SF_w)_{SKM}}{\%(SF_w)_t} \right| \times 100$$

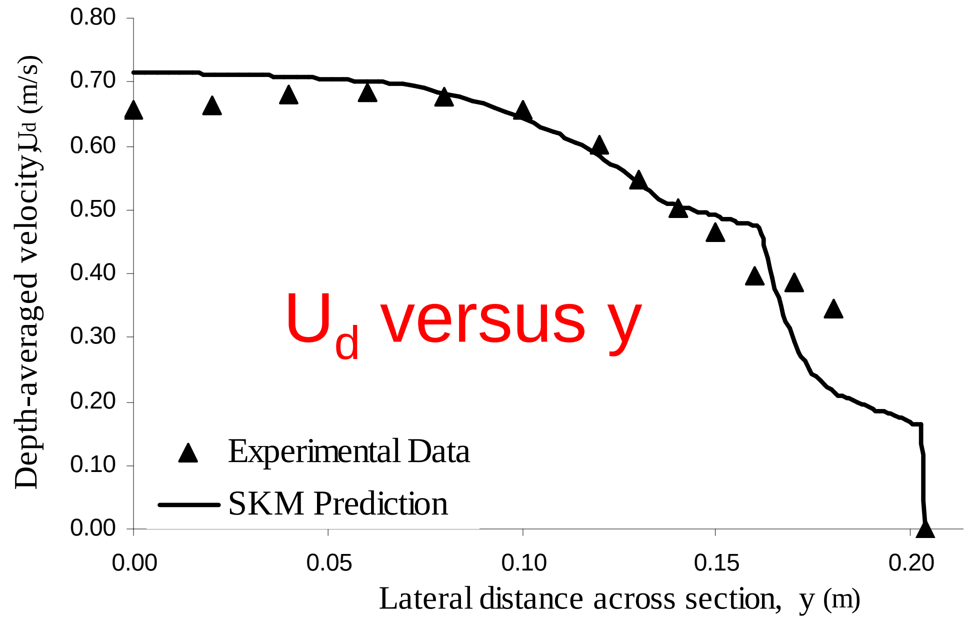

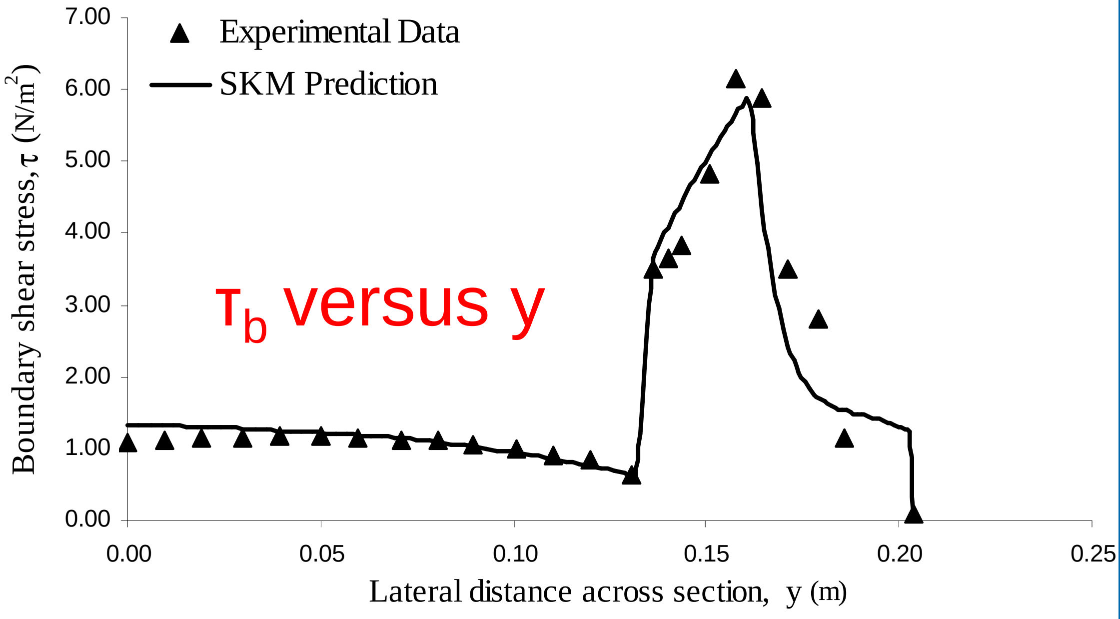

Al-Hamid Exp 18 H = 0.068 m

(Qdata= 14.09 l/s and QSKM= 13.86 l/s : Error = - 1.63%)

(%SFwdata= 68.32 and %SFwSKM= 68.01: Error = - 0.45%)